



Technical challenges for the new T2K High Angle TPCs

19 July 2024

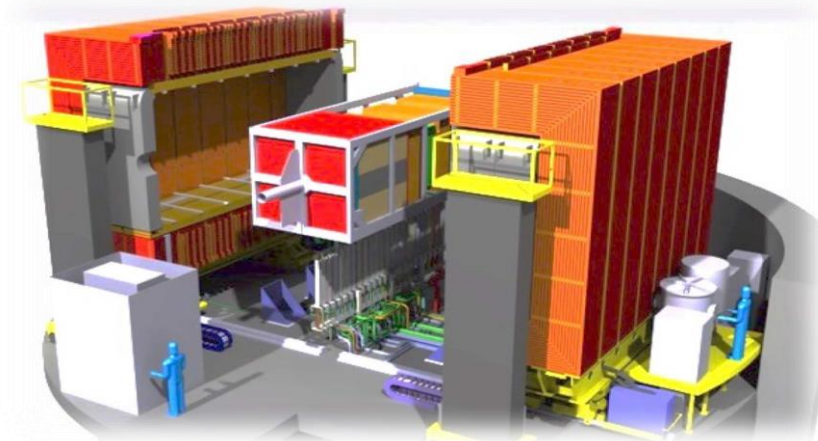
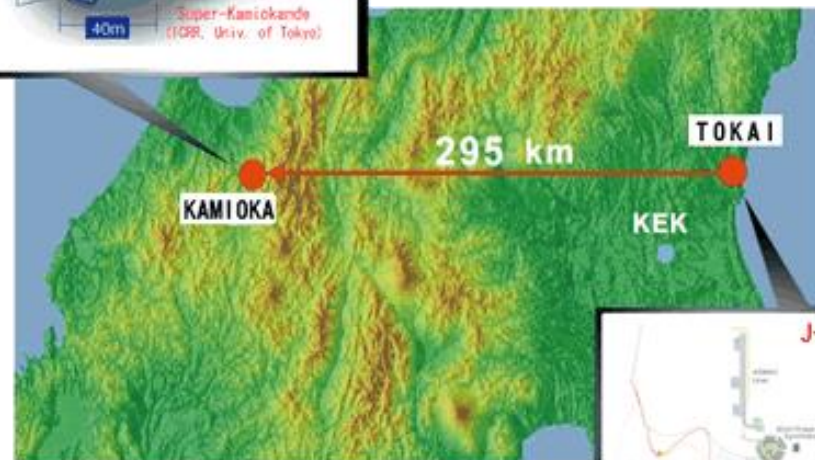
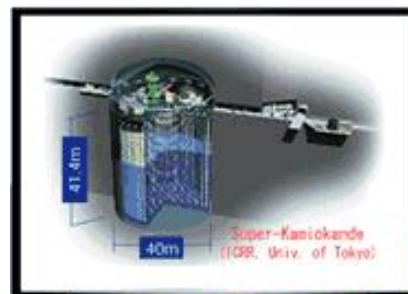
Stefano Levorato

on behalf of the T2K ND280 upgrade group



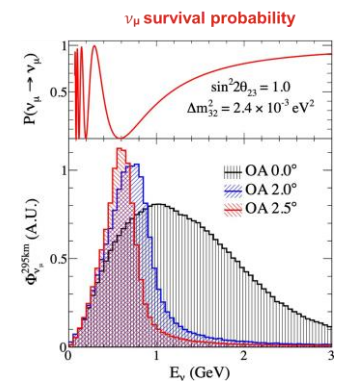
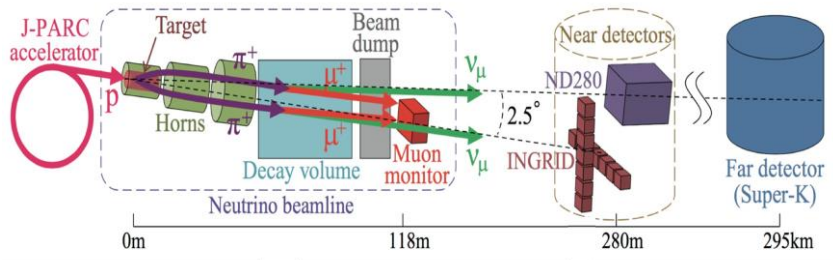
Outlook

- **The T2K ND280 experiment**
- **The ND280 upgrade project**
 - The motivations
 - The upgrade
- **The High Angle Time Projection Chambers (HATPC)**
 - Mechanical constrains
 - Electrical constrain and performance
- **The Encapsulated Resistive Anode Micromegas (ERAM)**
 - Construction
 - Quality assessment
- **Conclusions**



The T2K experiment and the role of ND280

High intensity ~ 0.6 GeV ν_μ beam produced at J-PARC (Tokai) $\rightarrow \nu$ or $\bar{\nu}$ mode by changing the horn polarity

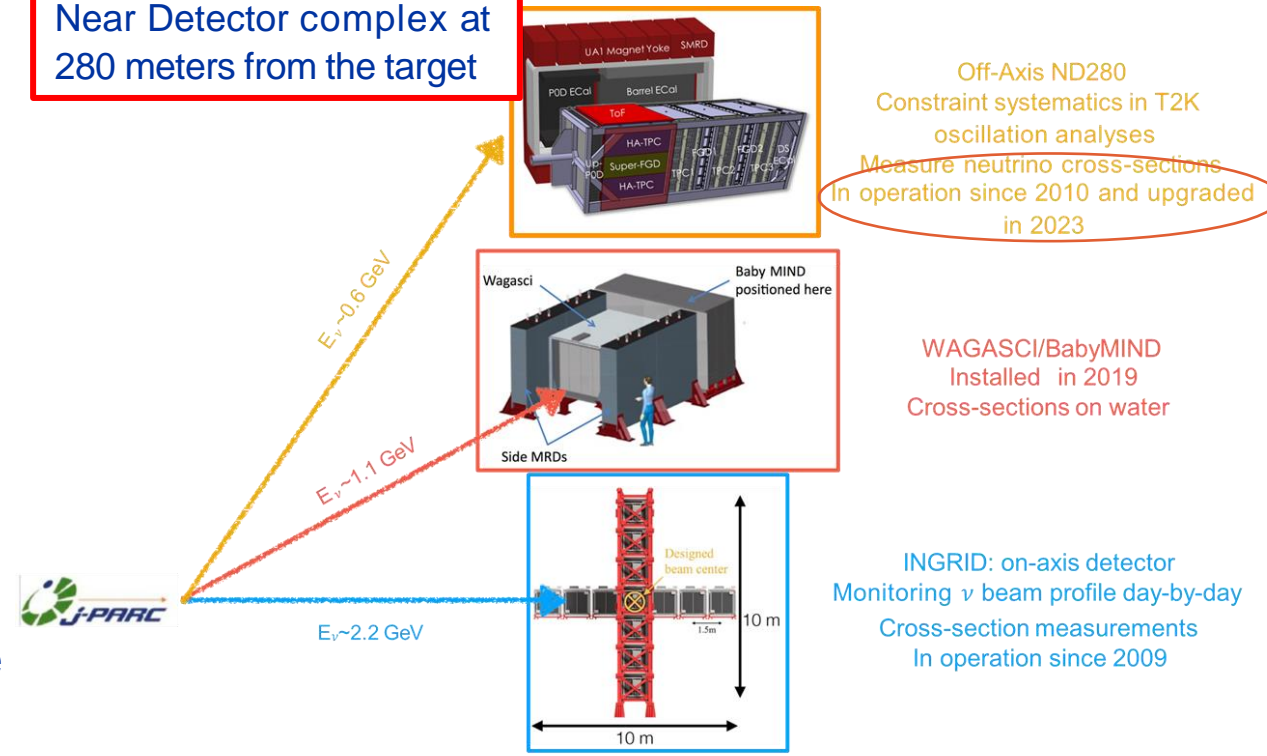


Neutrinos detected at the Near Detector (ND280) and at the Far Detector (Super-Kamiokande)

- ν_e and $\bar{\nu}_e$ appearance \rightarrow determine θ_{13} and δ_{CP}
- Precise measurement of ν_μ disappearance $\rightarrow \theta_{23}$ and $|\Delta m^2_{32}|$

ND to measure **un-oscillated beam flux** and **ν cross sections**

Near Detector complex at 280 meters from the target



Off-Axis ND280
Constraint systematics in T2K oscillation analyses
Measure neutrino cross-sections
In operation since 2010 and upgraded in 2023

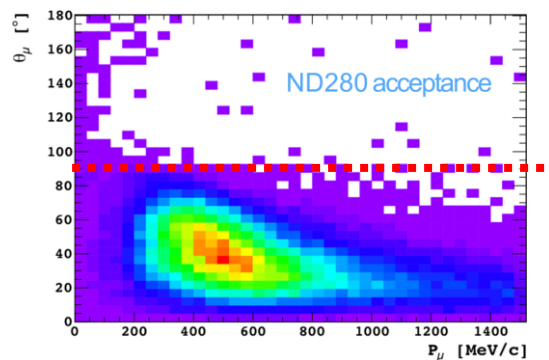
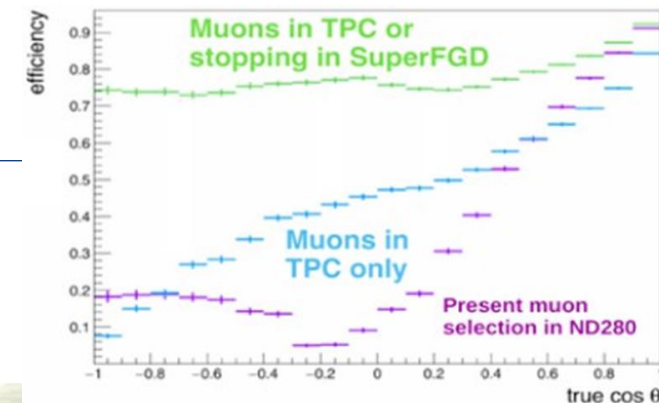
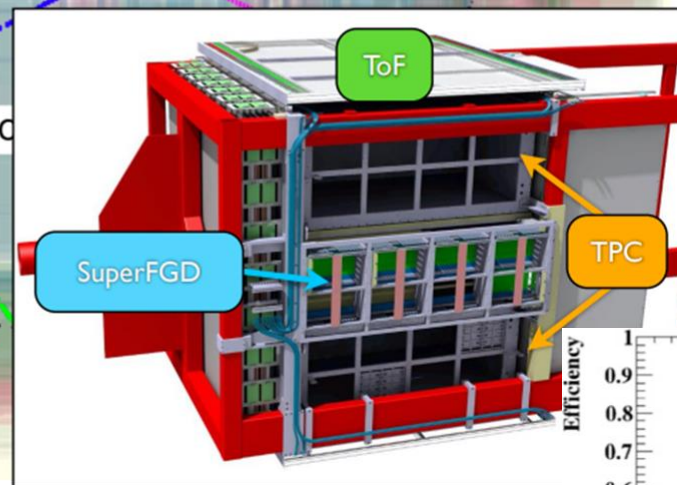
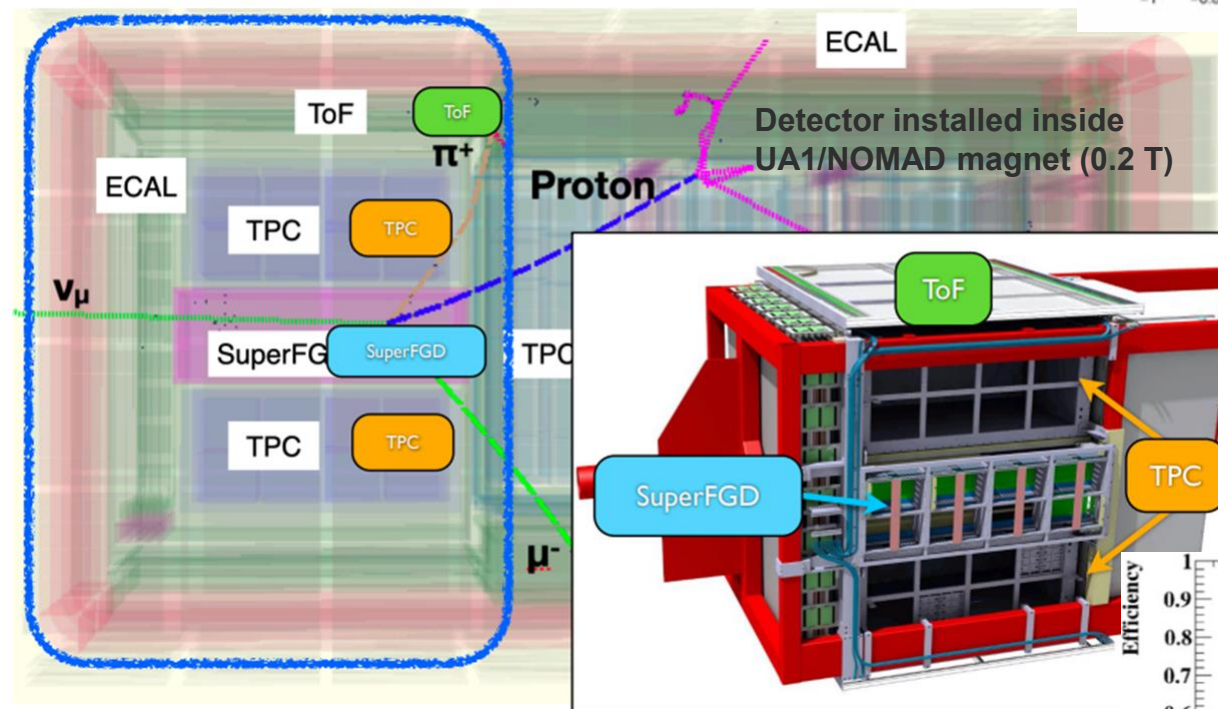
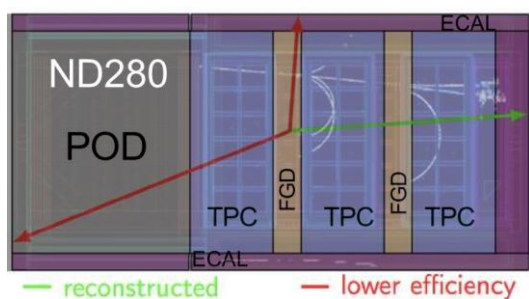
WAGASCI/BabyMIND
Installed in 2019
Cross-sections on water

INGRID: on-axis detector
Monitoring ν beam profile day-by-day
Cross-section measurements
In operation since 2009

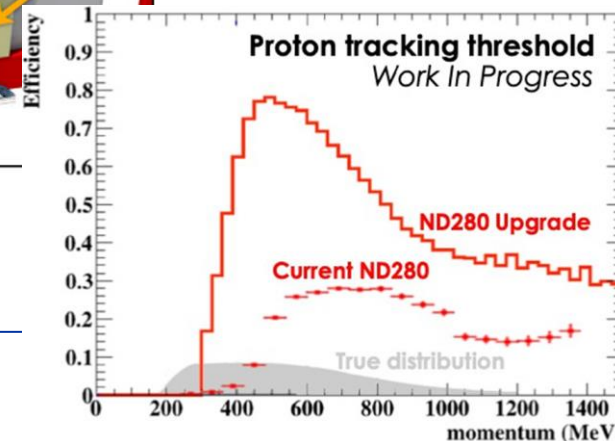
Several detectors installed to monitor the beam & reduce systematic uncertainties in oscillation analyses, and measure ν and $\bar{\nu}$ cross-sections

The ND280 experiment: the upgrade

- Reduced angular acceptance ν events, mostly reconstruct forward going tracks entering the TPCs
- Low efficiency to reconstruct low momenta protons

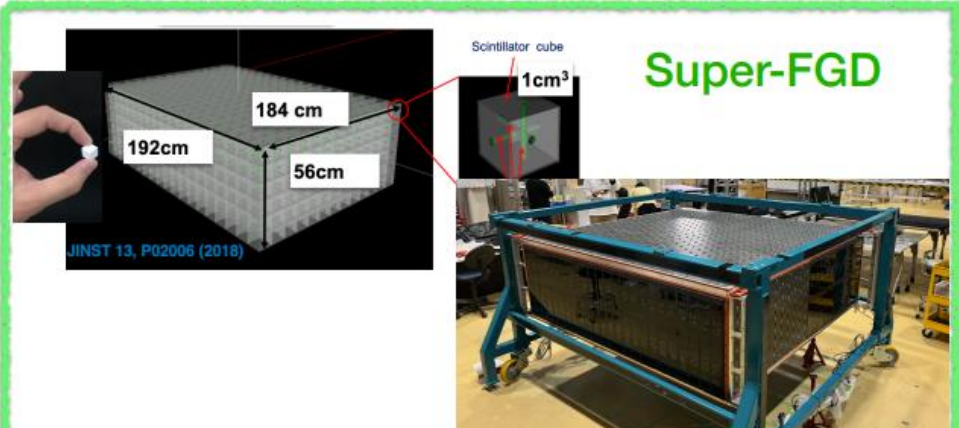


New detectors to extend acceptance for tracks at high angles



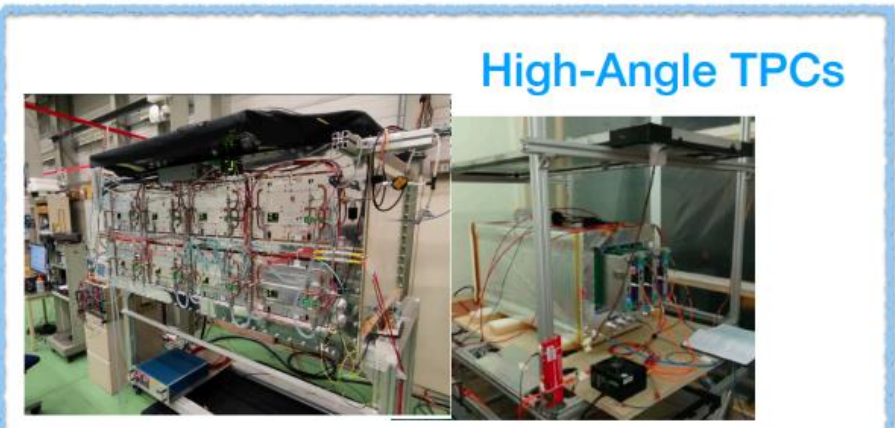
ND280: the upgrade detectors

Super-FGD




- * New concept of detectors, 2×10^6 1 cm^3 cubes
- * Each cube is read by 3 WLS → 3D view

High-Angle TPCs



- * New TPCs instrumented with Encapsulated Resistive Anode MicroMegas (ERAM)

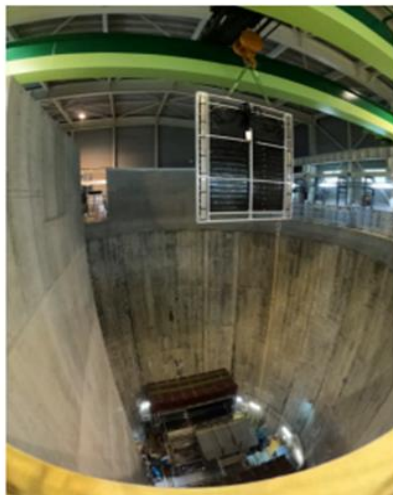
TOF



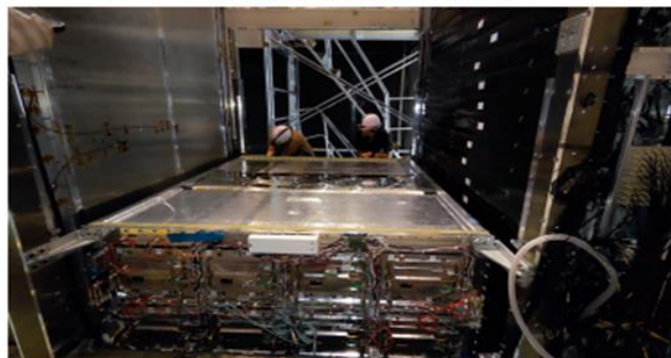
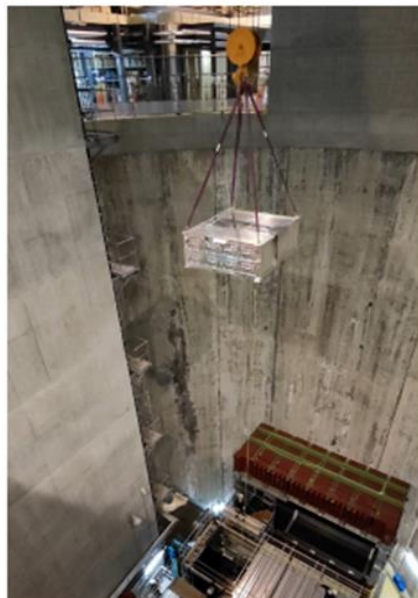
6 TOF planes to reconstruct track direction
Time resolution ~150 ps

ND280: installations at J-PARC

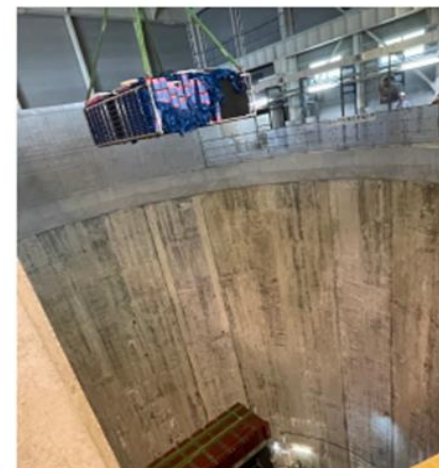
TOF installation (July 2023)



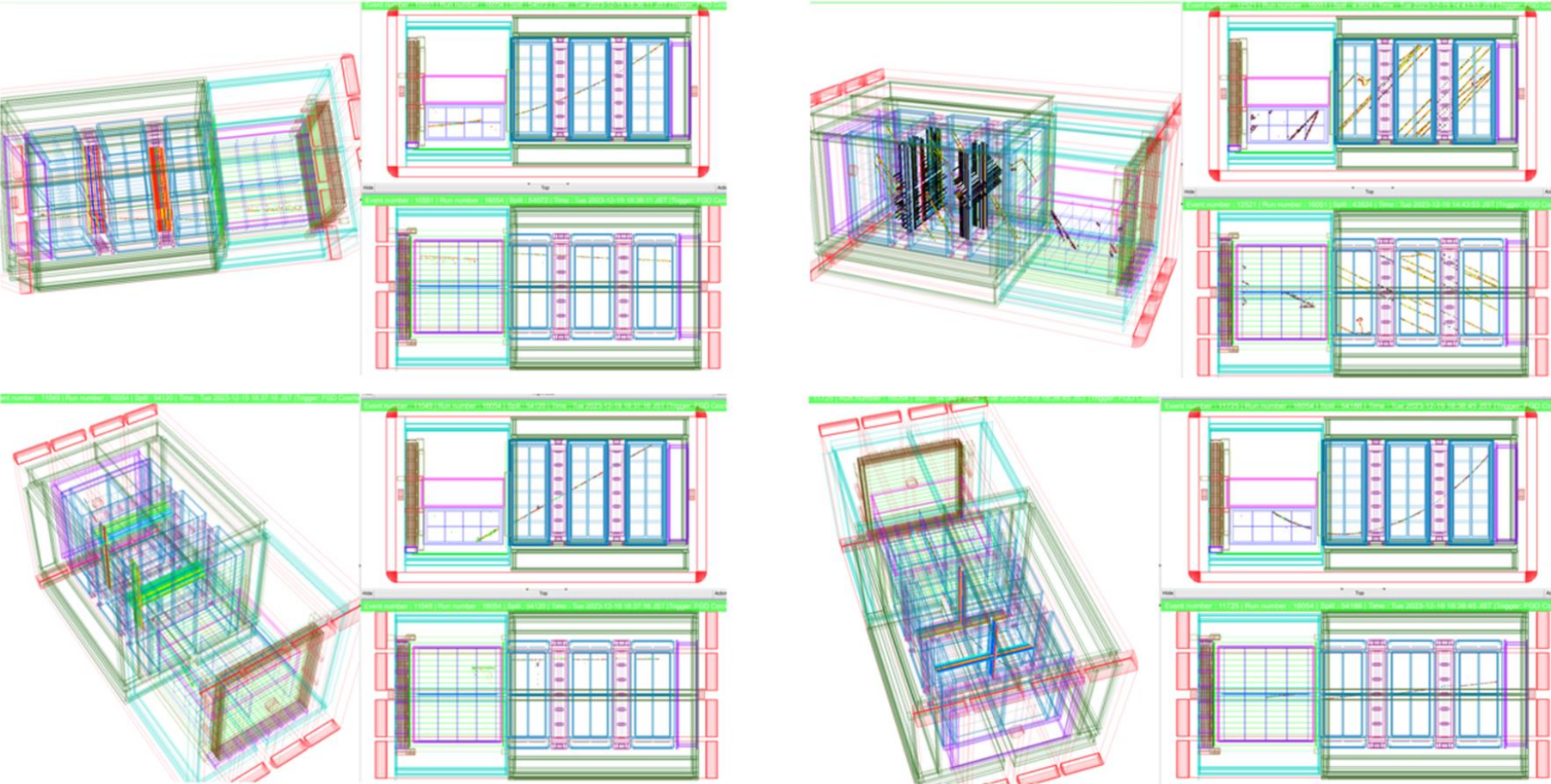
Bottom TPC installation (September 2023)



Super-FGD installation (October 2023)

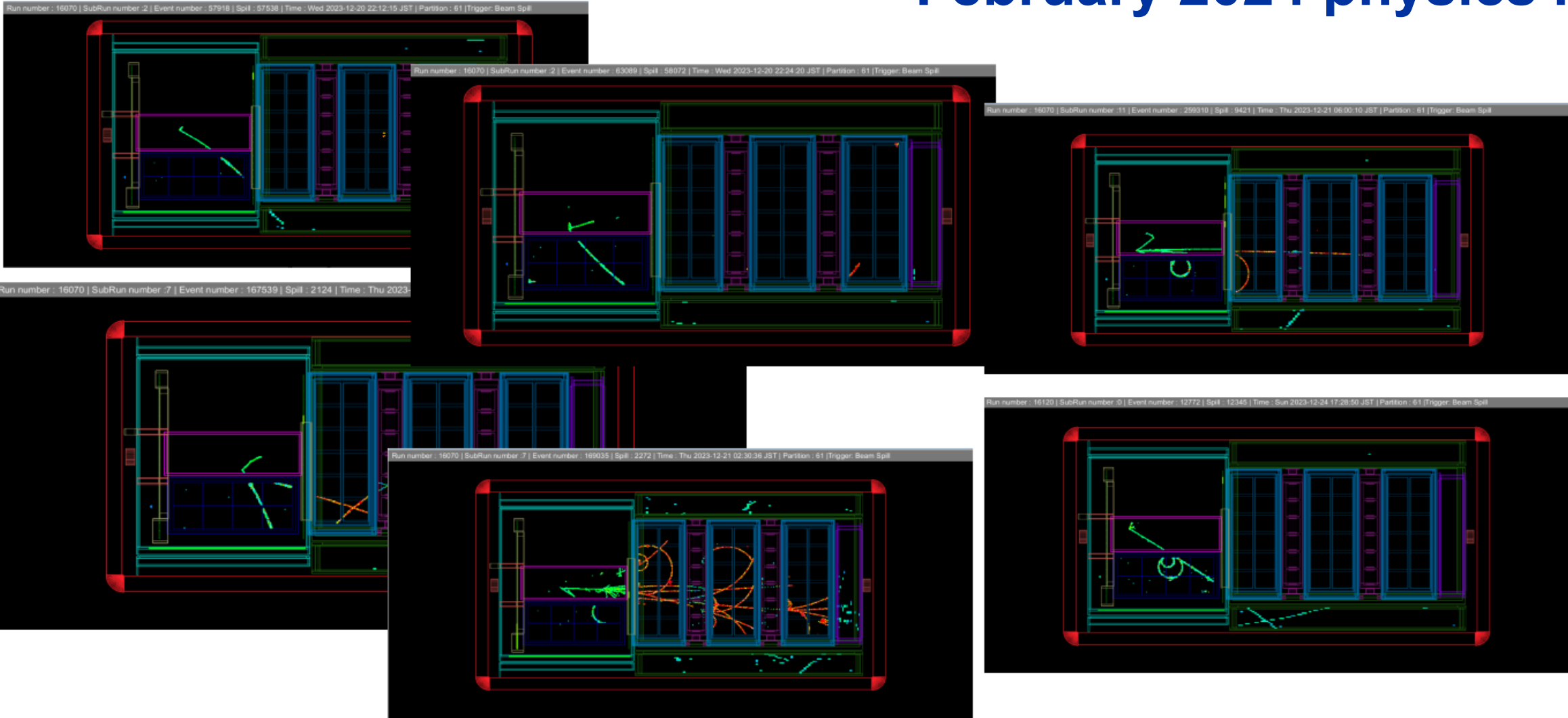


N280: commissioning at JPARC with cosmics

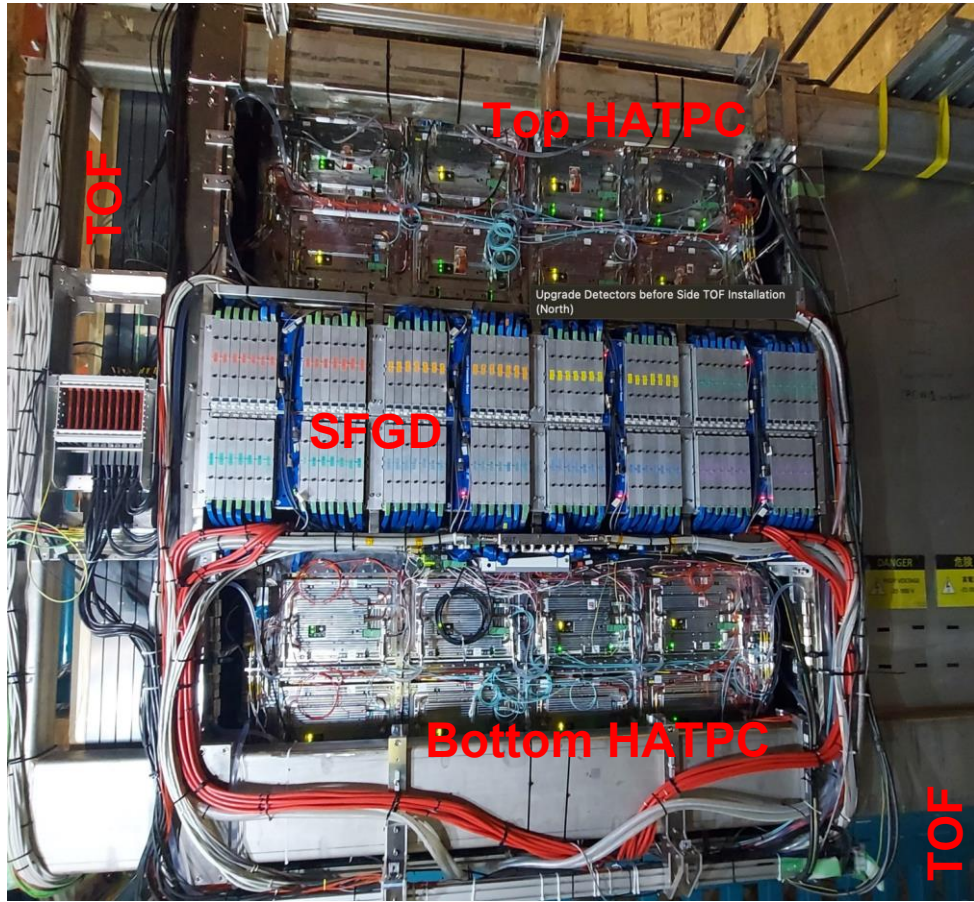
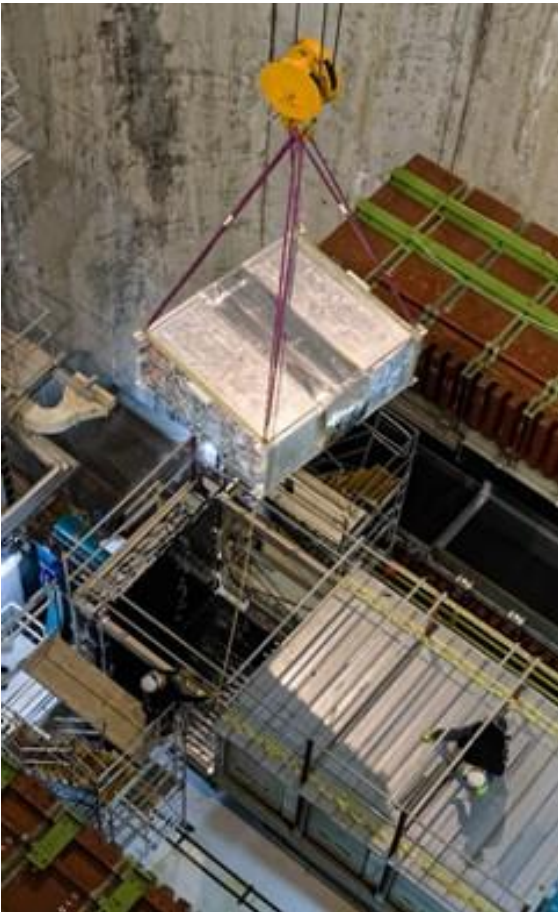


- Detector commissioning with and without magnetic field
- Alignment runs
- New software deployment
- New T2K gas system commissioning for both vertical and horizontal TPCs

N280: ν technical runs in December 2023 and February 2024 physics run



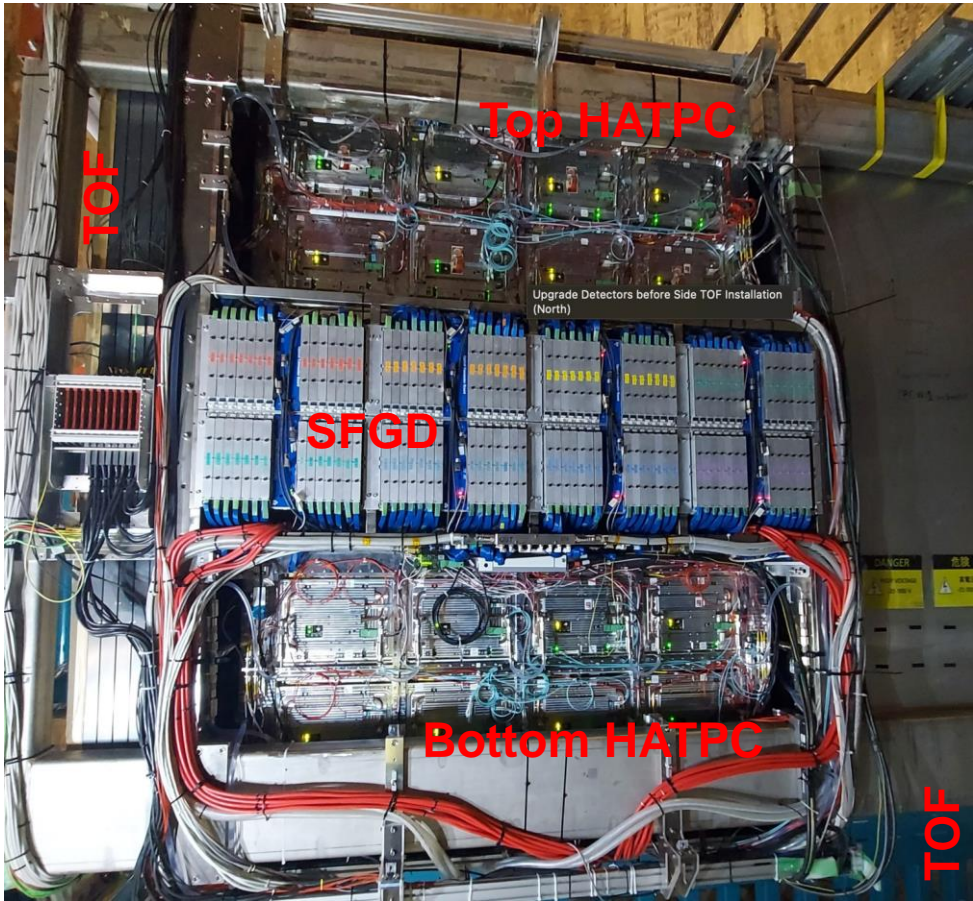
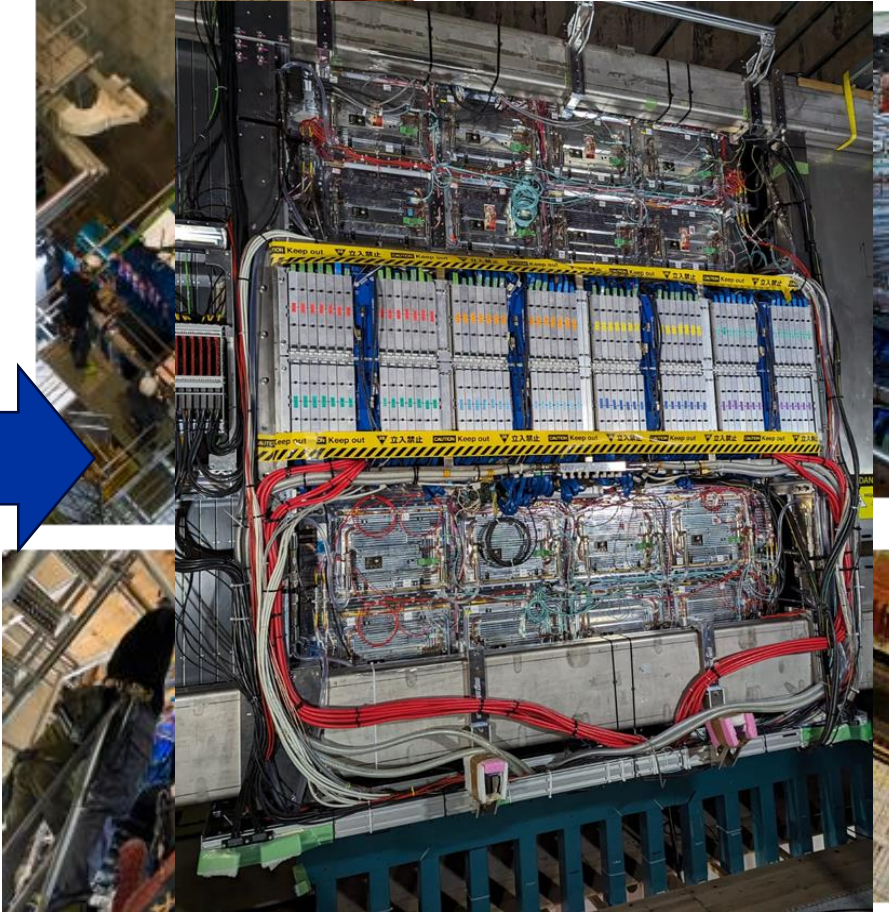
ND280: upgrade completed! Top-HATPC installed in the end of April 2024



ND280: upgrade completed! Top-HATPC installed in the end of April 2024

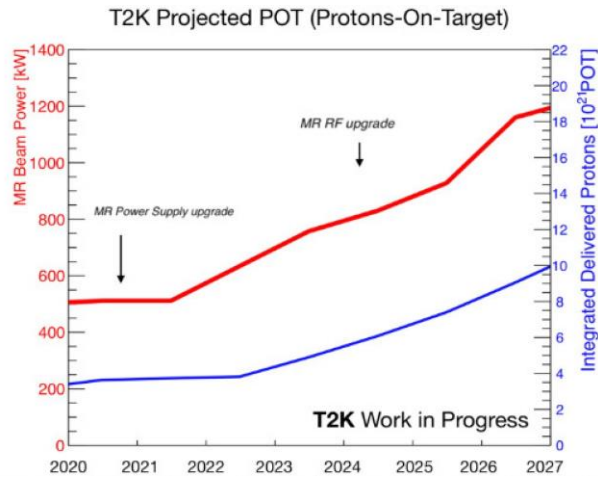


Installation of the Detectors of the ND280 upgrade successfully completed in May 2024!



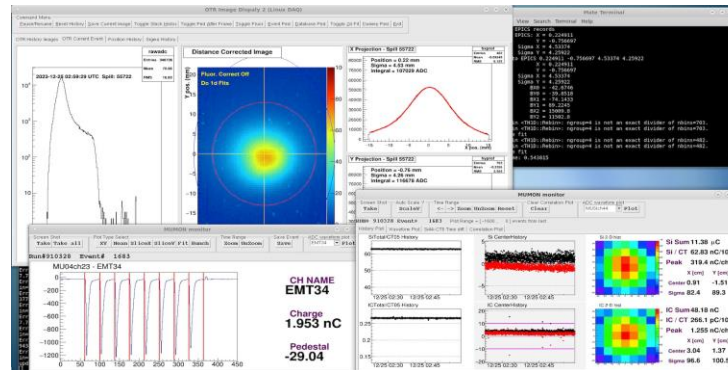
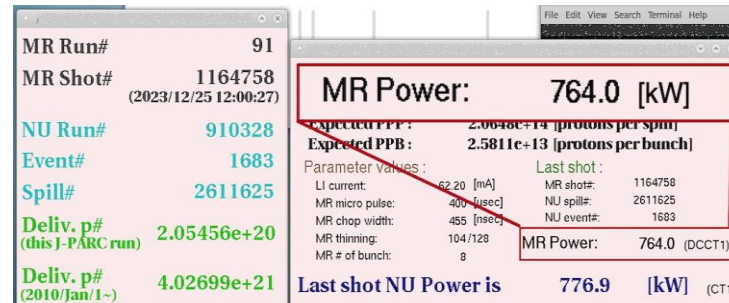
The T2K run schedule: beam upgrade

ν beam @ J-PARC: dedicated upgrade of the MR facility to reach the 1.3 MW beam power



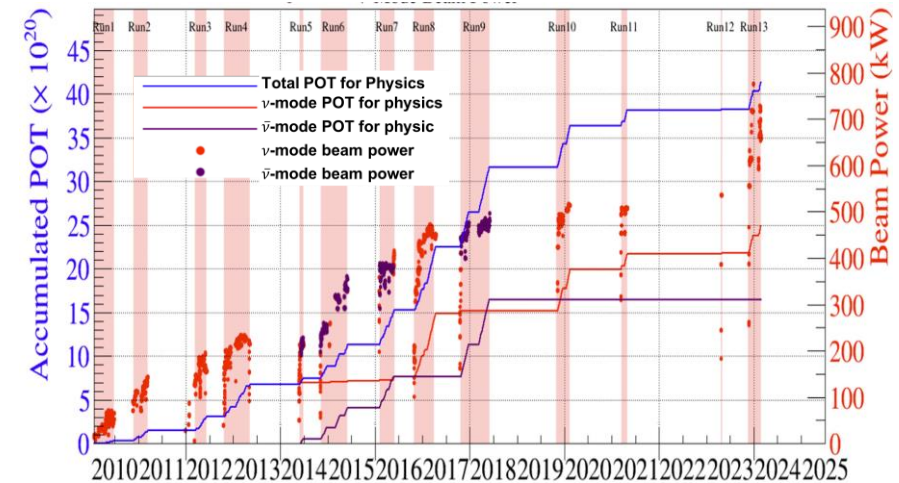
Beam and Window Parameters

	750 kW	1.3MW
	Design	T2KII path
Beam Energy [GeV]	30	30
Protons per spill [-]	3.30E+14	3.20E+14
Energy deposited per kg per proton [J/kg/proton]	2.52E-10	2.52E-10
Energy deposited per kg per pulse [J/kg/pulse]	83300	80640
Cycle time [s]	2.1	1.16
Spill length [s]	4.13E-06	4.11E-06
Number of bunches [-]	8	8
Bunch length [ns]	58	40
Gap length [ns]	523	541
Peak Heat Generation [J/m^3/s]	8.15E+14	1.14E+15
Beam sigma [mm]	4.24	4.24
Heat load per spill [J/cc/pulse]	378.18	366.11
Heat load per sec [W/cc]	180.09	315.61
Peak Temp per bunch [C]	19.78	19.15
Thermal stress per bunch [MPa]	61.27	59.32
Peak Temp per pulse [C]	158.27	153.22



Expect to select 20k ν_{μ} CC0pi interactions in the super-FGD for 0.2e21 POT (1 month)

December 2023 → Beam power increased from 500 to 760 kW stable mode
800 kW reached in 2024 for the first run with the fully upgraded ND280



Steady improvements to reach 1.3 MW by 2027 with an increase T2K statistics ~ a factor of 3 by 2027

The ND280 experiment: High Angle TPC highlights

- Field Cage (FC)
 - Assembly
 - Production
 - Characterization and Quality Assessment
 - Mechanical
 - Electrical
- Encapsulated Resistive Anode Micromegas (ERAMS)
 - Production of 50 sensors
 - Characterization
 - Detector response, signal and impact on reconstruction
- Impact on HATPC performance

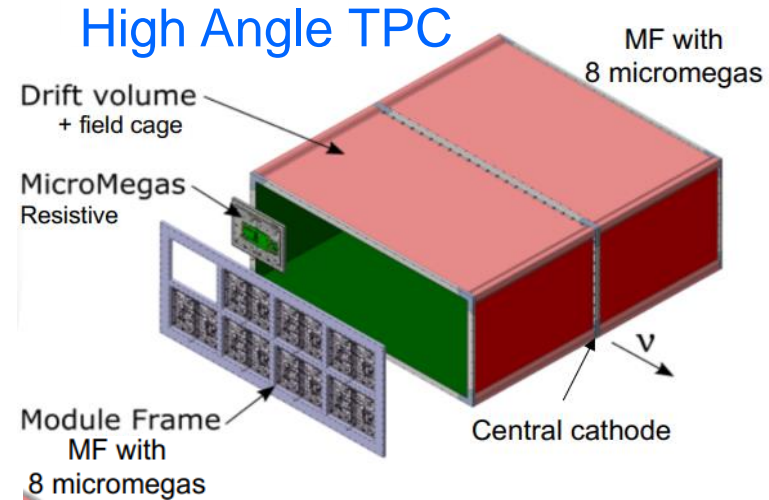
The ND280 experiment: physics requirements

Momentum resolution $\sigma_p/p < 9\%$ at 1GeV/c
(neutrino energy)

Energy resolution $\sigma_{dE/dx} < 10\%$
(PID muons and electrons)

Space resolution $O(500 \mu\text{m})$
(3D tracking & pattern recognition)

Low material budget walls $\sim 3\% X_0$
(matching tracks from neutrino active target)



Atmospheric pressure TPC

- Gas: T2K mixture (Ar-CF₄-isoC₄H₁₀ = 95-3-2)
- Gas contaminants better than O(10 ppm) level
- Drift length 1m
- Central Cathode @ -27kV
- E field unif. $< 10^{-3}$ @1cm from walls
- Low material budget, thin walls
- Active volume $\sim O(3\text{m}^3)$

Resistive MicroMegas sensors (ERAMs)

- Overall anode active surface $\sim O(3\text{m}^2)$
- Sampling length $\sim 80\text{-}160 \text{ cm}$
- pads $\sim 1\text{cm}^2$
- 10k+10k channels / TPC @ End Plates (Anodes)

HATPC: features, challenges, constrains and solutions

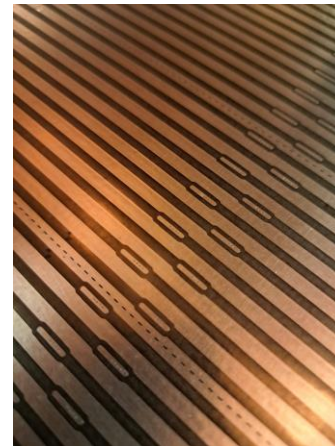
Mechanics and Electric Field uniformity

- Min dead space & max active volume in the dipole magnet
 - Rectangular shape & thinnest walls & field shaping electrodes incorporated into the walls
- Electric field uniformity better than 10^{-3} @1cm from walls
 - Mechanical accuracy: inner surfaces planarity & parallelism $\sim O(0.2\text{mm/m})$
 - Shaping Electrode design: Field and Mirror copper strip layers on two sides of a Kapton foil
- Low material budget walls
 - lightweight & lowest Z & robust (self supporting)



Electrical insulation Constrains

- HV insulation mantle $R > 1\text{T}\Omega\text{m}$ and volume resistivity, HV
 - geometry: several cm paths for charge from -HV strips to GND shielding (cathode flanges)
 - insulating materials: very high resistivity & dielectric strength



HATPC: features, challenges, constrains and solutions

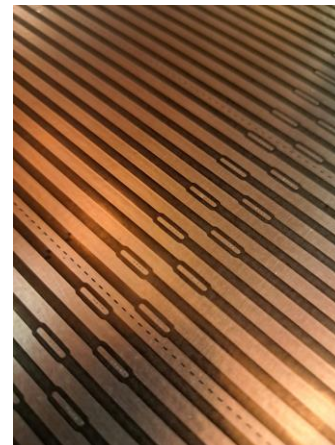
Building process: hand lay-up of composite materials on a Mould & polymerization in autoclave at high Pressure

- Autoclave dimensions
 - **Field Cage comprising two halves** (symmetrical flanges at central cathode position)
- Hand layup & large dimensions
 - several hours per process step → **very long pot life for epoxy resin**
- Mechanical accuracy of geometry → **resin curing at low T < O(40°C)**




Materials of choice

- lamination materials: **Aramid polymers** for peels (Twaron) and for honeycomb (Nomex paper)
- epoxy resin **limited choice: Resoltech 1054** combined with **quality control against contaminants** (moisture, ...)
- high insulation layers: **Kapton**
- box skeleton material: **high quality laminated G10**



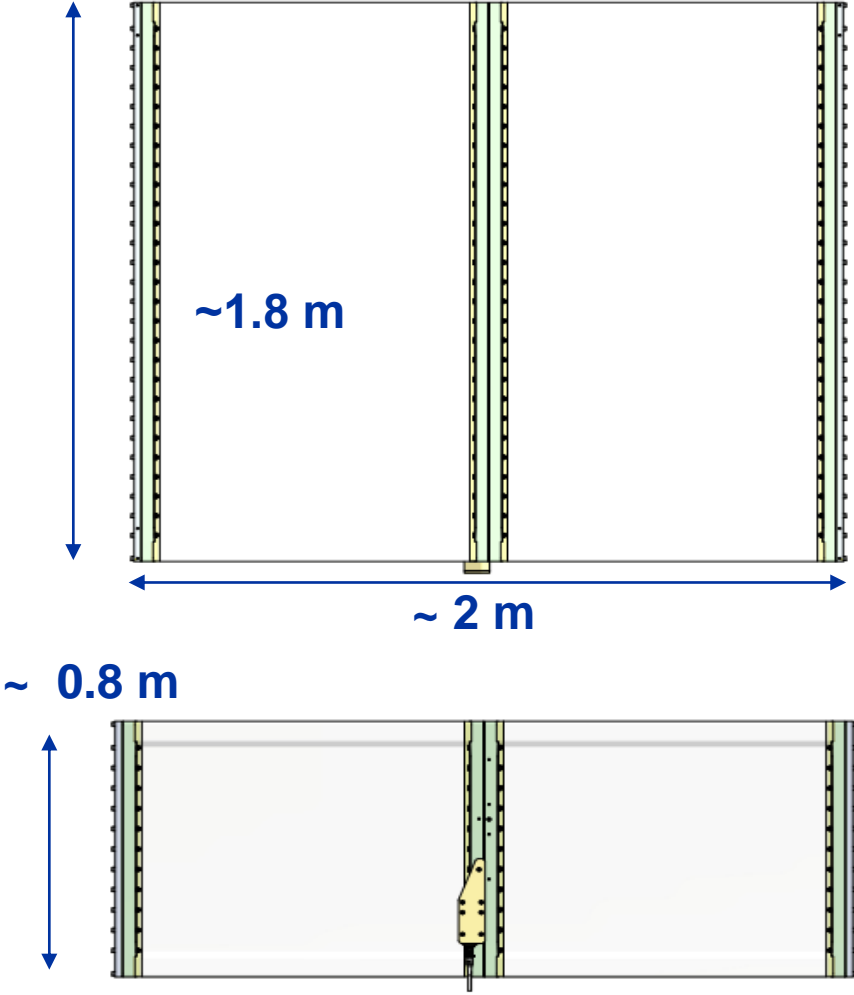
The ND280 experiment: High Angle TPC highlights

- Field Cage (FC)
 - Assembly and layout 
 - Production
 - Characterization and Quality Assessment
 - Mechanical
 - Electrical

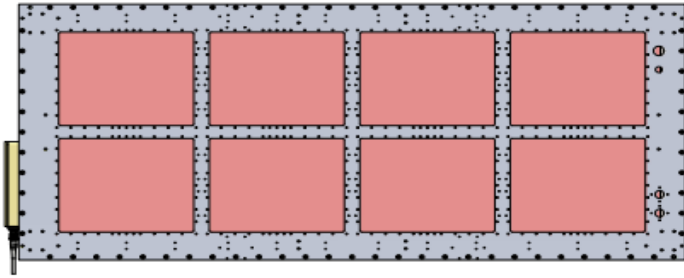
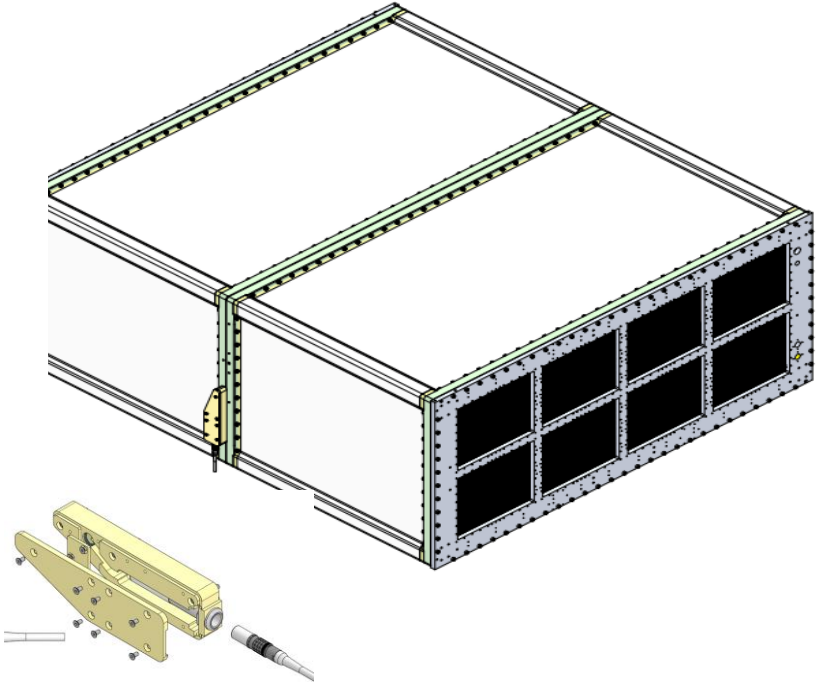
- Encapsulated Resistive Anode Micromegas (ERAMS)
 - Production of 50 sensors
 - Characterization
 - Detector response, signal and impact on reconstruction

- Impact on HATPC performance

Mechanical HATPC Field Cage assembly



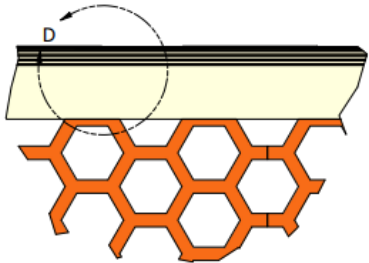
- HATPC in two half FCs
- Central cathode
- Special cathode flanges w/ HV ft
- Two End Plates (Al) supporting 8 Readout Modules each



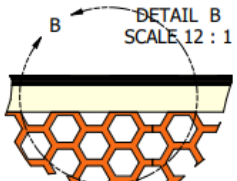
Field Cage: walls stack up layout

Inner surface

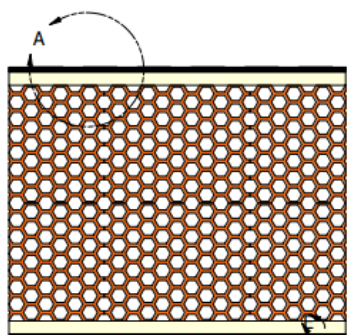
DETAIL D
SCALE 80 : 1



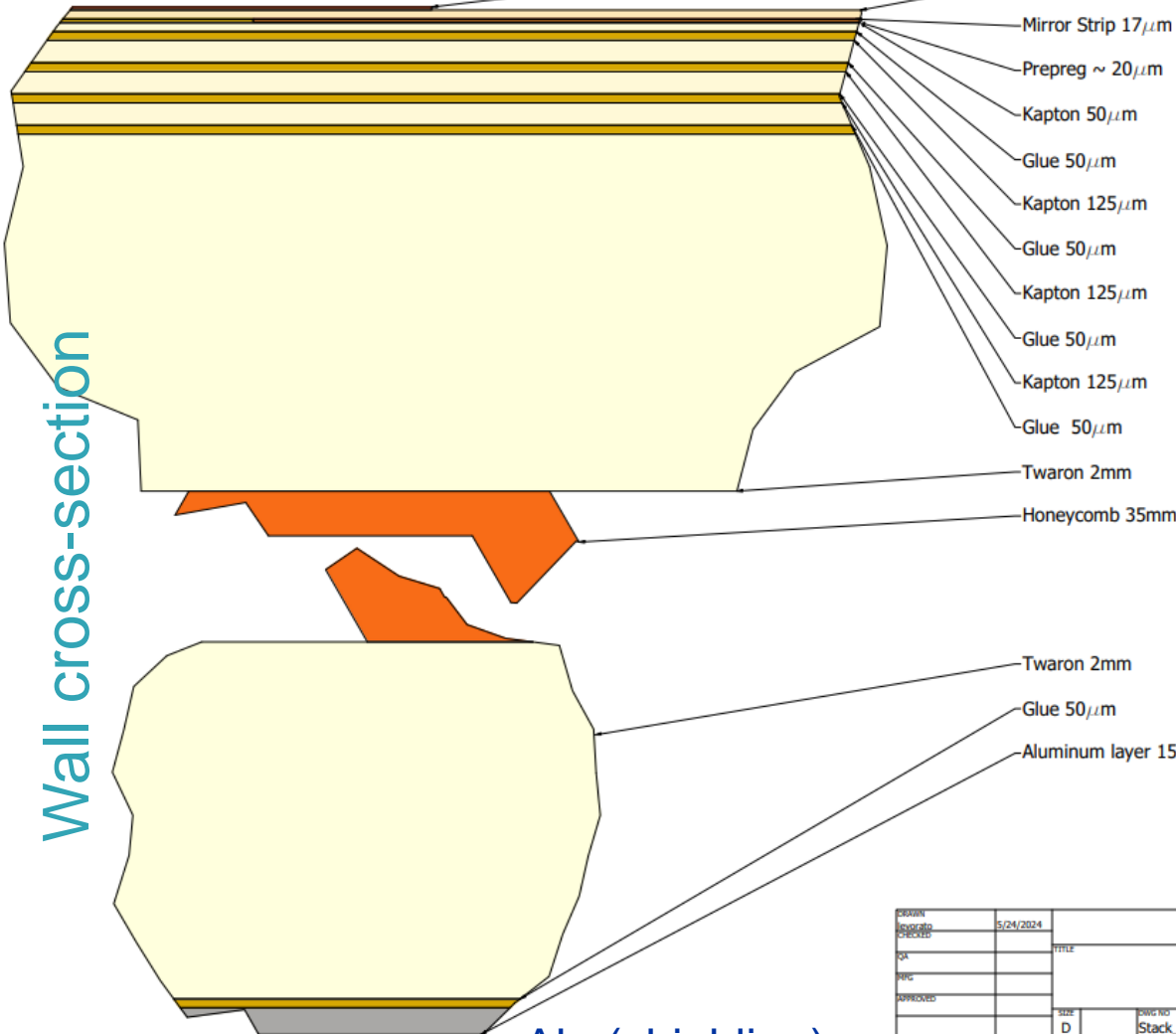
DETAIL B
SCALE 12 : 1



DETAIL A
SCALE 6 : 1



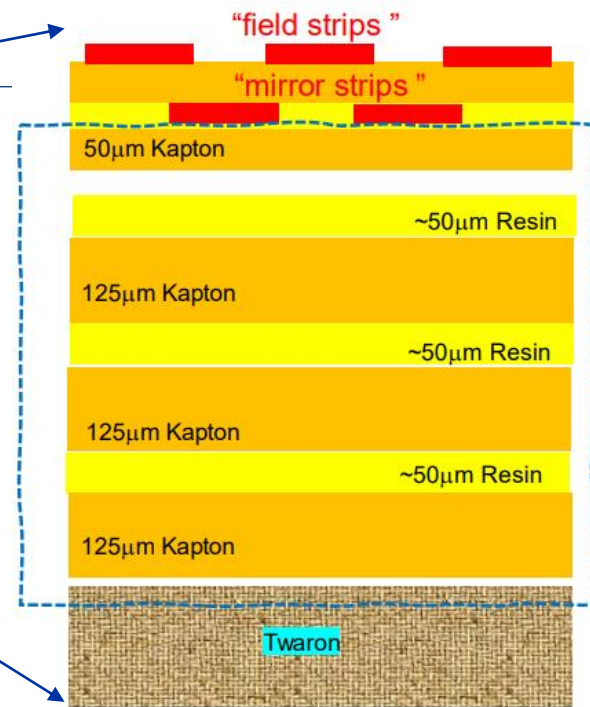
DETAIL E
SCALE 80 : 1



Wall cross-section

Alu (shielding)

DATE	5/24/2024	
DESIGNED		TITLE
QA		
ENG		
APPROVED		
	SIZE	DWG NO
	D	Stack.ne



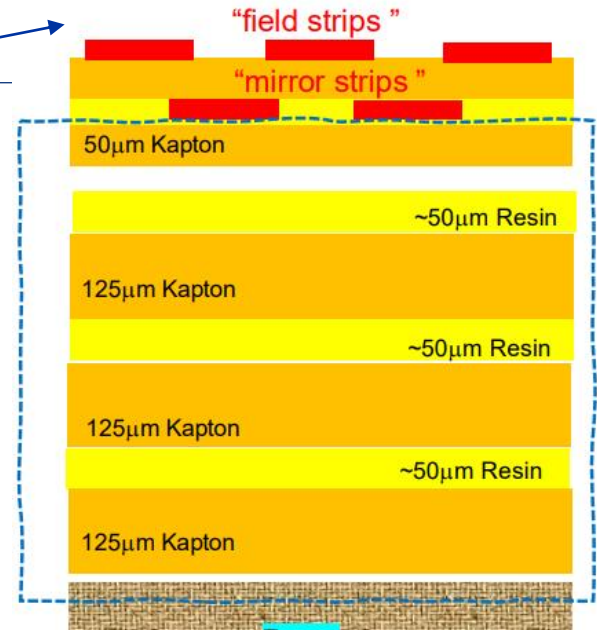
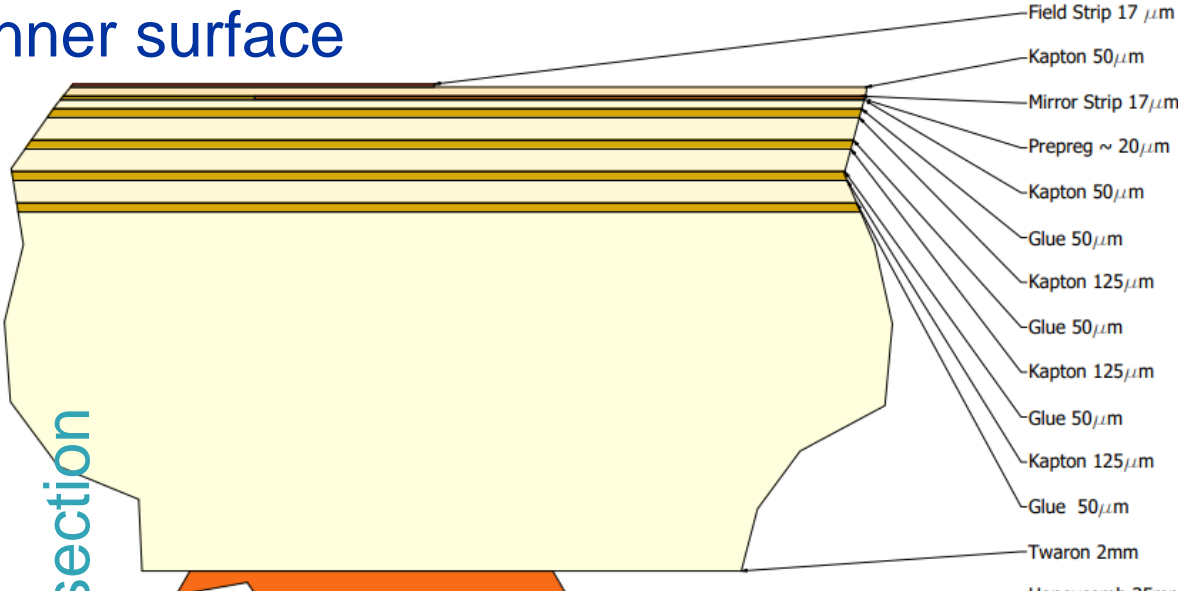
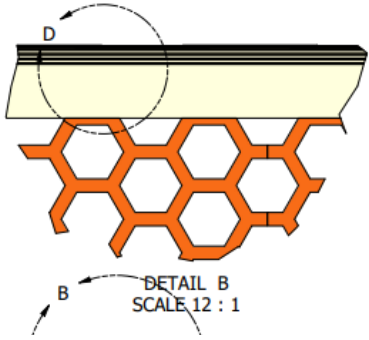
Wall thickness
~ 40 mm
~ 2% radiation length

Outer surface

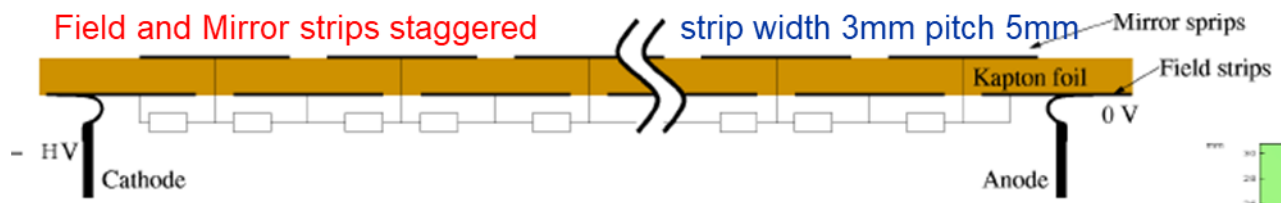
Field Cage: walls stack up layout

Inner surface

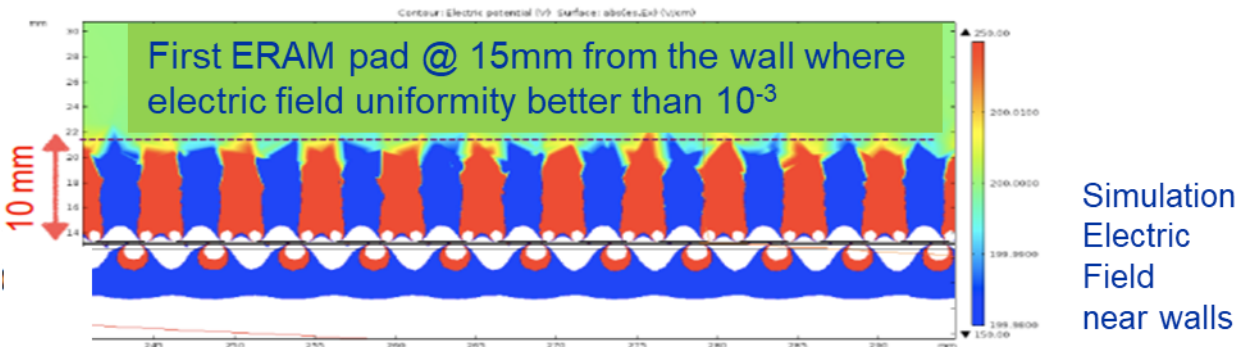
DETAIL D
SCALE 80 : 1



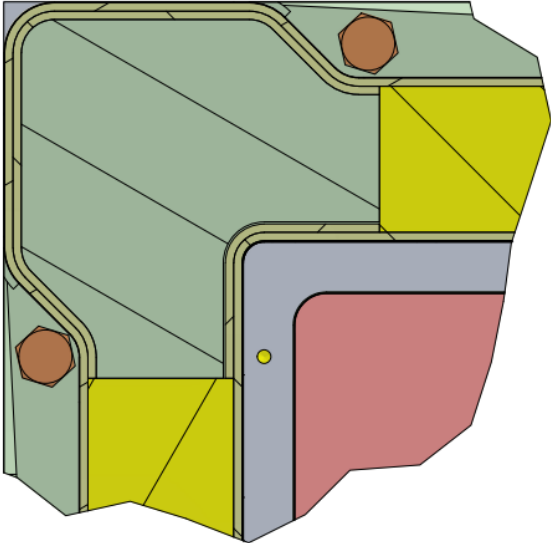
Electric field shaping by two Cu strips layers ('Field' and 'Mirror' strips)



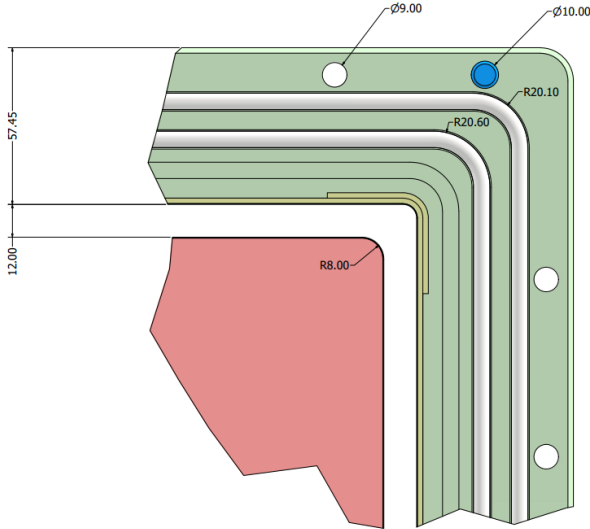
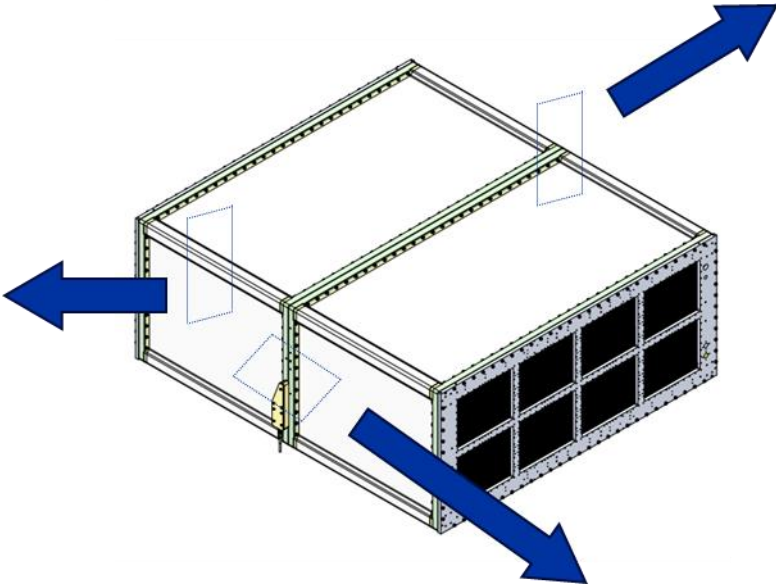
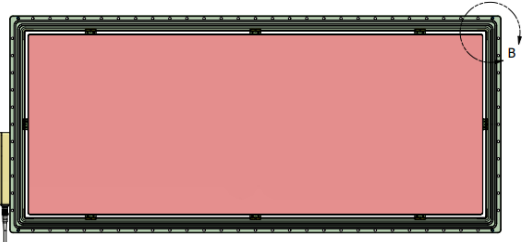
Double layer of strips on Kapton foil
 Dimensions = 5m (inner surface cage perimeter) x 1m (drift distance)
 Resistors soldered on the inner surface (contact Mirror strips by vias)



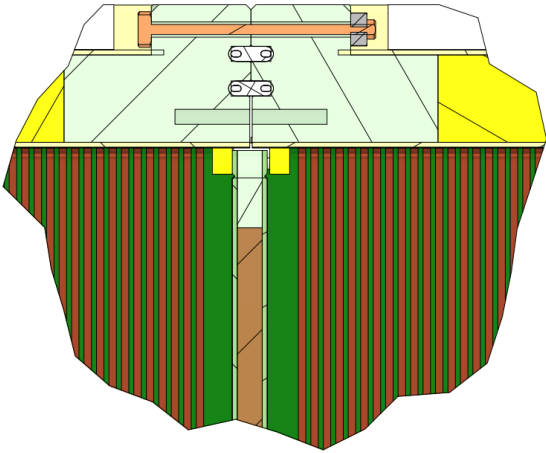
Field cage mechanical details



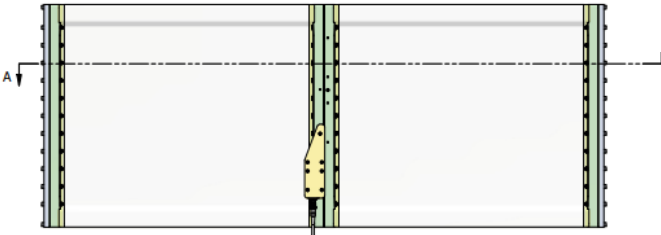
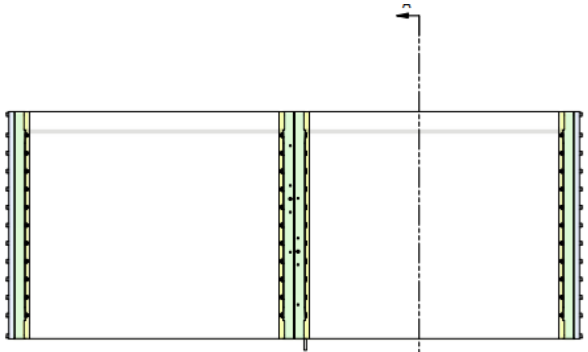
DETAIL C
SCALE 2 : 1



DETAIL B
SCALE 2 : 1



DETAIL B
SCALE 2 : 1



Field cage mechanical details: charge path to gnd

Flange thickness (5cm) too small for degrading -30kV to GND over a flat surface

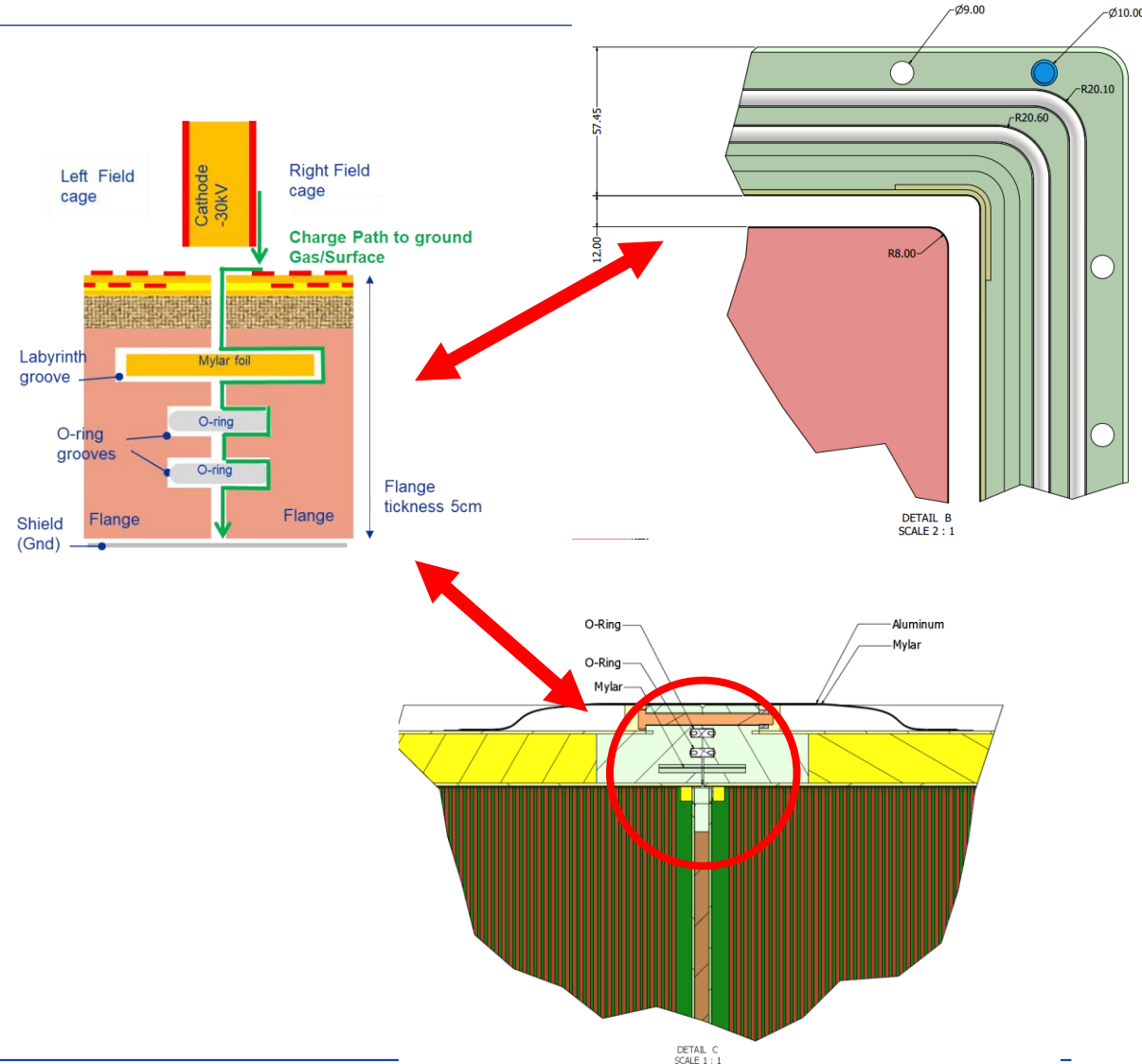
Three deep grooves

for extending the path from HV to GND for charge moving on surface and with gas flanges


~ 7cm thick labyrinth

~14 cm path length

→ voltage drop / path length < 3kV/cm



The ND280 experiment: High Angle TPC highlights

- Field Cage (FC)
 - Assembly and layout
 - Production
 - Characterization and Quality Assessment
 - Mechanical
 - Electrical
- 

- Encapsulated Resistive Anode Micromegas (ERAMS)
 - Production of 50 sensors
 - Characterization
 - Detector response, signal and impact on reconstruction

- Impact on HATPC performance

Field Cage building, assembling and characterization

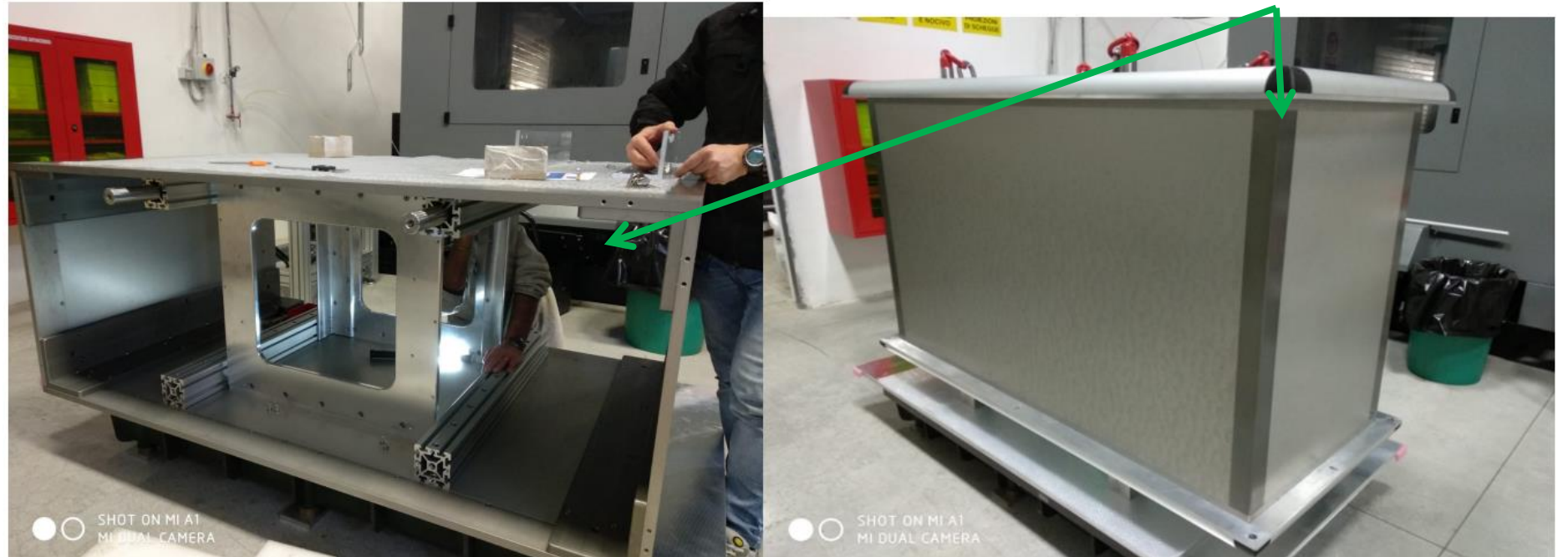
Production at NEXUS company (Barcelona) ~ 10 weeks

Validation, QC, electrical and mechanical assembly at CERN ~ 4 weeks

Mould building
(INFN)

Mold features

- 1cm thick Alu walls
- Anodized Surfaces
- Waviness compl. iso1302 N8
- Surfaces \perp and \parallel better than $80\mu\text{m/m}$
- Mount / unmount geom. reproducibility with high precision



Field Cage building, assembling & characterization at NEXUS Kapton Layer

Production at NEXUS company (Barcelona) ~ 10 weeks

Validation, QC, electrical and mechanical assembly at CERN ~ 4 weeks



5 m perimeter x 1m height (drift length)

- Mold preparation
- Inner Vacuum bag
- Strip Foil positioning
- Thick corners w/ Kapton tape
- Electrical tests on surfaces
- Resin samples electrical Tests

Strip foil (by CERN) alignment and lamination of 3 Kapton layers



- Kapton lamination
- Curing at 40C (fast)
- Electrical tests on surfaces and resin samples after curing



Field Cage building, assembling & characterization at NEXUS

Kapton Layer and inner Twaron

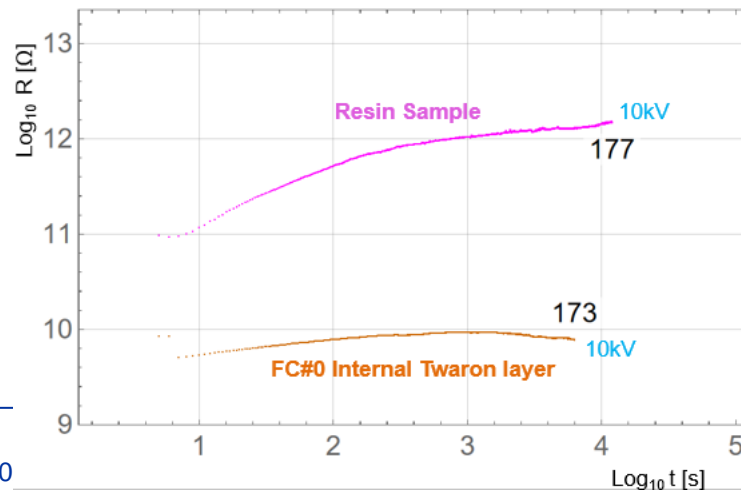
Inner Twaron peel lamination



- First Twaron layer lamination
- Curing at 40C (fast) in autoclave

Electrical tests

- Resin sample
- Inner Twaron layer



Quality controls – Resistivity of early Layers

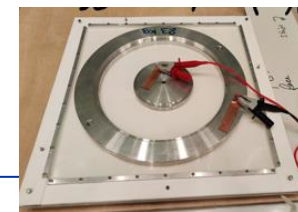
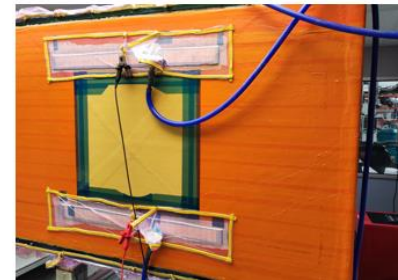
1) Resistance between mold and 40x45cm² electrode
 -> volume resistivity of layers



2) Surface resistivity of last layer Twaron



3) Resistance between two 6x80cm² electrodes
 -> mix of surface and volume resistivity



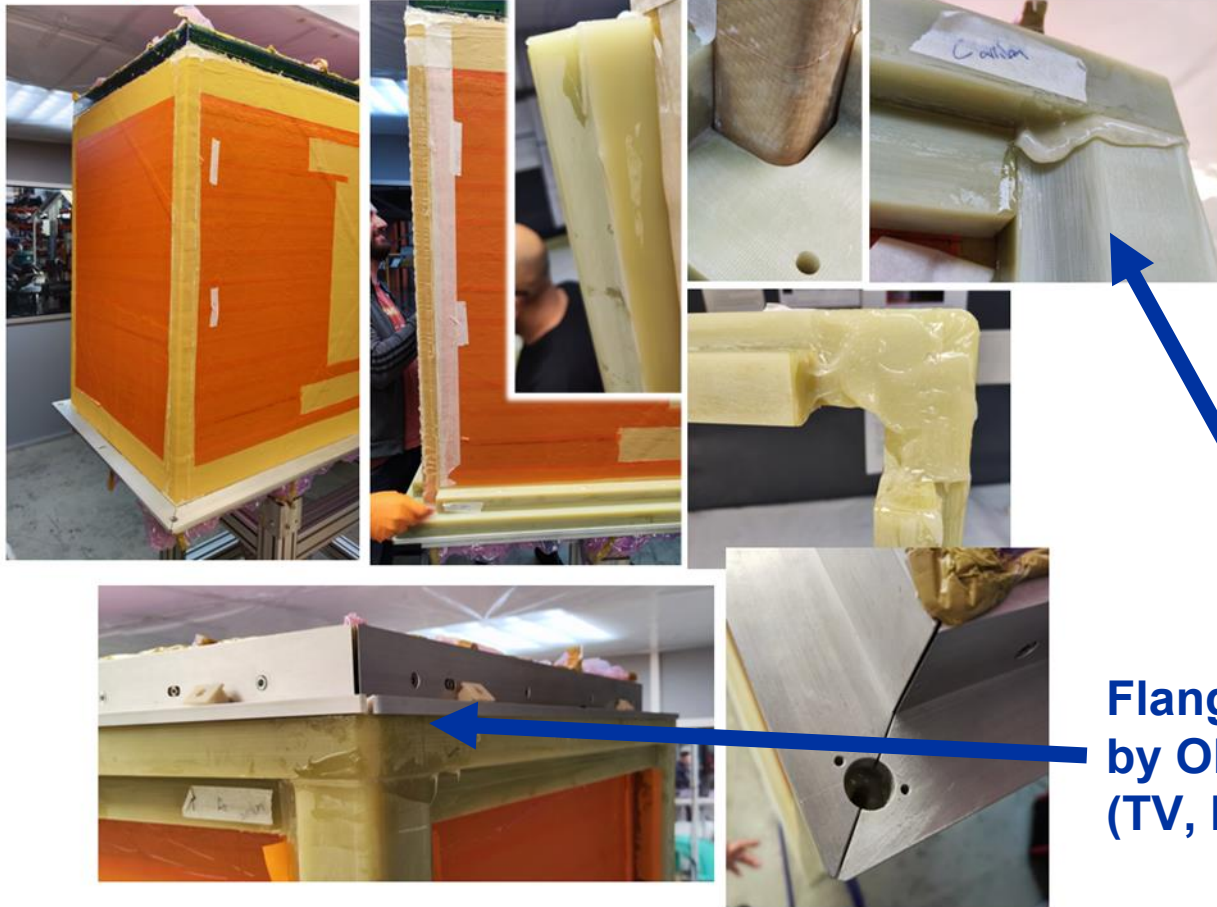
1) various methods and electrode types (optimizing contact)
 -> consistent measurements

2) Resin sample $\rho_s \sim 10 \text{ T}\Omega/\square$
 -> very good

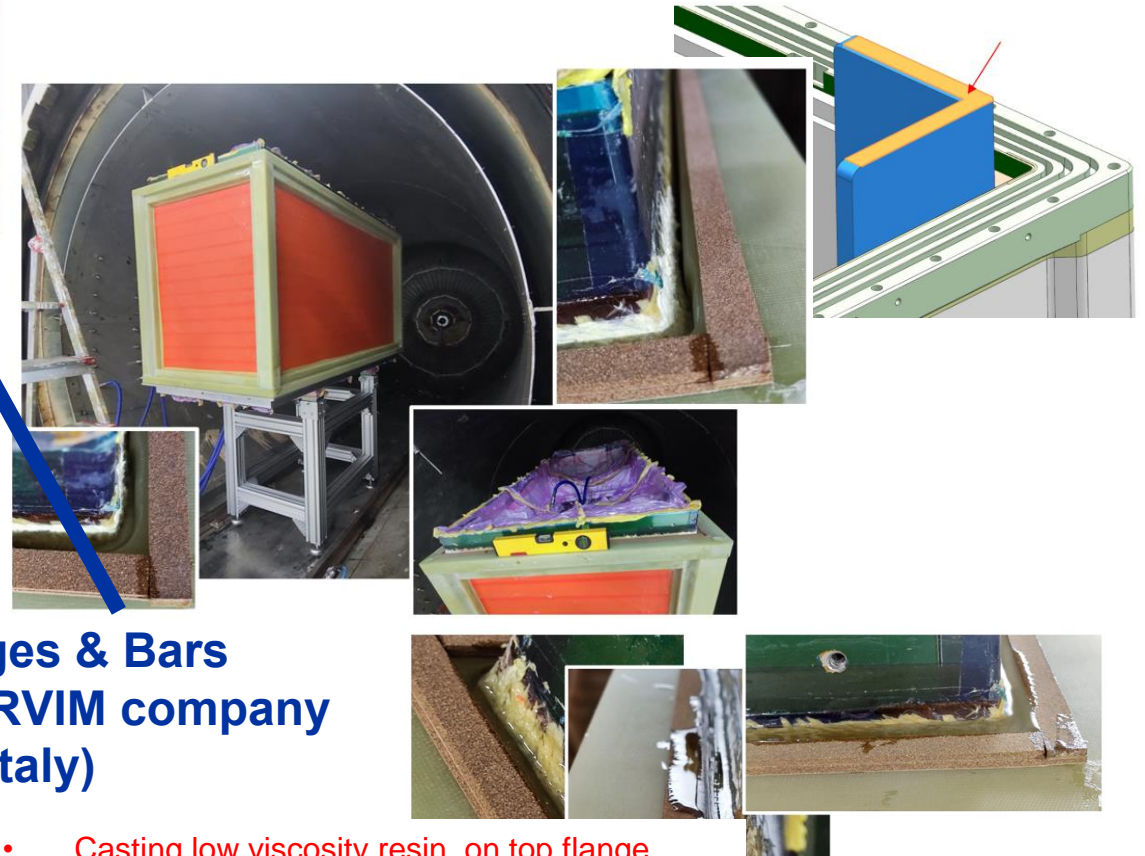
Field Cage building, assembling & characterization at NEXUS

Kapton Layer + inner Twaron + G10 Skeleton

Gluing G10 "skeleton"



Gluing G10 structural skeleton and casting resin on flanges for ensuring gas tightness



Flanges & Bars
by ORVIM company
(TV, Italy)

- G10 skeleton gluing
- Curing 40C in clean room

- Casting low viscosity resin on top flange
→ sealing flange to laminated layers
- Autoclave curing at 40C

Field Cage building, assembling & characterization at NEXUS Kapton Layer + inner Twaron + G10 Skeleton + HC + Ext Twaron

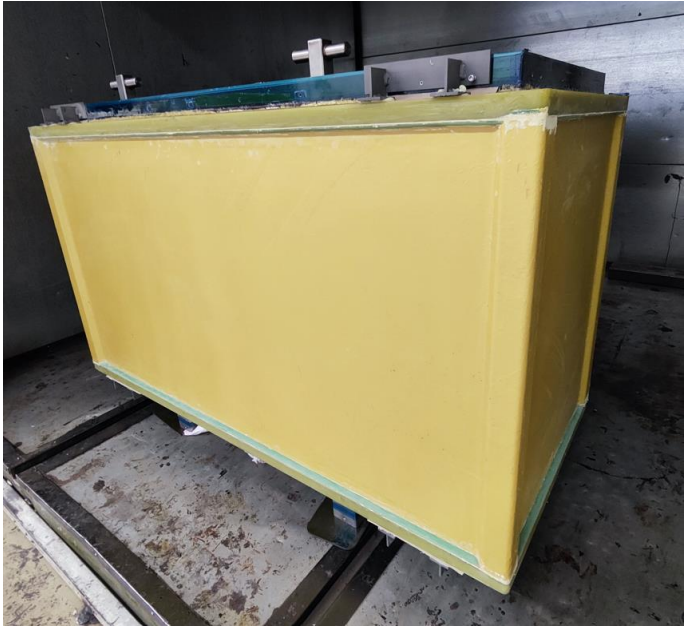
- Gluing Nomex Honeycomb
- Curing at 40C in oven



- Flipping the box top-bottom
- Resin casting on second flange
- Curing at 40C in autoclave
- Second Twaron peel lamination
- Curing at 40C in autoclave



Outer Twaron peel lamination

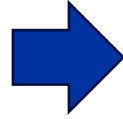


Post-curing at 40C in oven (lasting as long as possible)

Field Cage machining and final QC at Nexus

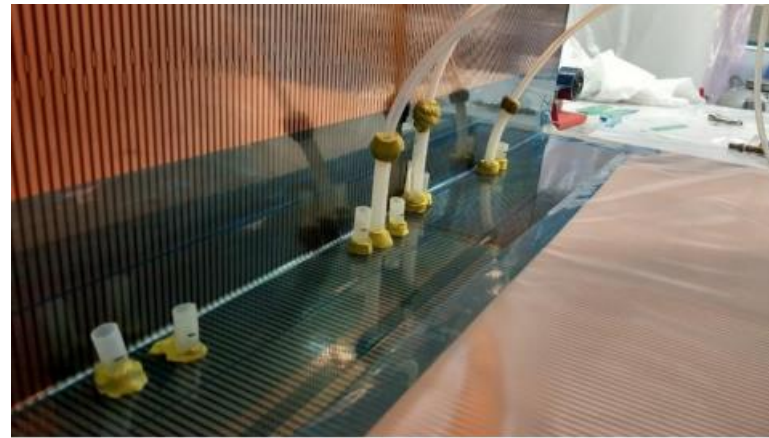


Vallmoll - Spain



Back to NEXUS company for

- Mould removal
- Very fine polishing of flanges
- Correction of defects (eg bubbles)



Shipment to CERN

Precision machining of cathode and anode flanges and surfaces finishing



The ND280 experiment: High Angle TPC highlights

- Field Cage (FC)
 - Assembly and layout
 - Production
 - Characterization and Quality Assessment
 - Mechanical
 - Electrical



- Encapsulated Resistive Anode Micromegas (ERAMS)
 - Production of 50 sensors
 - Characterization
 - Detector response, signal and impact on reconstruction

- Impact on HATPC performance

Field Cage assembling, characterization at CERN

Inner cage surfaces polishing

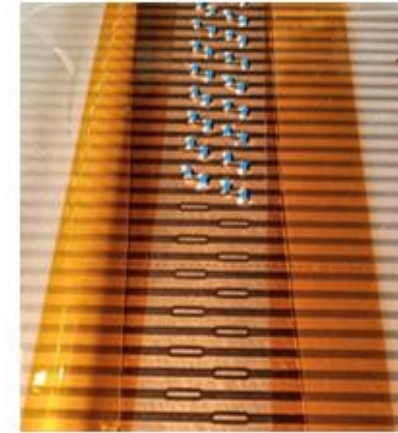


Checking grooves for o-ring and for charge labyrinth on cathode flanges

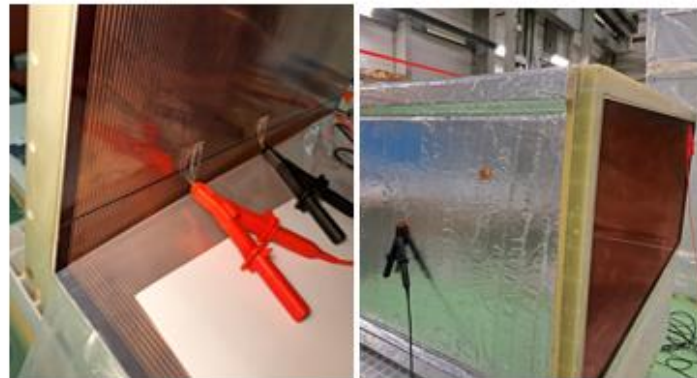
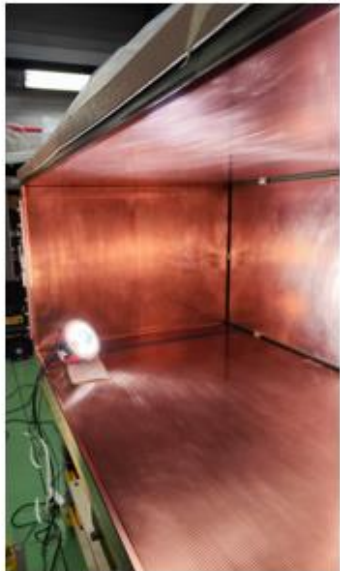
Looking for defects on strips and strip-strip short-circuits and repairing them



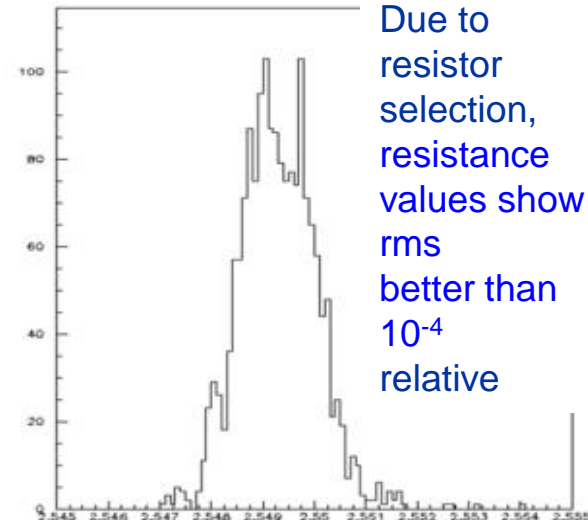
Soldering voltage divider resistors



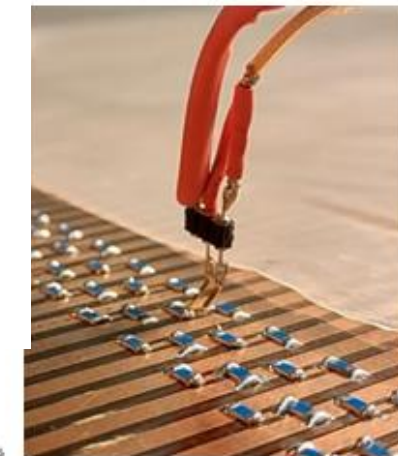
Two voltage dividers In parallel
~400 5.1M Ω resistors each:
Overall R ~ 1G Ω



Measuring strip-strip and strip-shield insulation at high voltage



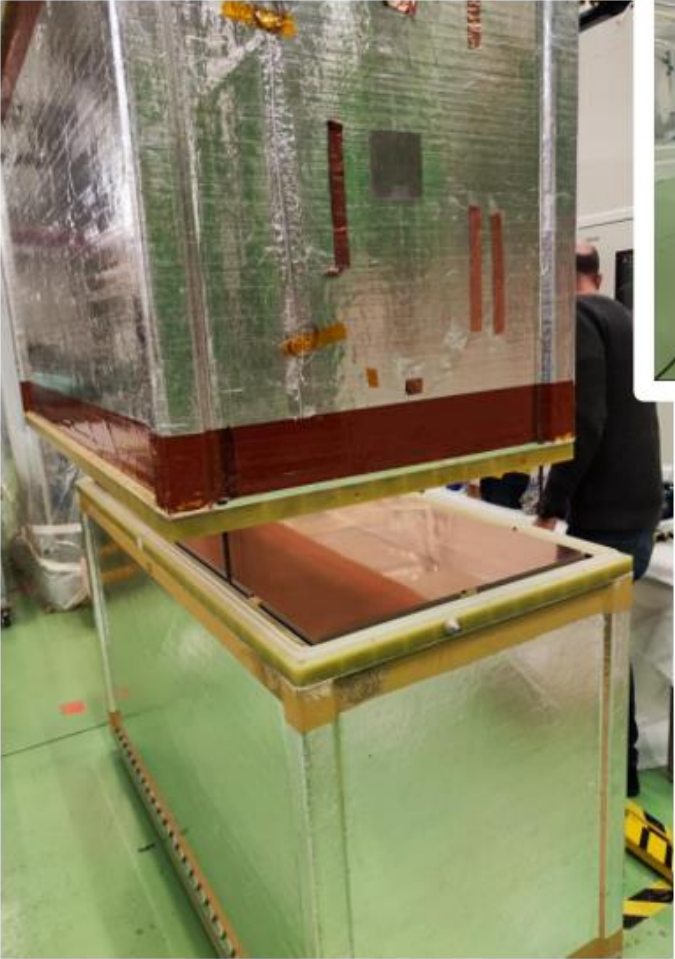
Measuring single resistors



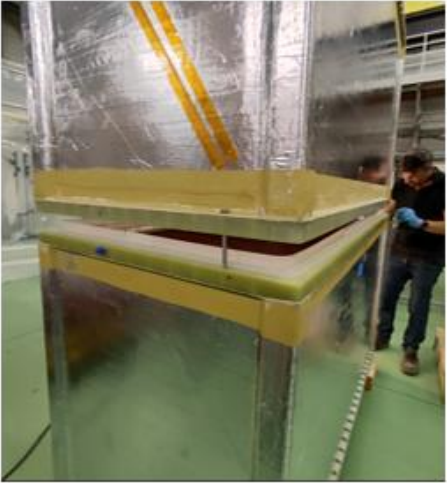
Mantle Resistance > 2T Ω ~ 2000 x voltage divider R

Field Cage assembling, characterization at CERN

Vertical assembly of two Field Cages into HATPC



Cathode assembly



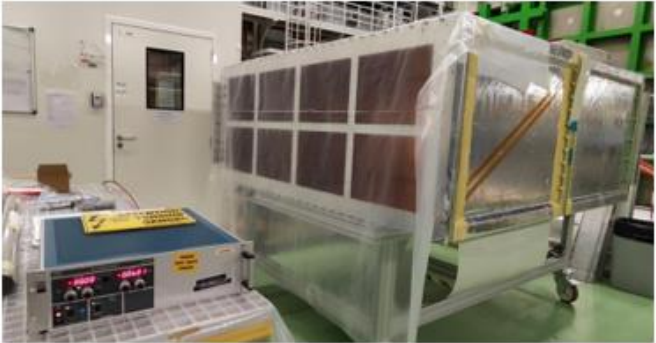
Cathode assembly



High Voltage feedthrough external connection



High voltage tests after assembly



Connection of last strips to cathode and to high voltage feedthrough

Field Cage assembling, characterization at CERN

1) He leak tested
sniffer (air + 30mbar of He)

2) Tested against gas density changes

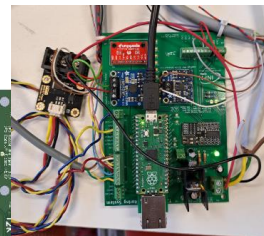
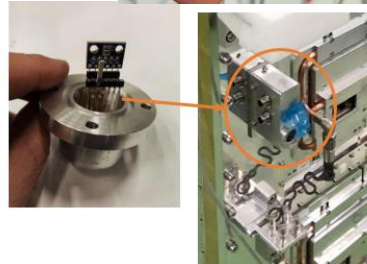
- He Over-pressure (+20mbar)
- Air Under-pressure (-20mbar)

Several T,P,RH sensors
Inside FC

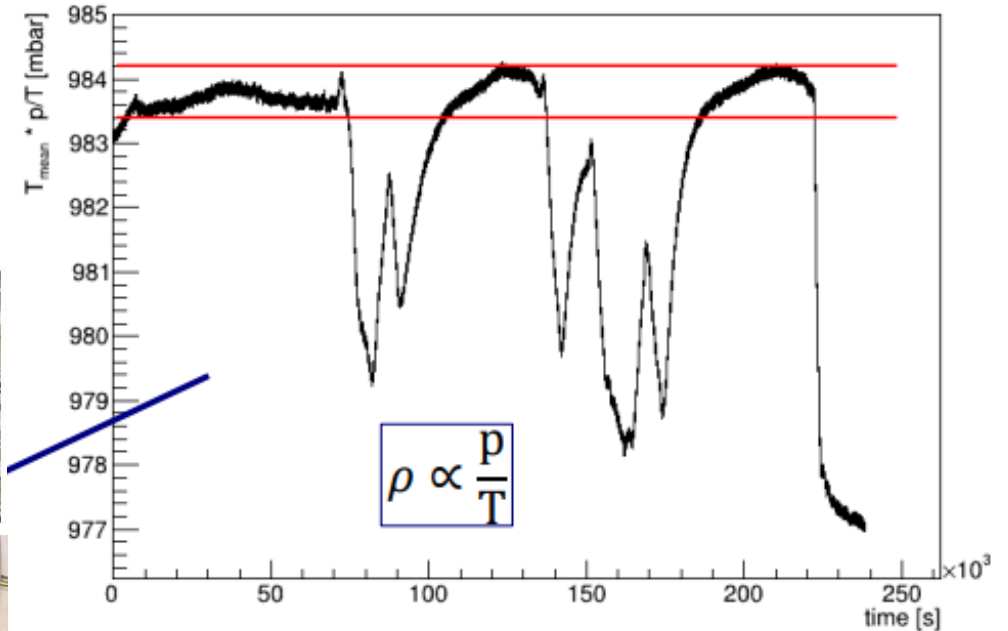
BME280 – T_{cage}, P, RH
IR sensor - T_{gas}
Thermocouple and Pt100
Voltage divider current meas.

Gas density corrected
for Volume variation (due to Pin - Pout)

$$= \frac{P_{in}(t)}{T_{in}(t)/T_{in}(0)} \left(1 - \frac{\Delta V}{V_0}\right) (P_{in} - P_{out})$$



Gas leakages qualification



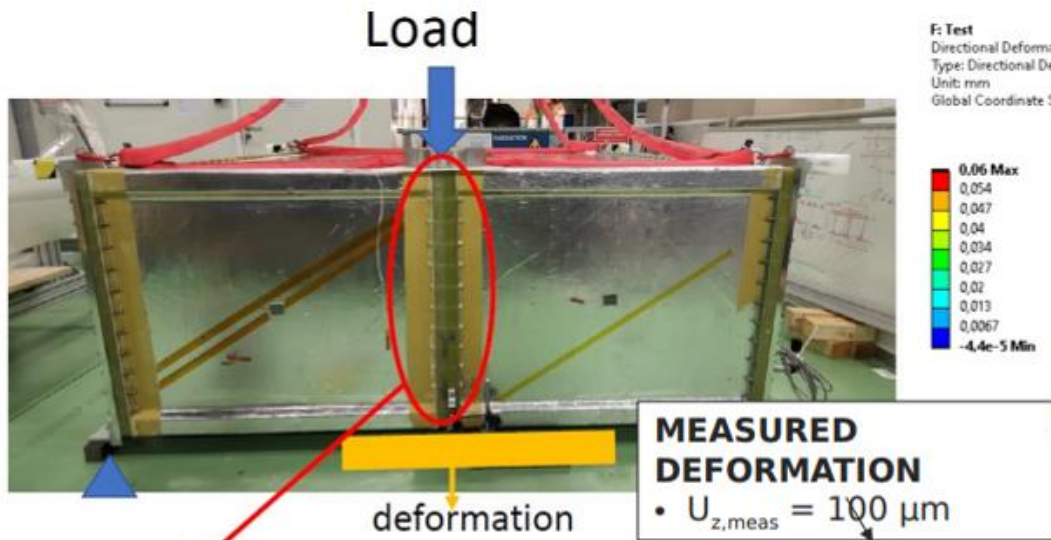
=> Overall Leak < 10⁻³ mbar L / s

Field Cage assembling, characterization at CERN

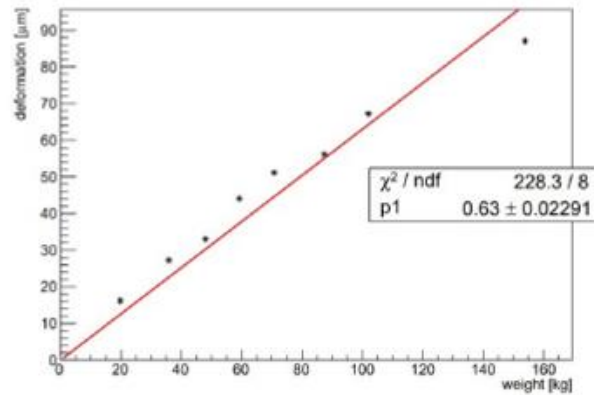
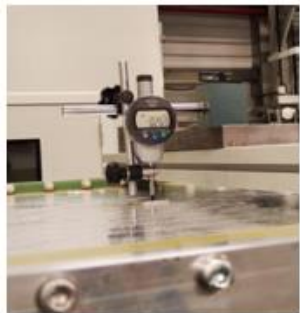
Mechanical qualification

Comparison with FEM models in fair agreement with

- load tests
- deformation vs pressure



G10 screws
(No metal near cathode)

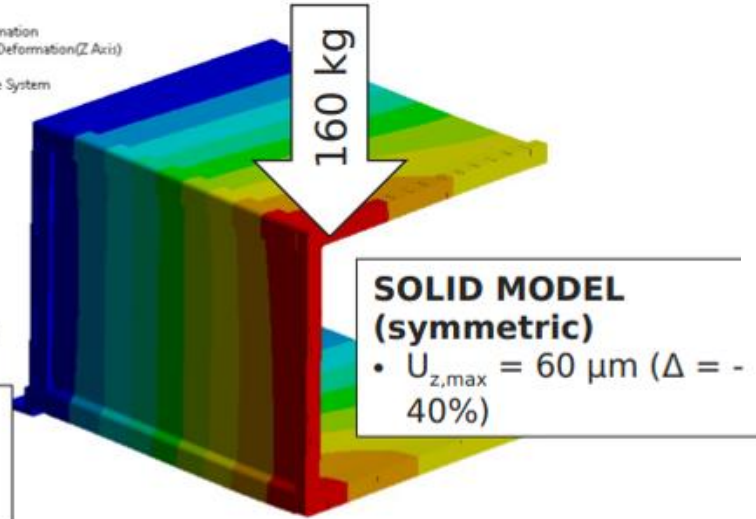


Load test performed up to 160 kg

Around $\sim 0.6 \frac{\mu\text{m}}{\text{kg}}$ of deformation w.r.t. horizontal position

F Test
Directional Deformation
Type: Directional Deformation(Z Axis)
Unit: mm
Global Coordinate System

0.06 Max
0.054
0.047
0.04
0.034
0.027
0.02
0.013
0.0067
-4.4e-5 Min

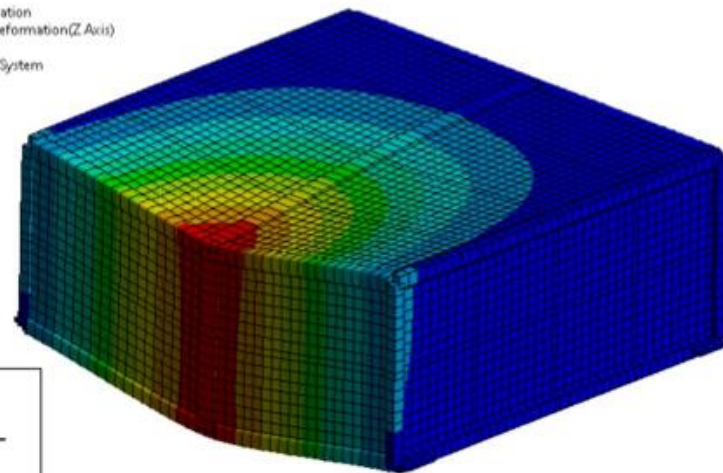


F Test
Directional Deformation
Type: Directional Deformation(Z Axis)
Unit: mm
Global Coordinate System

0.07 Max
0.061
0.052
0.044
0.035
0.026
0.018
0.0091
0.00049
-0.0081 Min

SHELL MODEL

- $U_{z,max} = 70 \mu\text{m}$ ($\Delta = -30\%$)

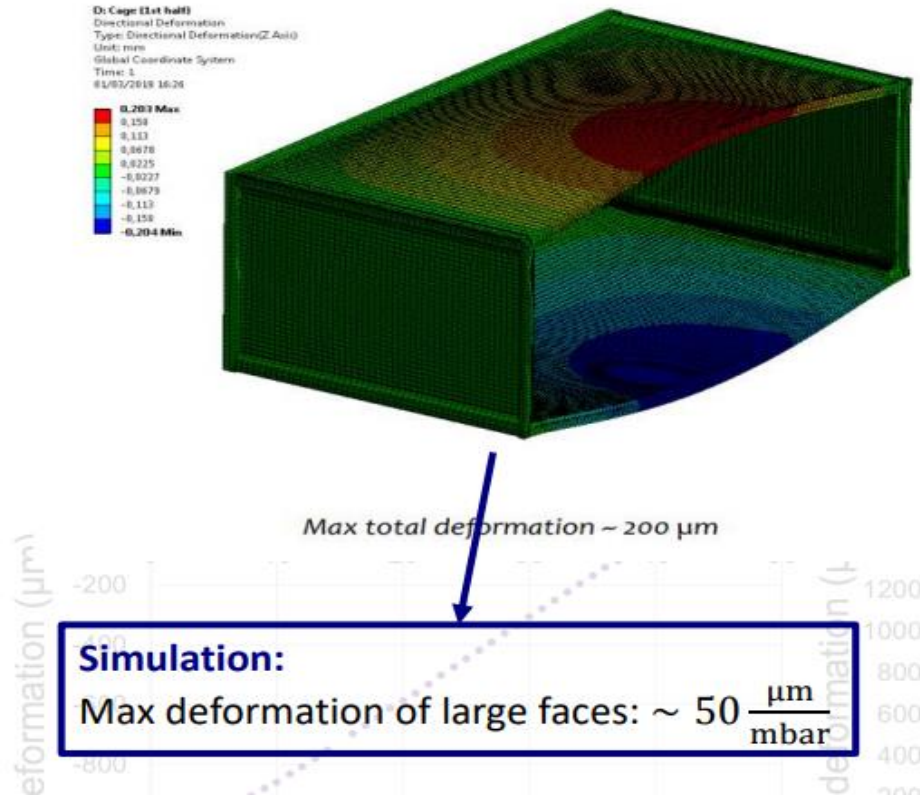


Field Cage assembling, characterization at CERN

Mechanical qualification

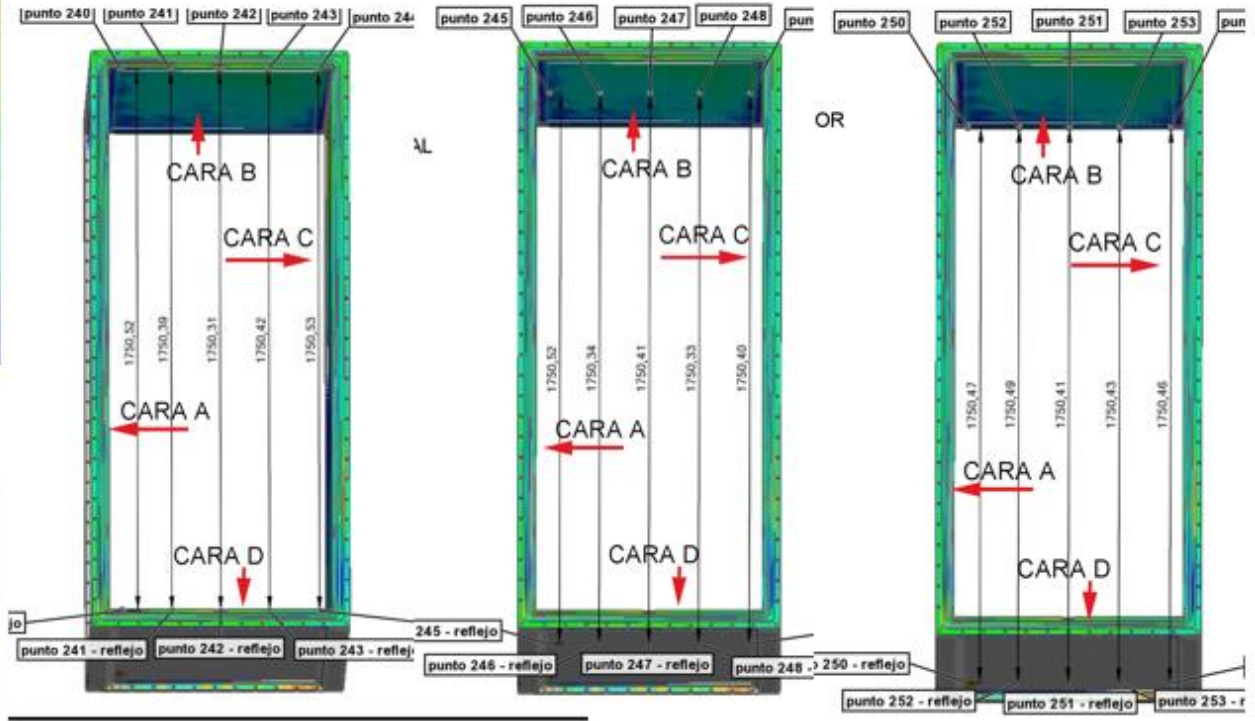
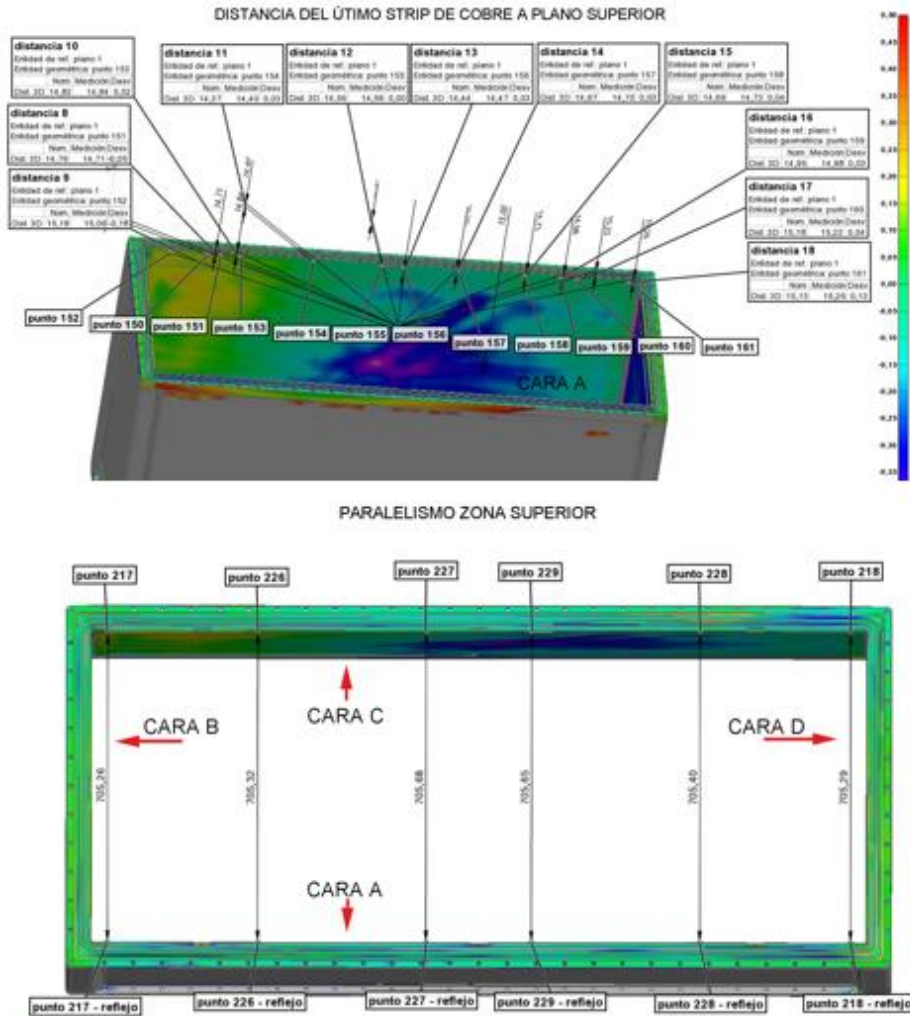
Comparison with FEM models in fair agreement with

- load tests
- deformation vs pressure



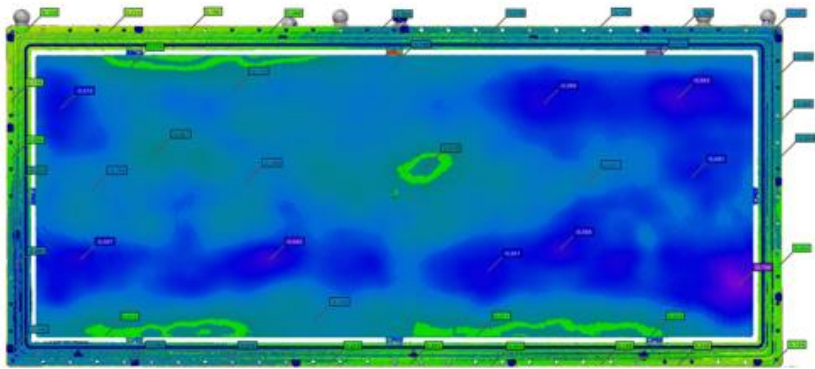
Field Cage assembling, metrology at Nexus

Tolerances and specifications at a level better than $300\mu\text{m/m}$ for planes parallelism and orthogonality and better than ISO1302-N8 for waviness are respected with few localized acceptable exceptions

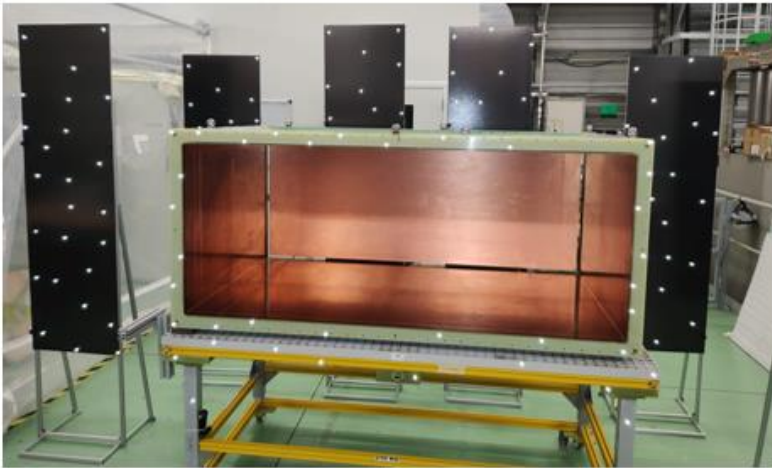
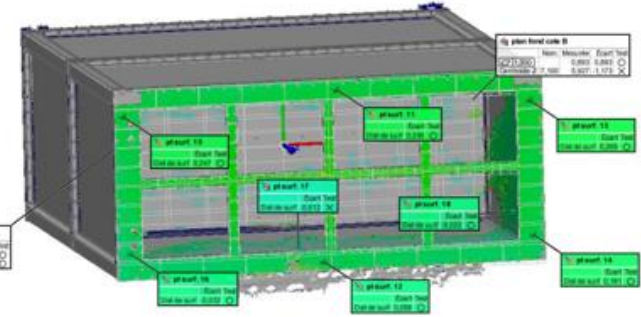
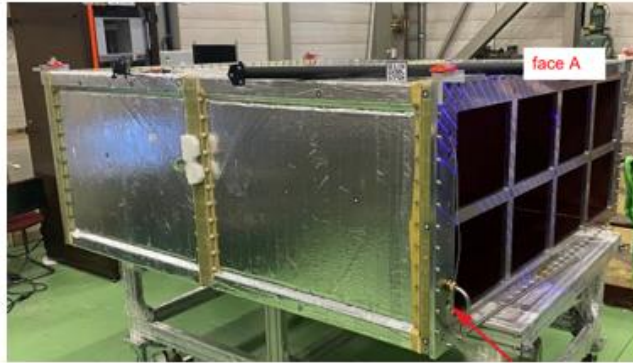


Reached limits of composite material technique
Large dimensions and hand lay-up

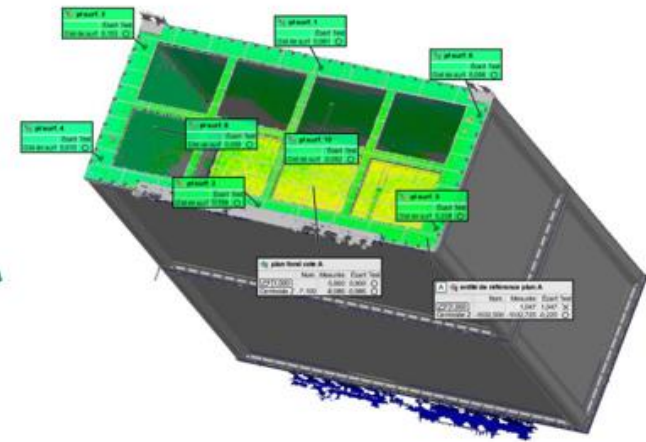
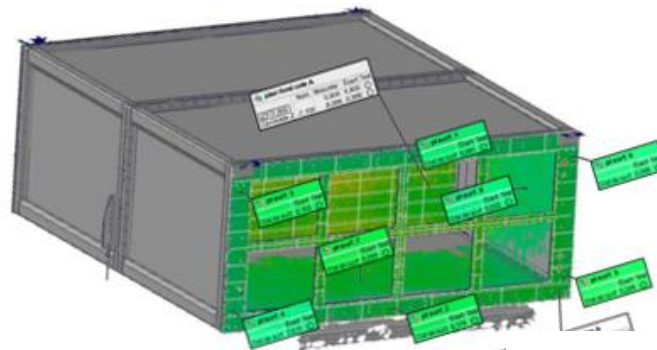
Field Cage assembling, metrology at CERN



Metrology at CERN Top-HATPC
(2024, single whole TPC 3D metrology)



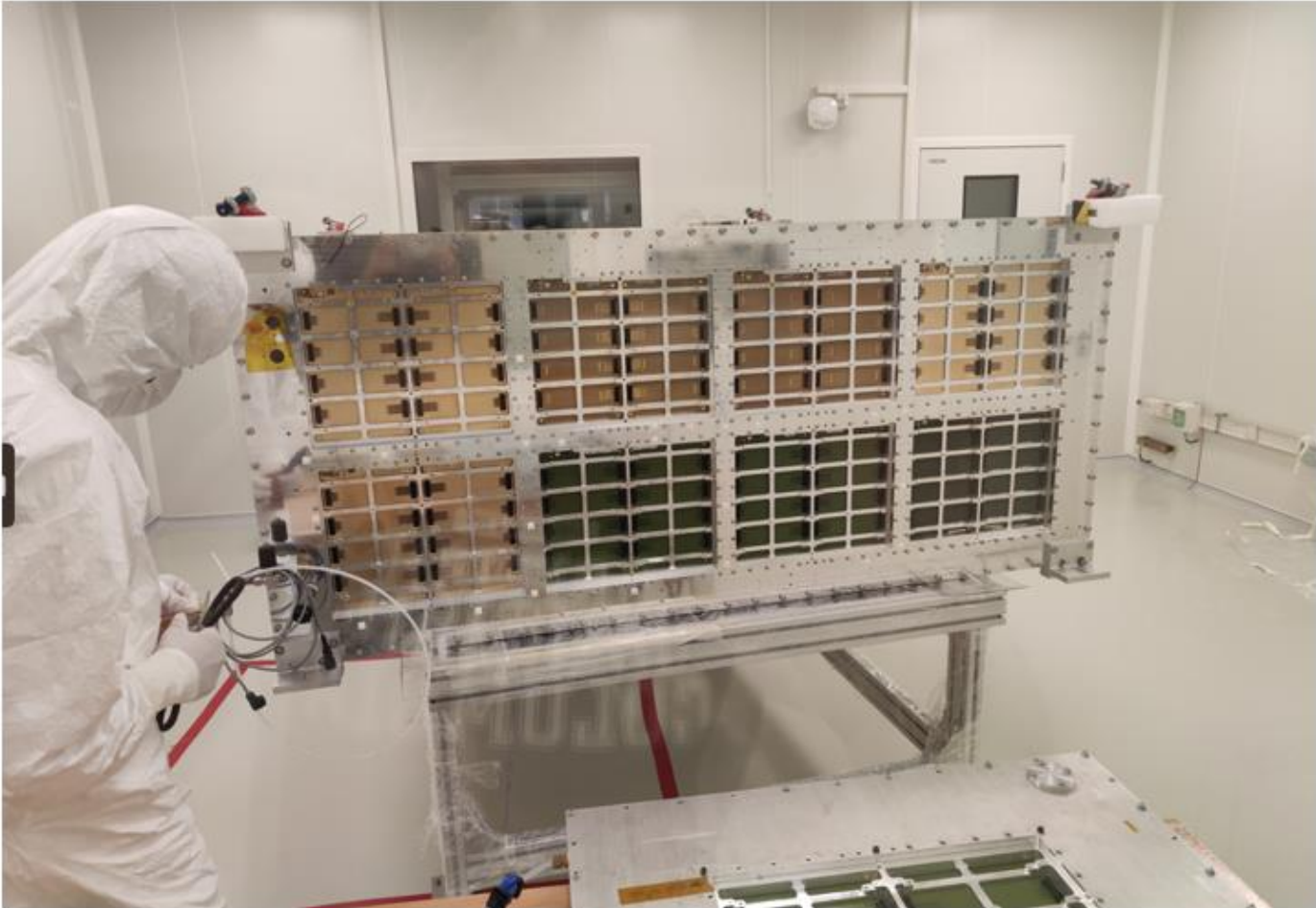
Metrology at CERN Bottom-HATPC (2023)
(Two separate cages and cathode)



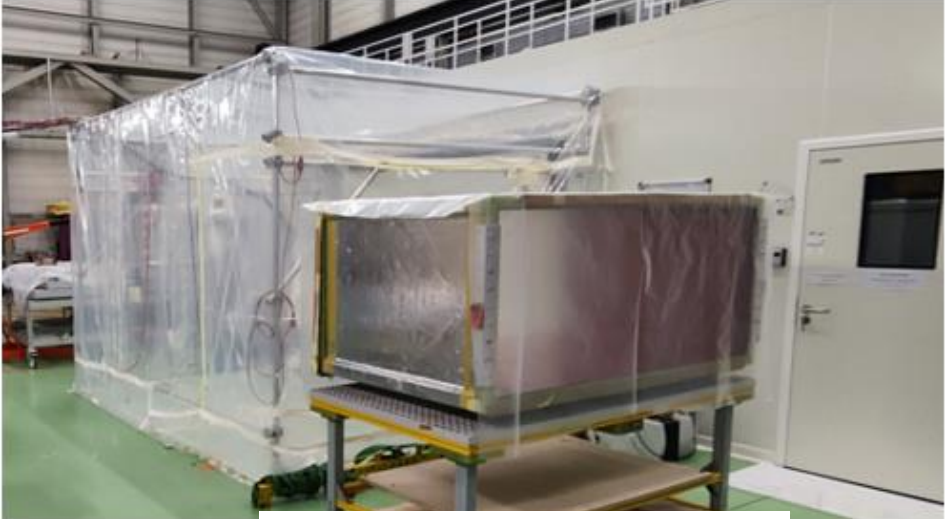
Measured internal geometry after assembly agrees with nominal CAD with pull better than 300 μ m with few localized, acceptable exceptions

Field Cage assembling, ERAM installation

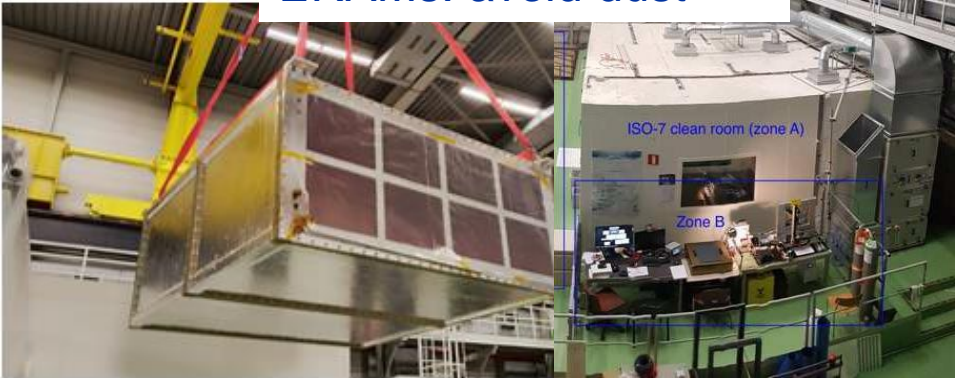
Assembly the 16 ERAMs in Clean room for each TPC



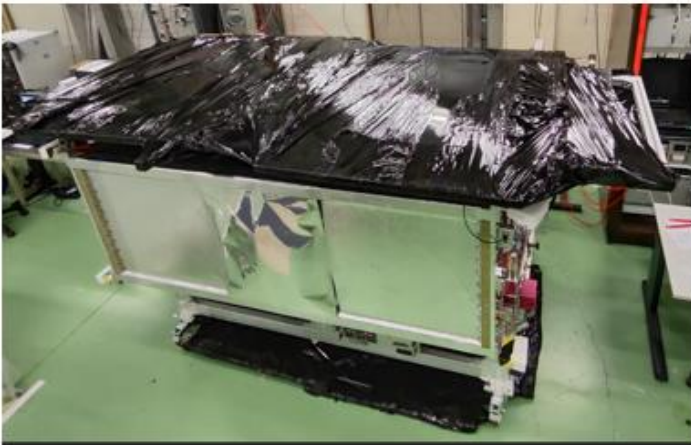
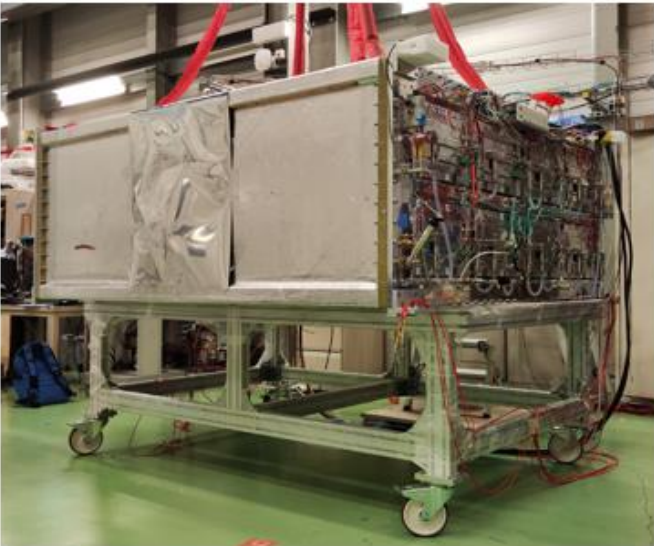
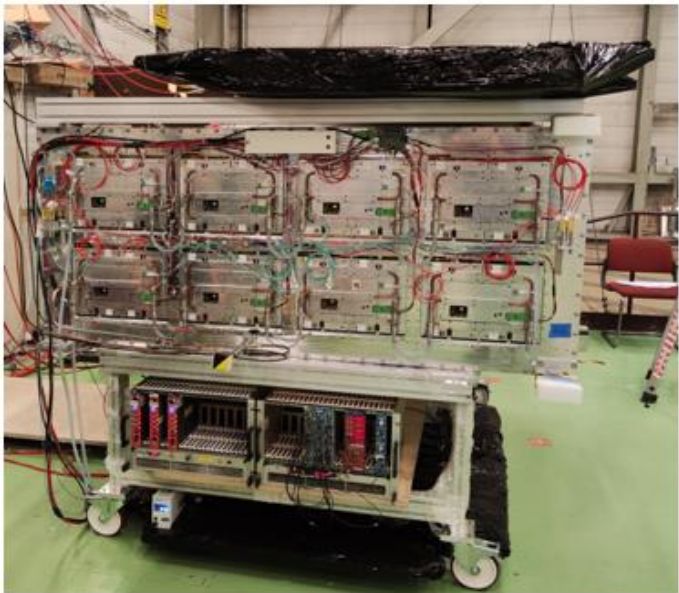
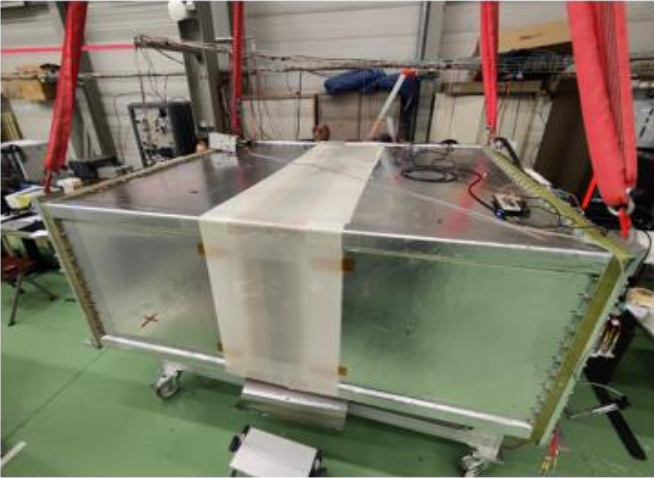
Grey tent area in front of Clean Room large entrance for enhanced clean conditions



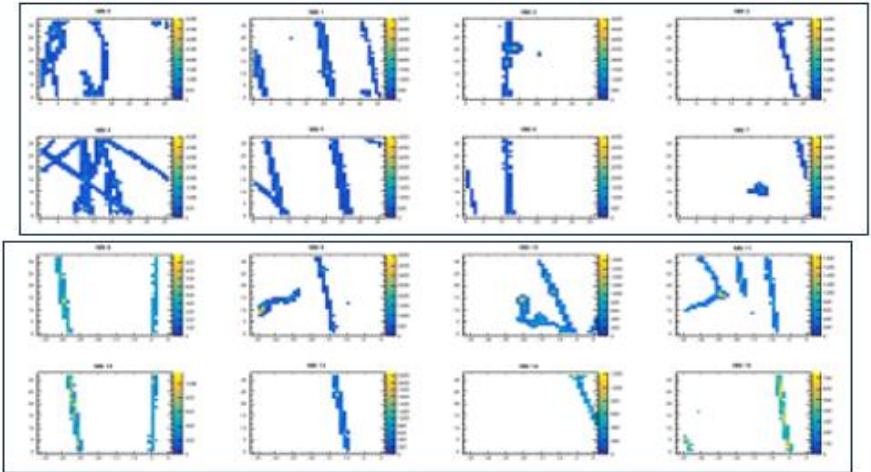
ERAMs: avoid dust



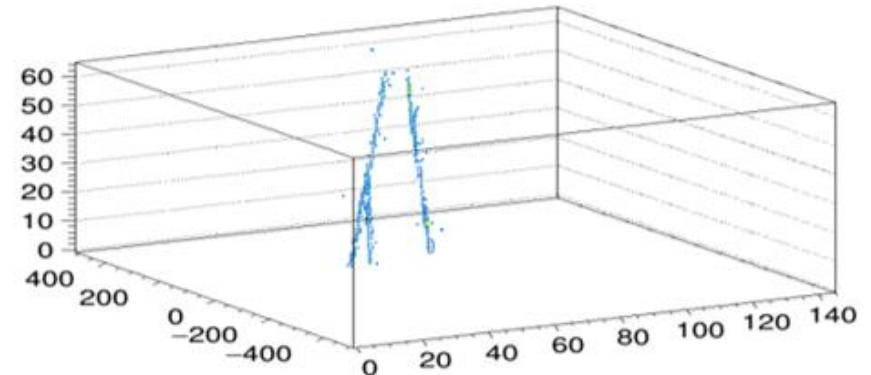
Field Cage assembling, commissioning with cosmics



Cosmic shower ewnt Projection on Anode End Plate 2

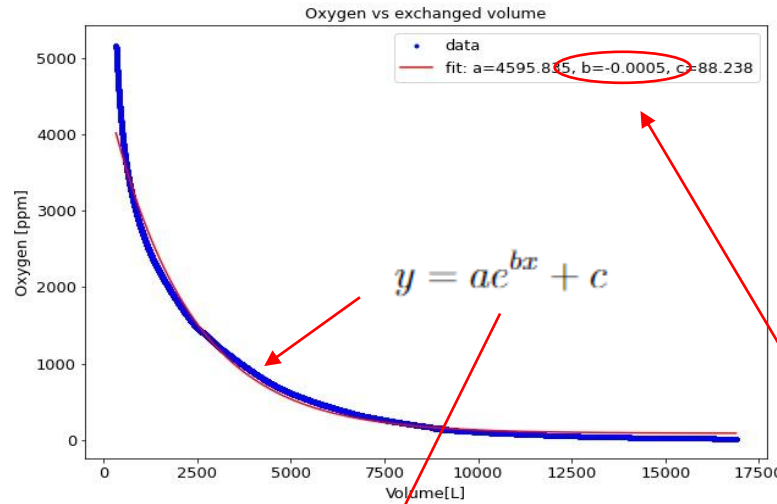
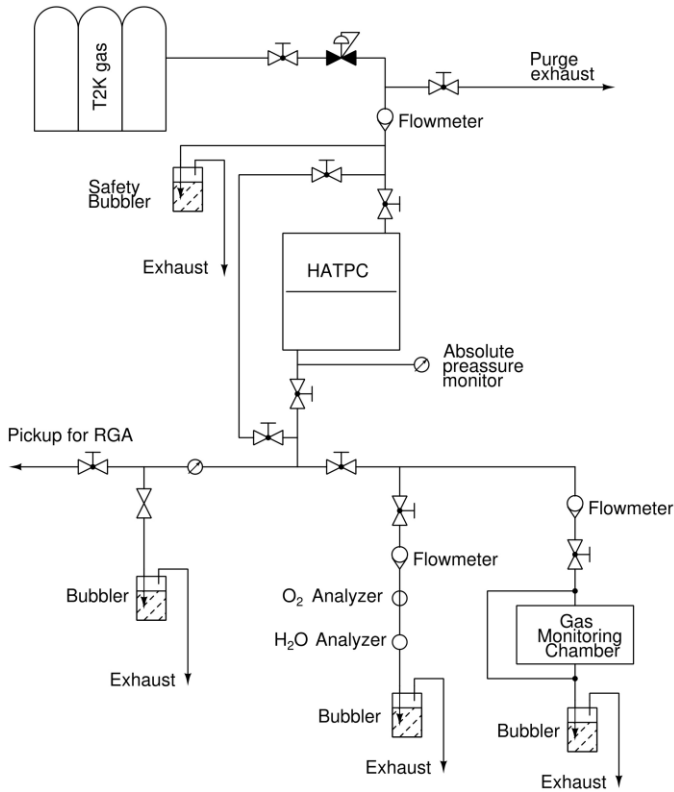


Projection on Anode End Plate 1



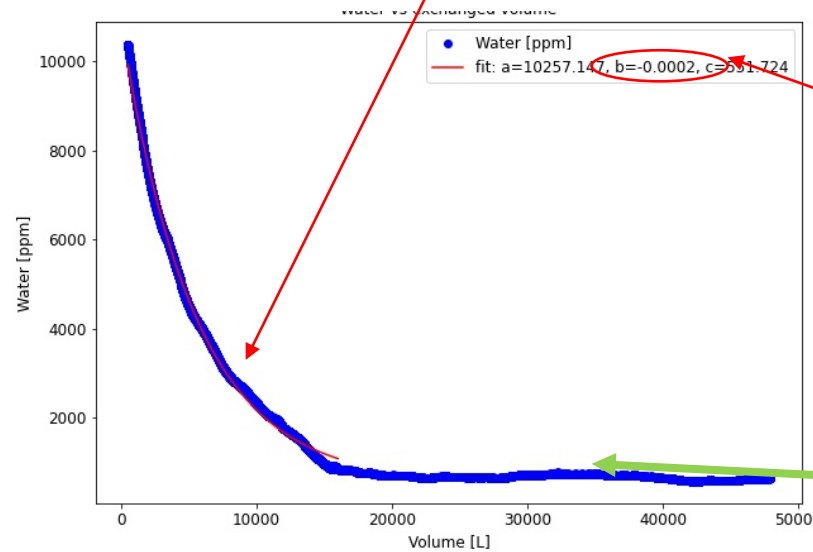
Cosmic tracks interaction ewnt

Field Cage assembling, commissioning: gas contamination at CERN



Water and Oxygen contamination evolution

Large amount of water uptake by Kapton: 2% in mass, with respect to dry Kapton, ~ about 70 g → purging time ~ a couple of months



Different dragging coefficient ? Under investigation

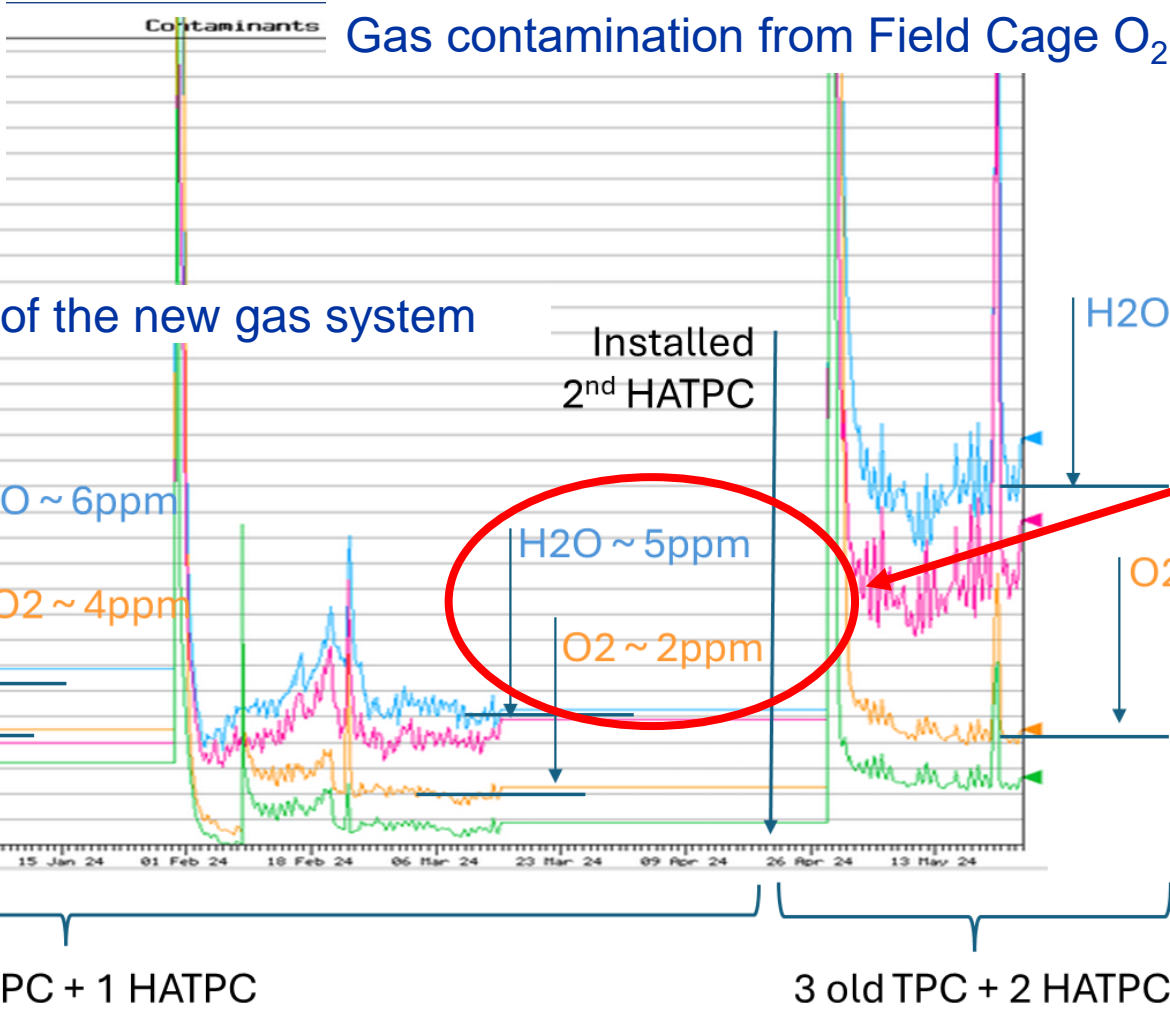
$$\frac{dc(t)}{dt} + \frac{f}{V}c(t) = \delta$$

δ water desorption from walls → 0.06 g/day water removal / desorption (long)

Field Cage assembling, commissioning: gas contamination at J-PARC

New gas system (CERN)
 Overall recirculation
 flow ~ 500 l/h per TPC with
 overall few % fresh gas injection

Gas contamination from Field Cage O₂ and H₂O

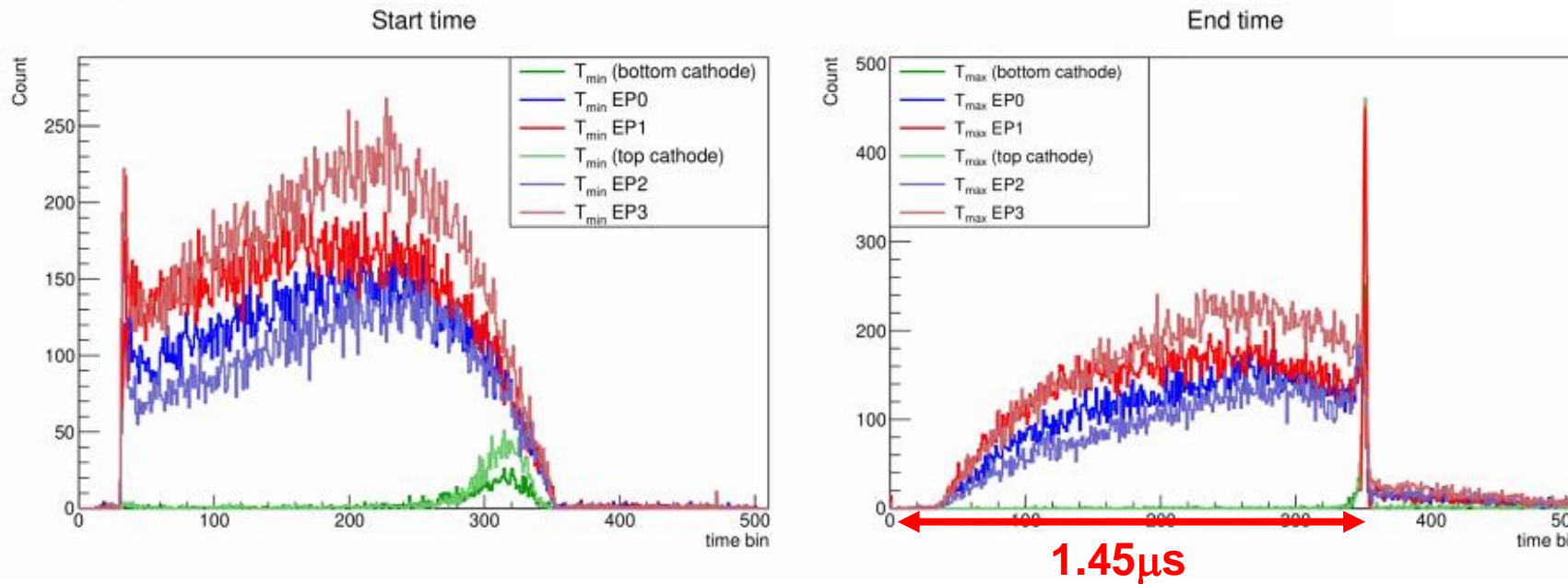


Excellent Performance of the new gas system

Typical operational values

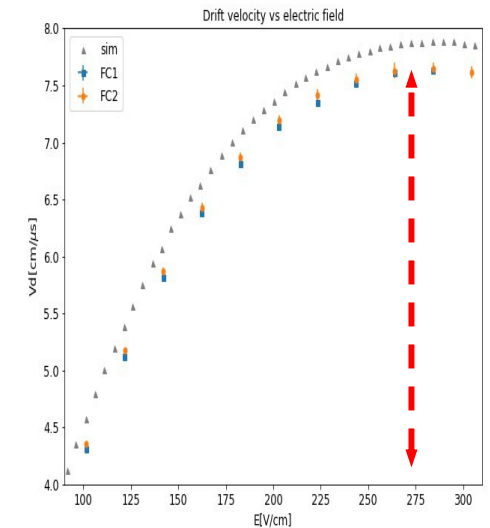
Field Cage assembling, commissioning: drift velocity measurement

Drift velocity



Perfect agreement with expectations (Magboltz)

Gas contamination H₂O ~ 10 ppm H₂O @ J-PARC All TPCs
 Drift velocity in bottom HATPC: 7.769 ± 0.005 cm/μs
 Drift velocity in top HATPC: 7.772 ± 0.005 cm/μs



Gas contamination from Field Cage – O₂ and H₂O included
 500 ppm H₂O @ CERN Bottom TPC

The ND280 experiment: High Angle TPC highlights

- Field Cage (FC)
 - Assembly and layout
 - Production
 - Characterization and Quality Assessment
 - Mechanical
 - Electrical

**An outsider: Field Cage 0 ?
Electrical Issues, what we understood...
and learnt**

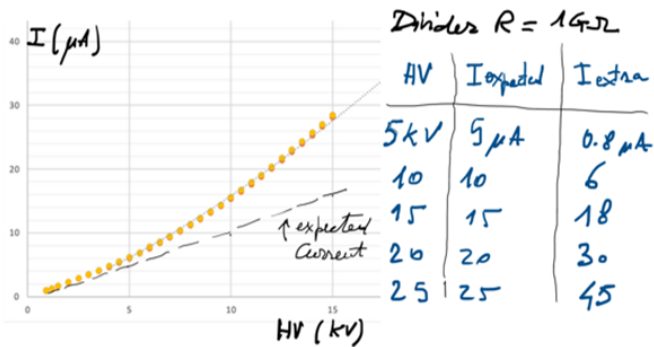
Insulation issue in full scale FC0 prototype

Innermost layers stack (first full-scale FC prototype)

Material	Thickness
Cu Strips on Kapton foil (electrodes)	Cu 17 μ m / Kapton 50 μ m / Cu 17 μ m
“Coverlay” (strip insulation / protection)	Glue 20 μ m / Kapton 25 μ m
Aramid Fiber Fabric (Twaron™)	2mm

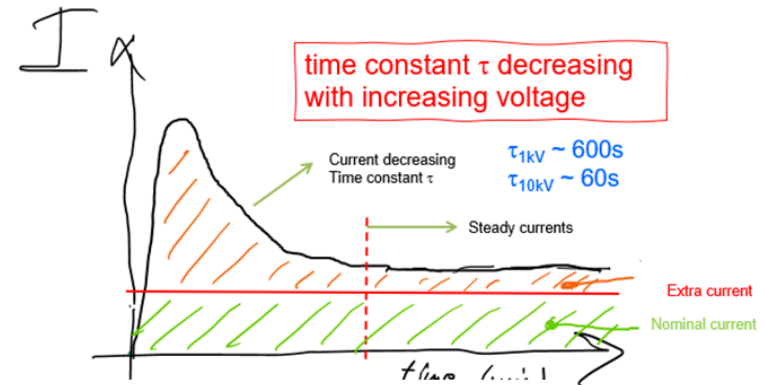


Current drawn by voltage divider starting in large excess wrt nominal at power on and slowly decreasing to lower value but still in excess



I_{extra} increasing non linearly with voltage

Current drawn by voltage divider starting in large excess wrt nominal at power on and slowly decreasing to lower value but still in excess



Observed extra-currents in excess w. r. t. expected from voltage divider

Insulation issue in full scale FC0 prototype

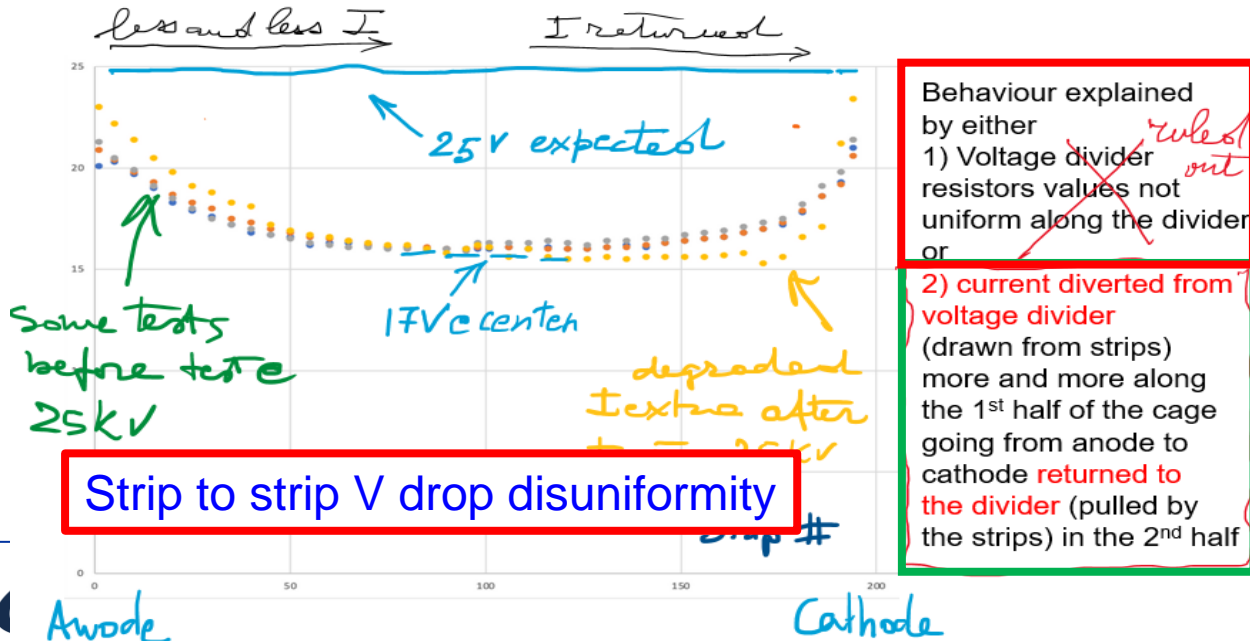
Innermost layers stack (first full-scale FC prototype)

Material	Thickness
Cu Strips on Kapton foil (electrodes)	Cu 17 μ m / Kapton 50 μ m / Cu 17 μ m
"Coverlay" (strip insulation / protection)	Glue 20 μ m / Kapton 25 μ m
Aramid Fiber Fabric (Twaron™)	2mm

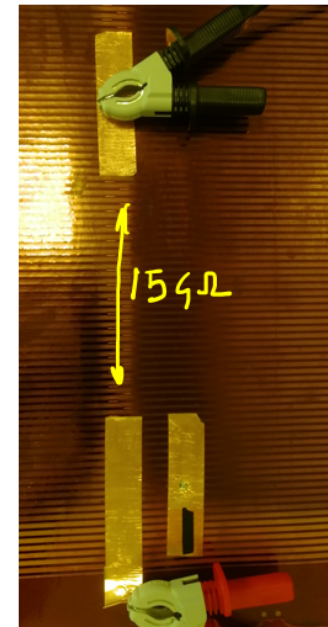


Strip-Strip Potential difference of the strips @ 5kV

Voltage difference between Field strips (every 5 strips)
ie $V_1-V_2, V_5-V_6, V_{10}-V_{11}, \dots$ $V_1 = \text{anode}, V_{196} = \text{cathode}$



Measurement of Surface resistance of strip foil (resistors removed)



Resistance between single strips is very high $O(T\Omega)$
...but when joining some tens of strips to form a single large electrode then finite resistances are measured

Example: measured $R \sim 15 \text{ G}\Omega$ @ 1kV between two electrodes formed by 20Field+20Mirror strips each (surface of single electrode is huge $\sim 0.5\text{m}^2$)
! No voltage divider there, ie all strips disconnected

Resistance is

- Independent of the distance between electrodes
- Linearly dependent of the number of the strips
- not a surface resistance !

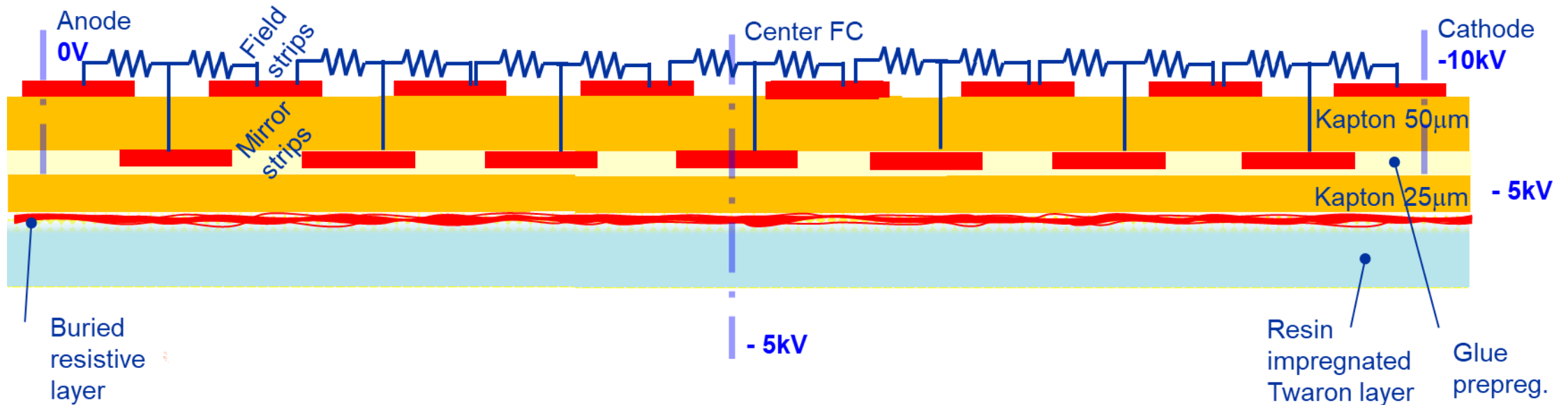
Measured R is rising with time (slow) up to saturation
- when repeating measurement, go faster to saturation
- when inverting polarity of electrodes, slow again
→ looks like due to dielectric polarization / relaxation
→ or capacitor charging trough high resistance

Find similar value of Resistance for same dimension electrodes formed in the Field Cage and on a strips foil when aluminum foil is placed underneath the foil → next

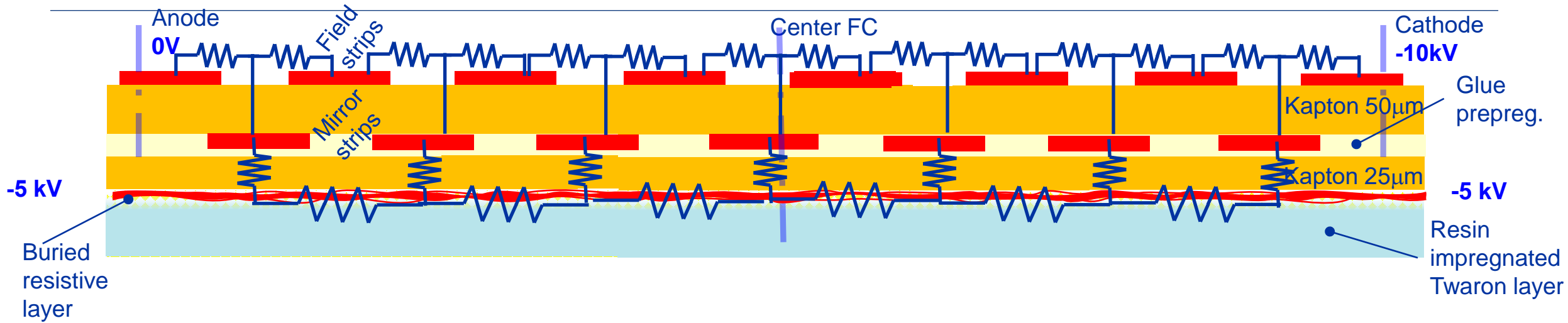
Buried resistive layer: a possible explanation

All observed features could be explained by the combination of two factors:

- 1) Presence of a resistive layer buried underneath the Kapton coverlay layer protecting the mirror strip
- 2) Low resistivity of the coverlay Kapton layer



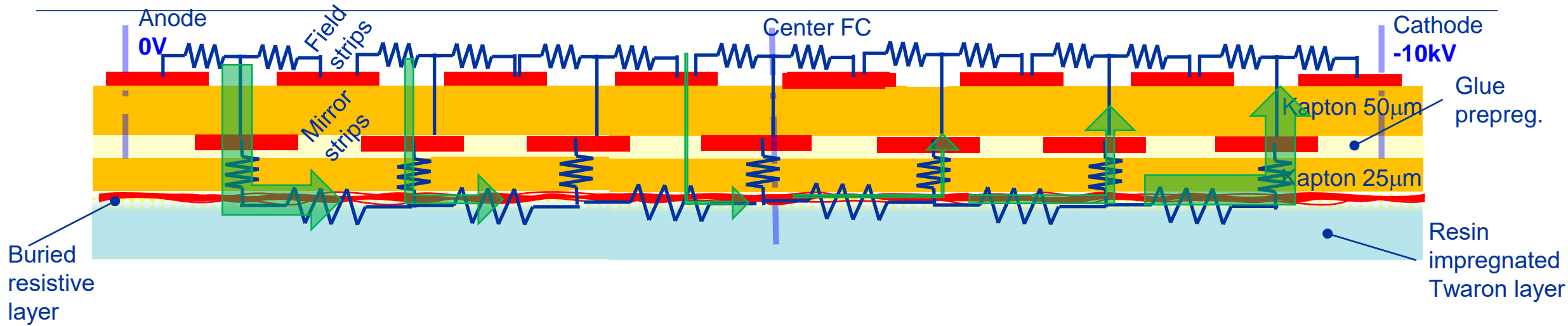
Buried resistive layer: phenomenology



After applying HV after applying HV (eg -10kV) to the cathode, two phases:

- 1) Transient state:** in time scale depending on the contaminated layers resistivity (in our case very short $O(10s)$ time scale) the buried resistive layer become ~ equipotential (setting at intermediate potential -5kV) by **drawing charge from the strips**
- 2) Steady state:** Mirror strips on the Anode, first half convey current to the buried layer, while mirror strips on the Cathode side draw currents from the buried layer

Buried resistive layer: phenomenology



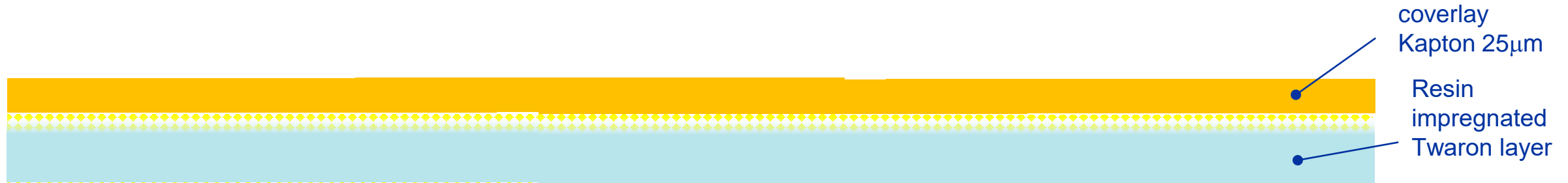
After applying HV after applying HV (eg -10kV) to the cathode, two phases:

- 1) Transient state:** in time scale depending on the contaminated layers resistivity (in our case very short $O(10s)$ time scale) the buried resistive layer become \sim equipotential (setting at intermediate potential -5kV) by **drawing charge from the strips**
- 2) Steady state:** Mirror strips on the Anode, first half convey current to the buried layer, while mirror strips on the Cathode side draw currents from the buried layer

Buried resistive layer: verification

In fact we **verified** the following

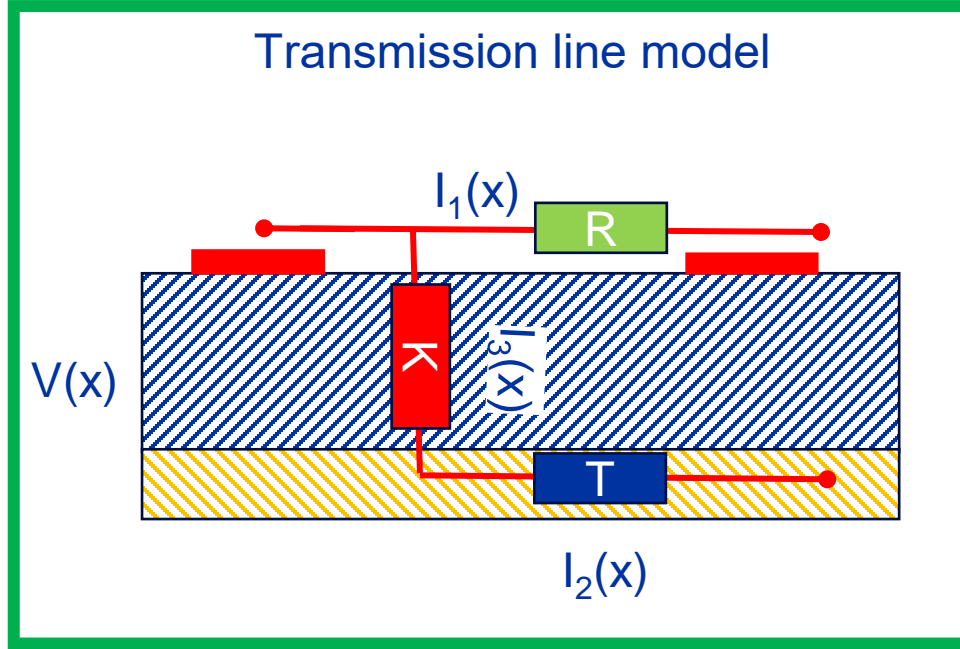
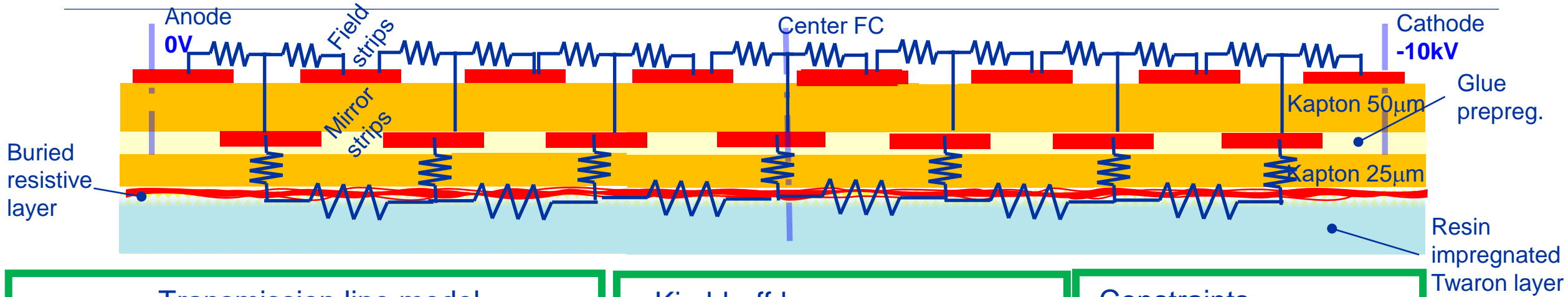
- 1) Coverlay Kapton volume resistivity $\sim 1\text{G}\Omega\text{cm}$ much lower than datasheet)
- 2) Twaron layer facing the coverlay featured **surface resistivity $\sim 1\text{G}/\square$**



Both features could on turn be explained by the **accidental use of antistatic spray (resistive)** on the back of the strip foil (ie on the coverlay) after the strip foil was fixed on the Mould, in order to keep the huge foil surface (5m^2) clean from dust and other possible contaminants. The **spray contaminated both the Kapton coverlay** (being very easily adsorbed) and the **innermost layer of the Twaron** (being mixed with the resin which impregnates the fiber fabric, during the Twaron lamination phase)

We could not exclude alternative sources of **contamination affecting the resin** and making it resistive (eg presence of water if epoxy not treated in vacuum after mixing)

Buried resistive layer: electrical model



Kirchhoff law

$[K]=\Omega m, [T]=\Omega/\square, [R]=\Omega$

$$T \frac{dI_3(x)}{dx} + RI_1(x) - KI_2(x) = 0$$

$$\frac{dI_1(x)}{dx} + I_3(x) = 0$$

$$\frac{dI_2(x)}{dx} - I_3(x) = 0$$

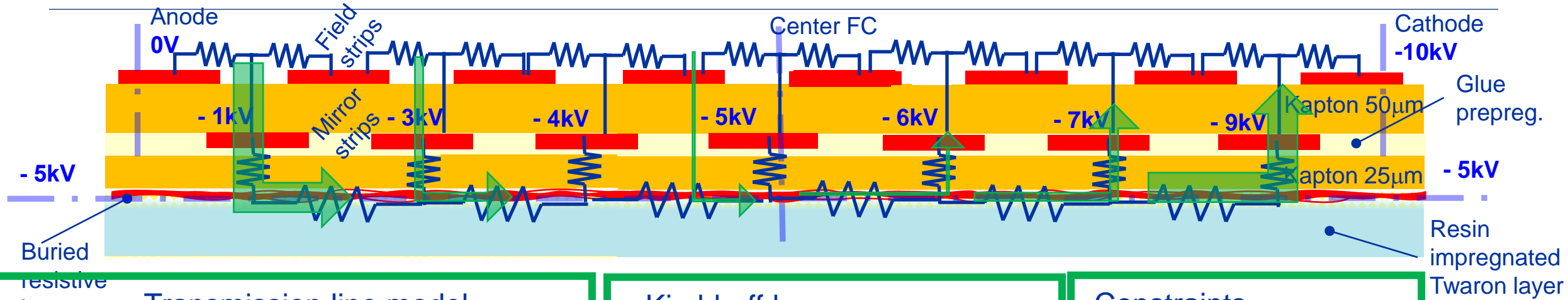
Constraints

$$I_1(0) + I_3(0) = I_1(L) - I_3(L)$$

$$I_2(0) = I_3(0) \quad I_2(L) = -I_3(L)$$

Symmetry $\frac{dI_3(x=L/2)}{dx} = 0$
(middle of the cage)

Buried resistive layer: electrical model results



Transmission line model

Kirchhoff law

Constraints

The electric field in the active volume is non uniform

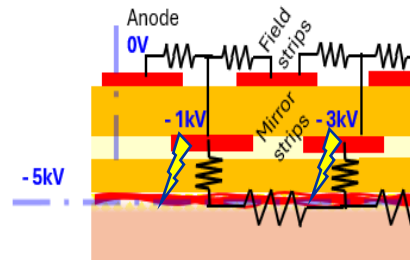
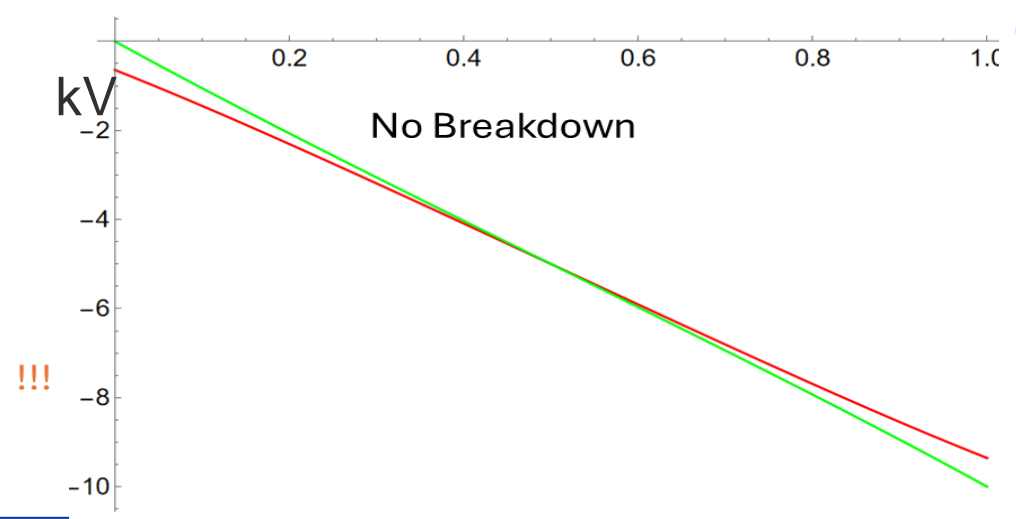
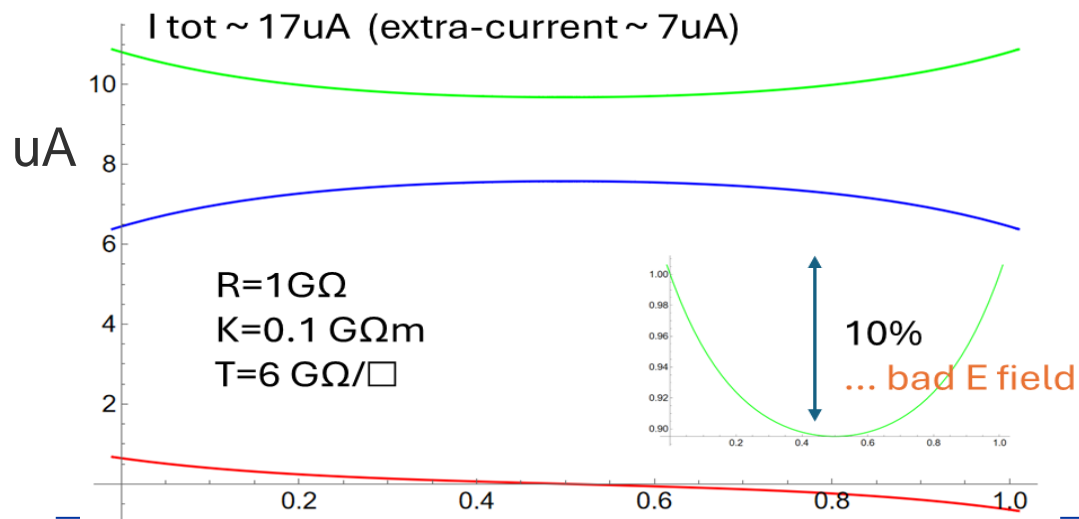
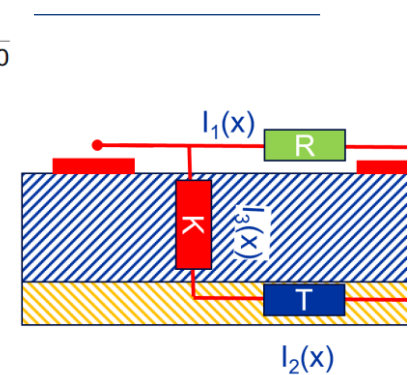
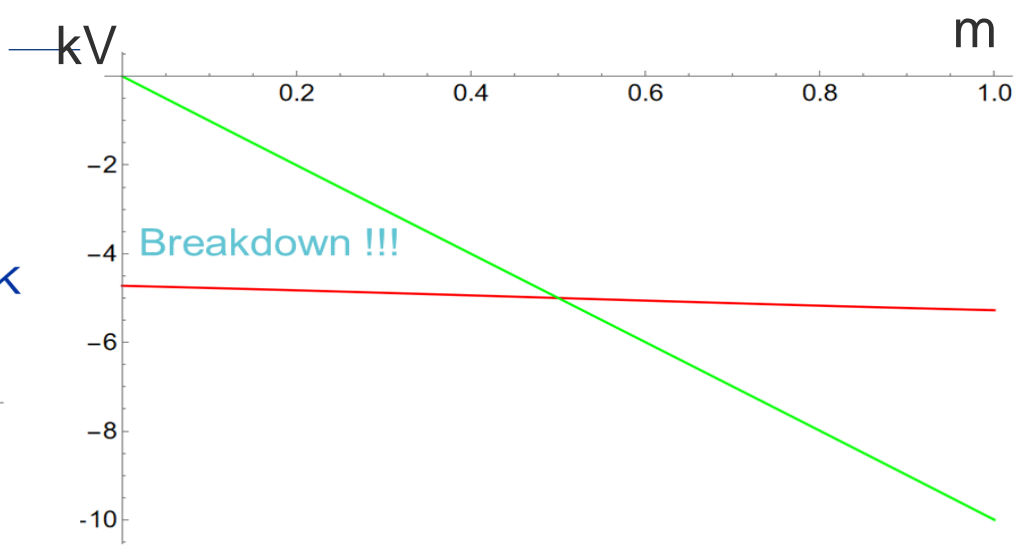
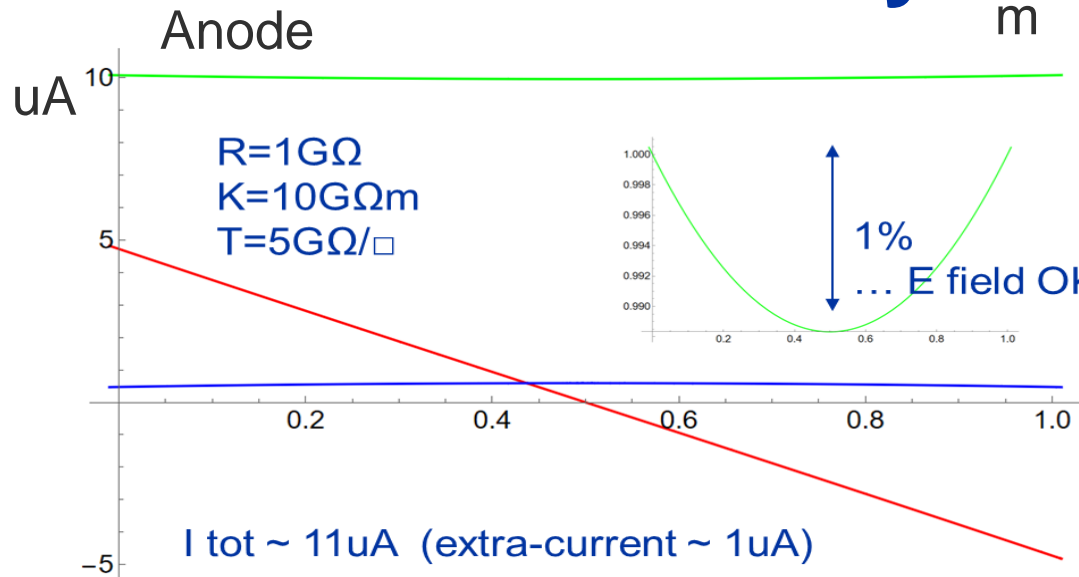
Due to the spurious voltage divider formed in parallel to the regular one

$V(x)$

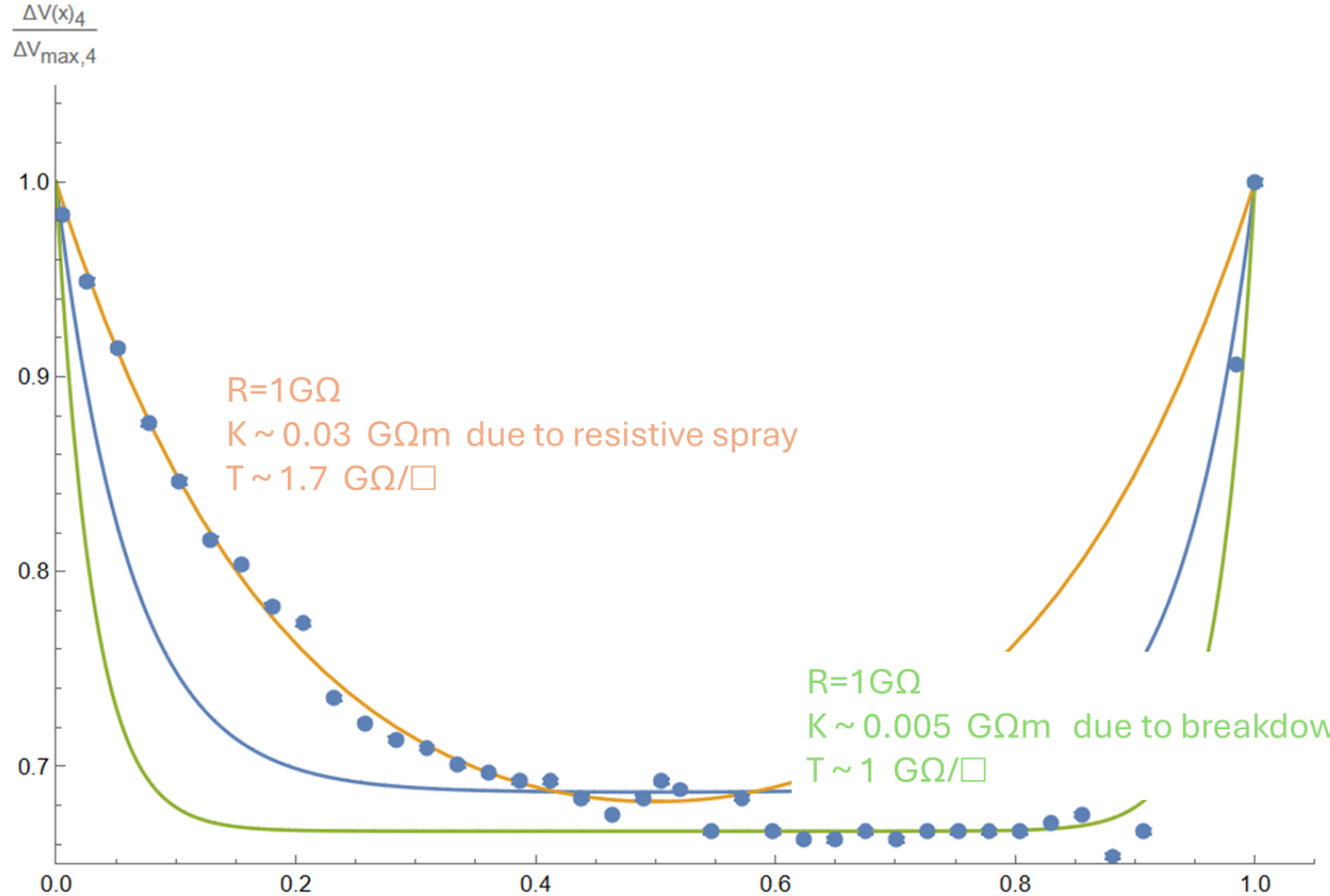
$V(x)$

dx

Buried resistive layer: electrical model results

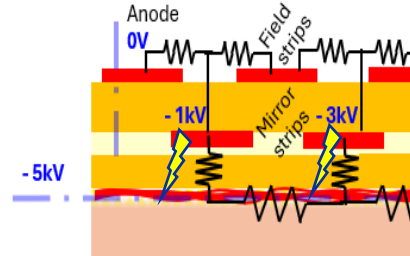
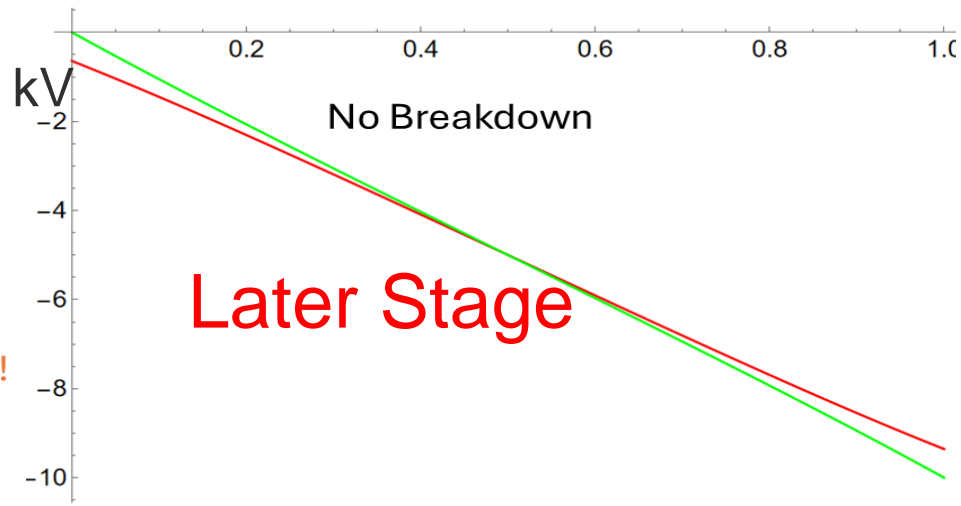
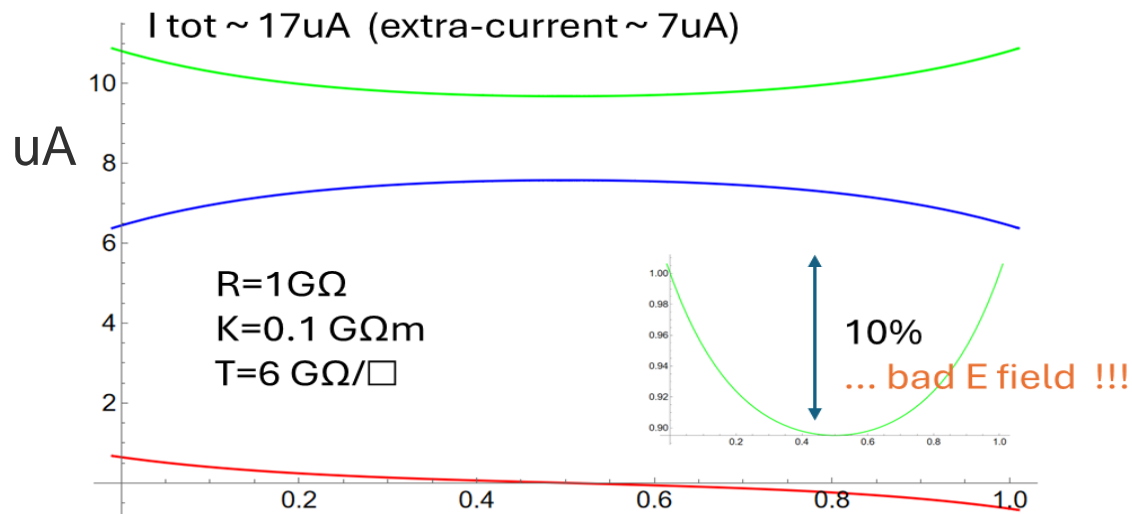
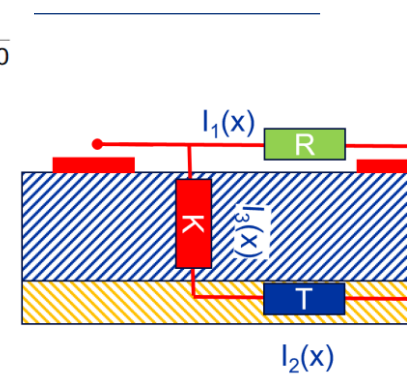
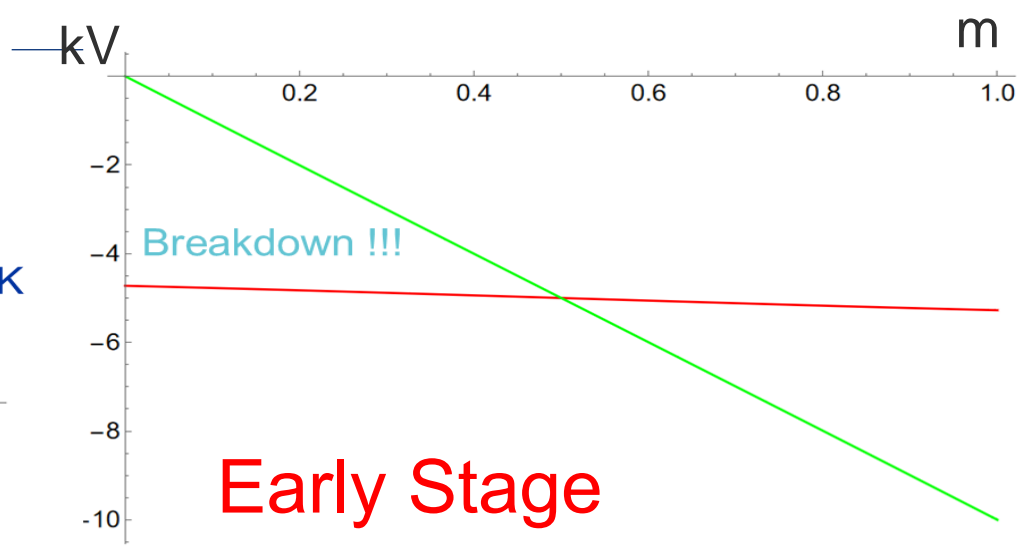
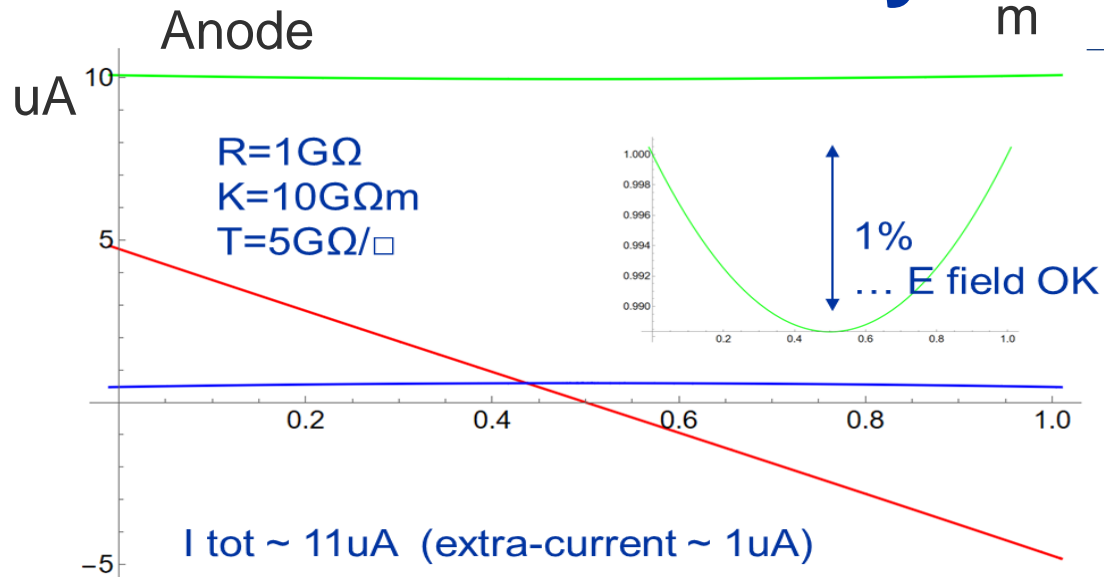


Buried resistive layer: fit to the data



25 μm Kapton
 Breakdown observed
 at values much lower
 than datasheet

Buried resistive layer: electrical model results



Final layout, materials and procedures fixed for the series production

Key points to avoid failures

- **no resin contamination !!!** Note: usually glues and resins are the weakest points
- Interpose between strips and Twaron layers a **“thick” layer of insulator** featuring
 - High resistivity $\rho_v > 10^{15} \Omega\text{cm}$
 - Dielectric strength $> 150\text{kV/mm}$

Final layout of the stack: **minimal changes to design**

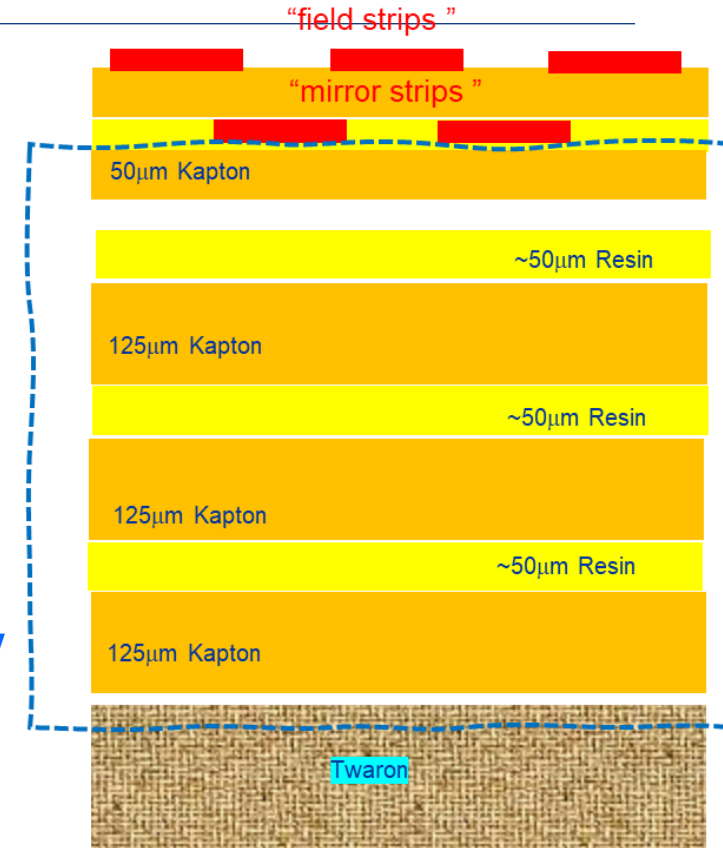
- new strip foil w/ thicker Kapton coverlay $50\mu\text{m} + 25\mu\text{m}$ glue (produced at CERN, gluing in vacuum with press)
- 3 layers of Kapton: $125\mu\text{m} + 50\mu\text{m}$ resin each (to be laminated on the back of strip foil on the mold)

thickness Kapton+Resin $\sim 0.5\text{mm}$ \rightarrow “vertical R” below 1 strip $O(10\text{T}\Omega)$ @ 10kV

Materials: Same insulating materials (Kapton + Aramid) and same resin (Resoltech)

Production procedure **and enhanced countermeasures and QC**

- Minimize moisture trapped in wall layers: drying in oven Kapton & Twaron just before use
- QC epoxy contamination \rightarrow proper control of mixing and de-gassing process (new mixing / degassing tools and QC) and **... avoid antistatic spray...**
- QC electrical resistivity measurements after each early step in the production



The ND280 experiment: High Angle TPC highlights

- Field Cage (FC)
 - Assembly and layout
 - Production
 - Characterization and Quality Assessment
 - Mechanical
 - Electrical

- Encapsulated Resistive Anode Micromegas (ERAMs) 
 - Production of 50 sensors
 - Characterization
 - Detector response, signal and impact on reconstruction

- Impact on HATPC performance

ERAM: MicroMegas with DLC resistive foil

Resistive layer enables **Charge spreading**

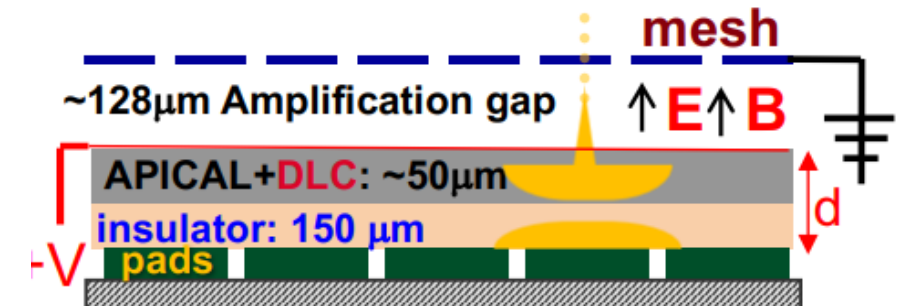
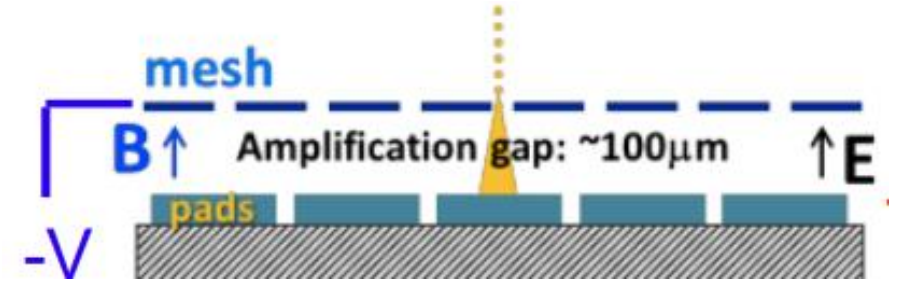
- space resolution below $500\mu\text{m}$ with larger pads
- less FEE channels (lower cost)
- improved resolution at small drift distance (where transverse diffusion cannot help)

Resistive layer prevents charge build-up and hides sparks

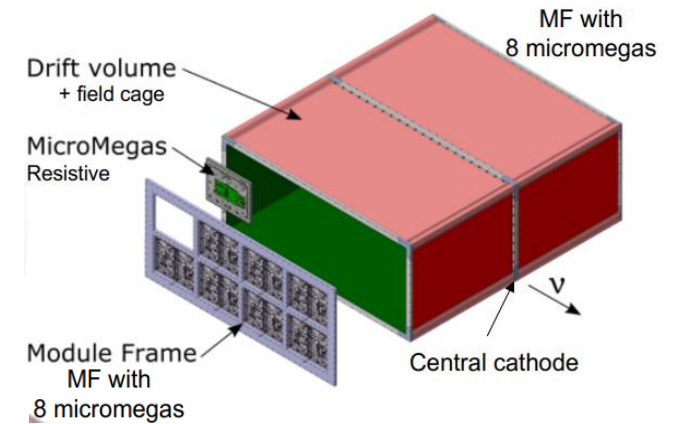
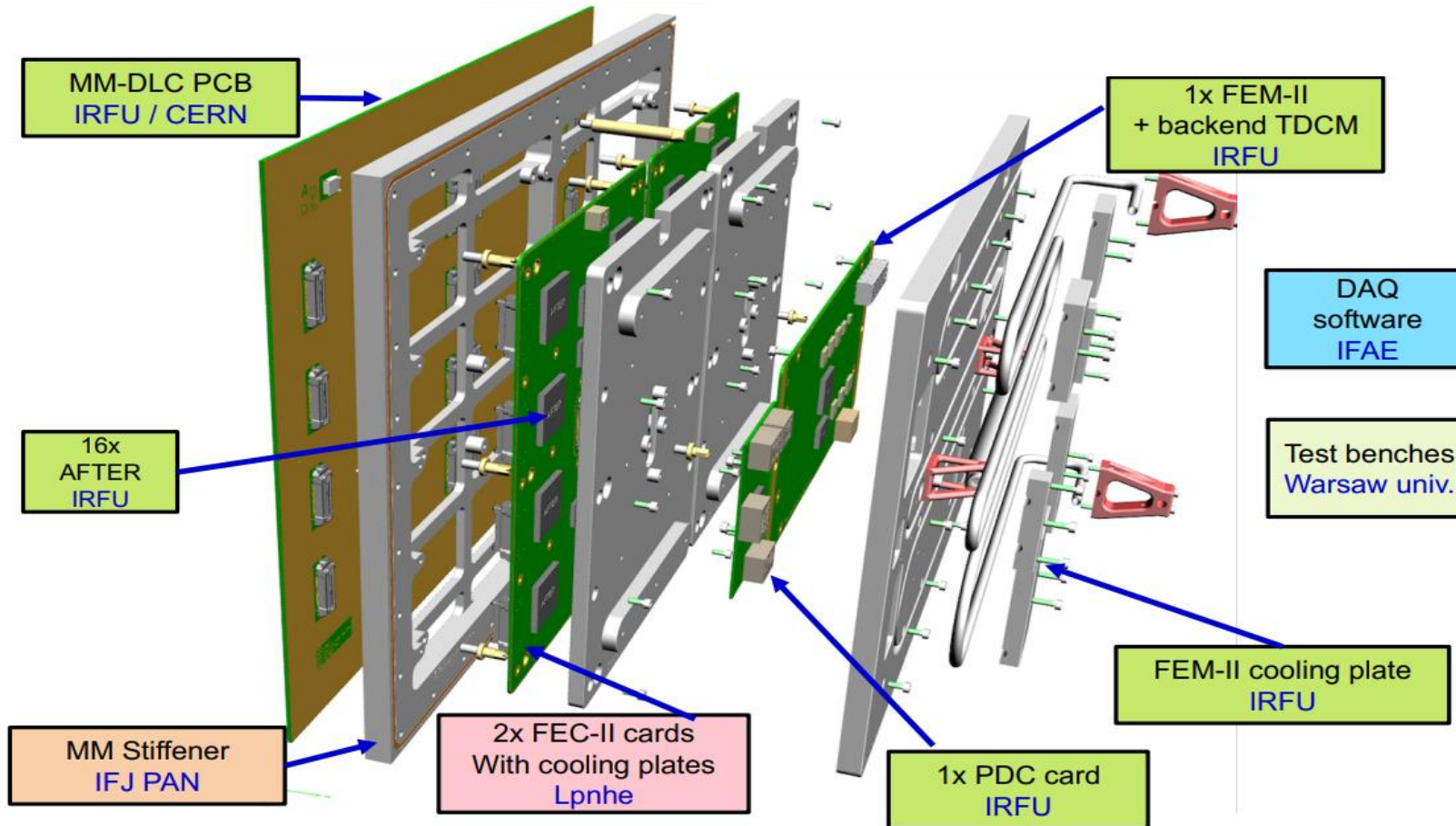
- enables operation at higher gain
- no need for spark protection circuits for ASICs
 - compact FEE → max active volume

Resistive layer encapsulated and properly insulated from GND

- Mesh at ground and Resistive layer at +HV
- improved field homogeneity → reduced track distortions
- better shielding from mesh and DLC → potentially better S/N



ERAM Module breakout



8 + 8 ERAMs per HATPC

Very compact Electronics → parallel to the detector

36x32=1152 pads : 2 x 576 ch. FEC + 1 FEM2 + 1 PDC

Charge spread on low resistivity foil

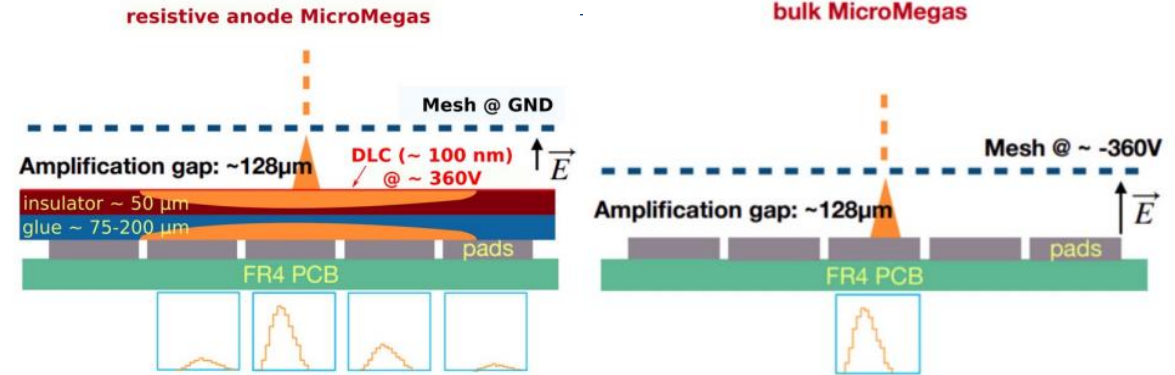
Charge Spreading 2D telegraph eqn. solution
time scale is driven by RC

R- surface resistivity
C- capacitance/unit area

Gaussian spread

$$\frac{\partial \rho}{\partial t} = h \left[\frac{\partial^2 \rho}{\partial r^2} + \frac{1}{r} \frac{\partial \rho}{\partial r} \right] \rightarrow \rho(r, t) = \frac{RC}{2t} e^{-r^2 RC / (4t)}$$

$$\sigma_r = \sqrt{\frac{2t}{RC}} \left\{ \begin{array}{l} t \approx \text{shaping time (few 100 ns)} \\ RC_{[ns/mm^2]} = \frac{180 R_{[M\Omega/\square]}}{d_{[\mu m]}/175} \end{array} \right.$$



Final ERAM layout choice for series production:

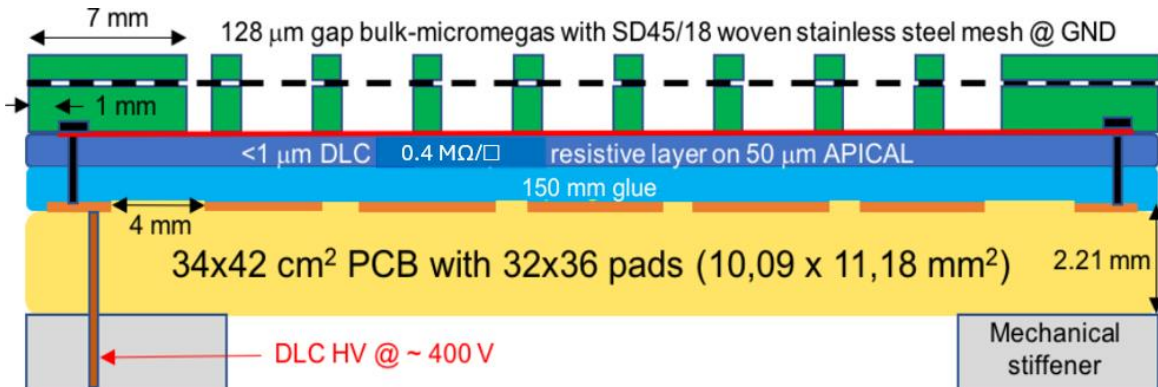
Considering pads of 11x10 mm² parameters

- 400 kΩ/□ DLC resistivity – low resistivity
- 150 µm thickness glue – C_{dLC-pad/gnd} ~ O(20pF)

→ RC ~ O(100ns/mm²)

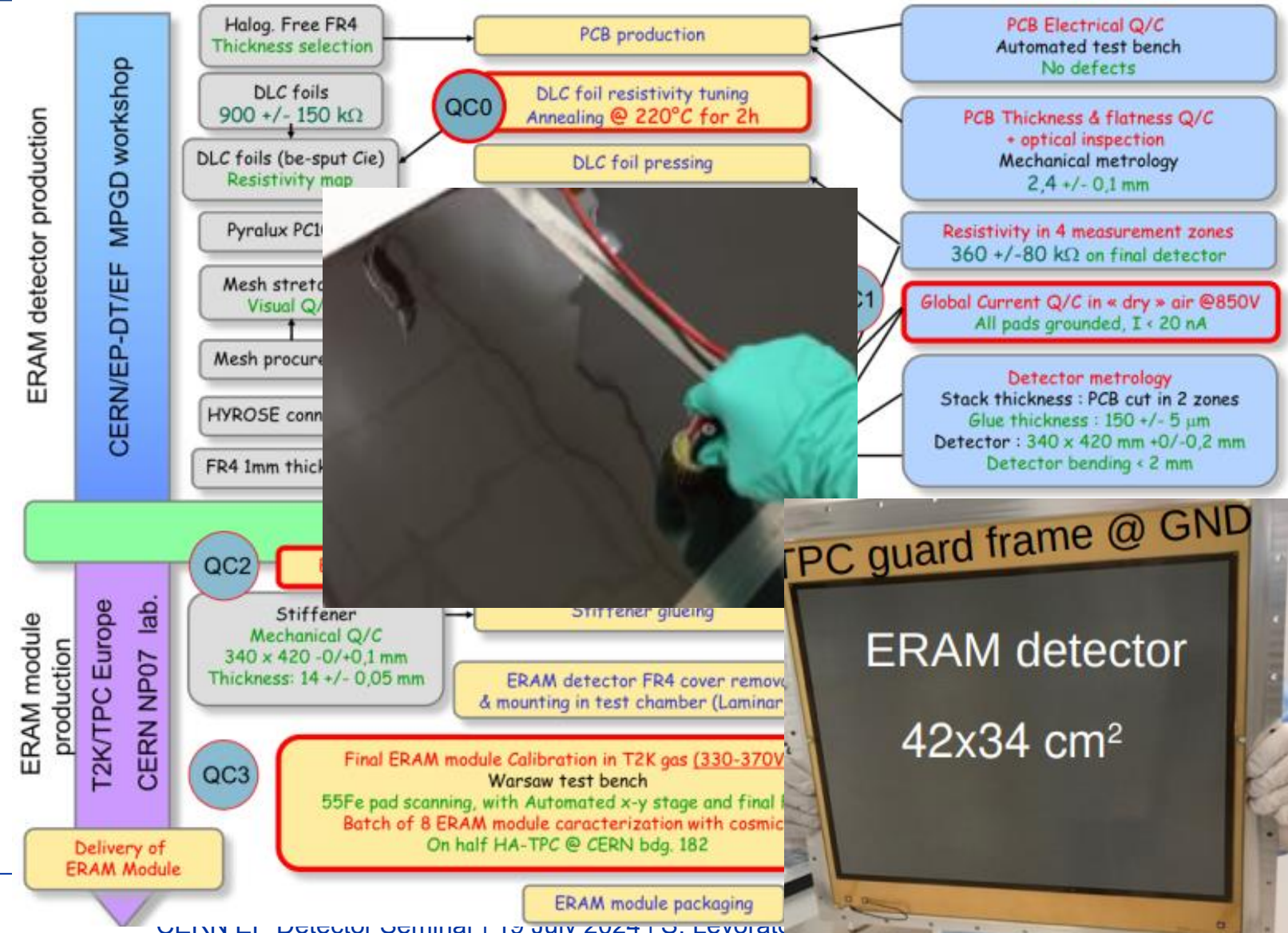
Trade-off optimal charge spread VS spark protection

Gain not affected by resistivity
(transparency to induced signals is guaranteed)

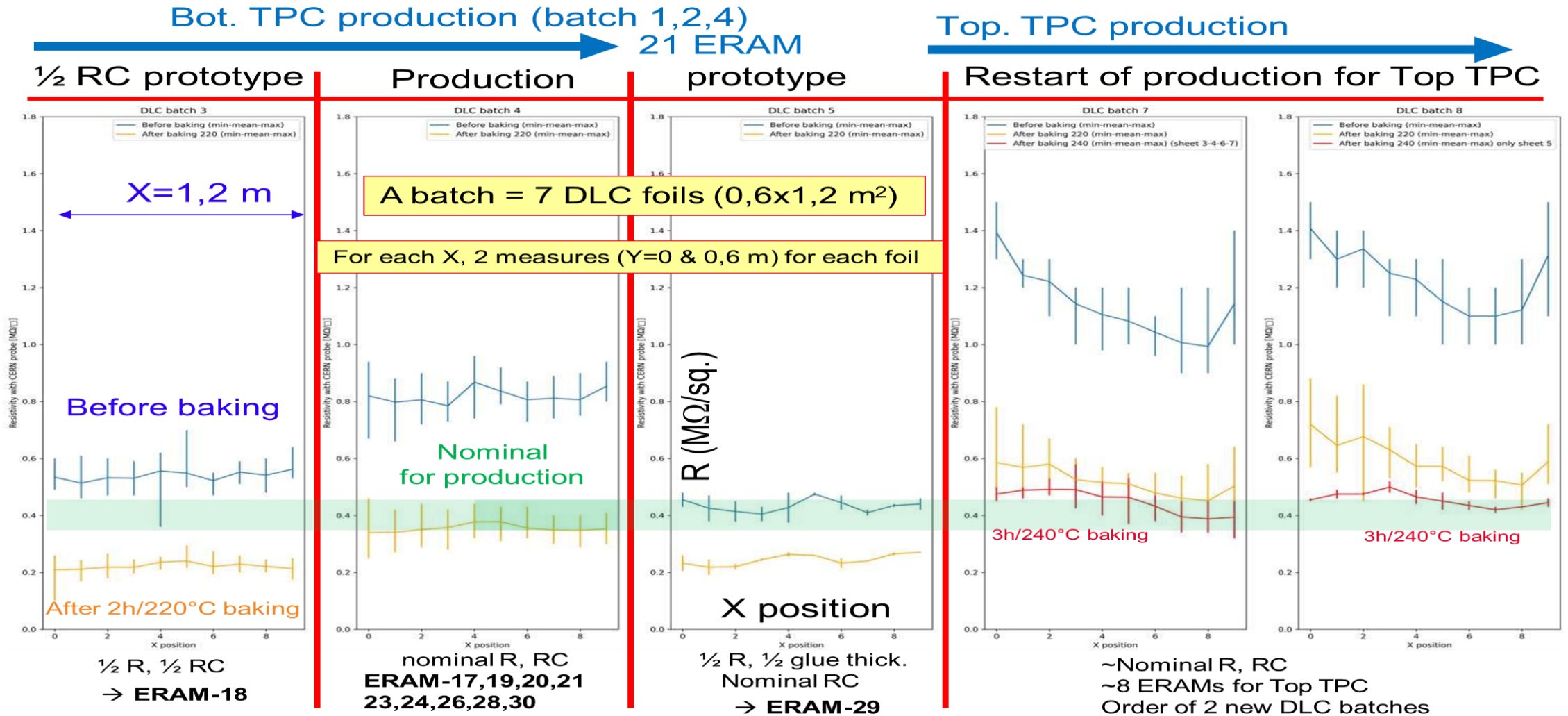


ERAM production ~ 50 detectors

- Crucial steps in production (CERN MPGD workshop)**
- 1) Selecting DLC foil resistivity**
 - Large variations from DLC provider
 - Value stable after annealing
 - 2) Gluing steps by Pressing**
 - DLC to PCB
 - Stiffener to DLC-PCB



DLC layer: foil selection, QC



The ND280 experiment: High Angle TPC highlights

- Field Cage (FC)
 - Assembly and layout
 - Production
 - Characterization and Quality Assessment
 - Mechanical
 - Electrical

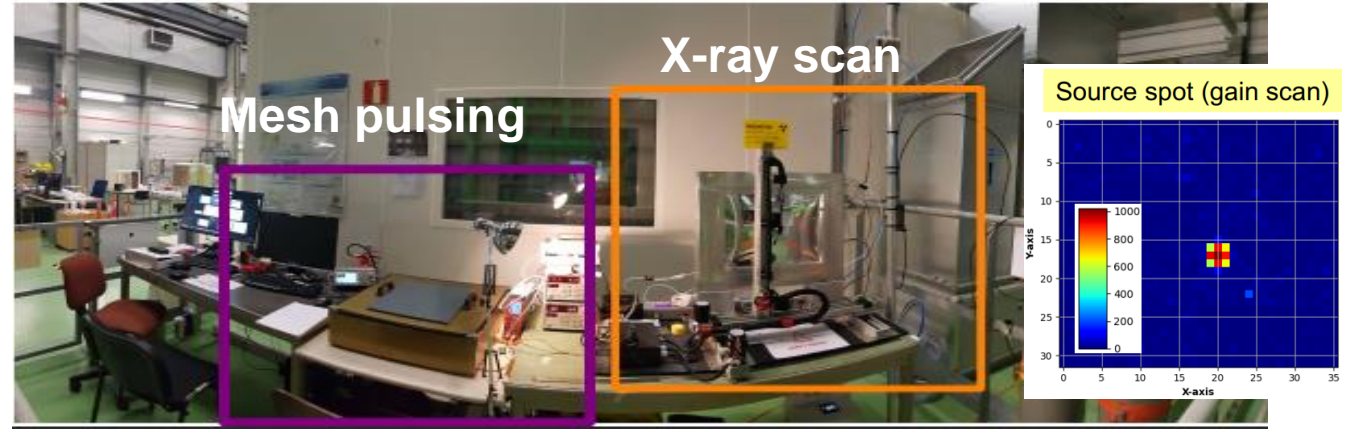
- Encapsulated Resistive Anode Micromegas (ERAMS)
 - Production of 50 sensors
 - Characterization
 - Detector response, signal and impact on reconstruction
- 

- Impact on HATPC performance

ERAM Series production experience: X-ray scan

X-rays Test Bench at CERN
 fundamental to

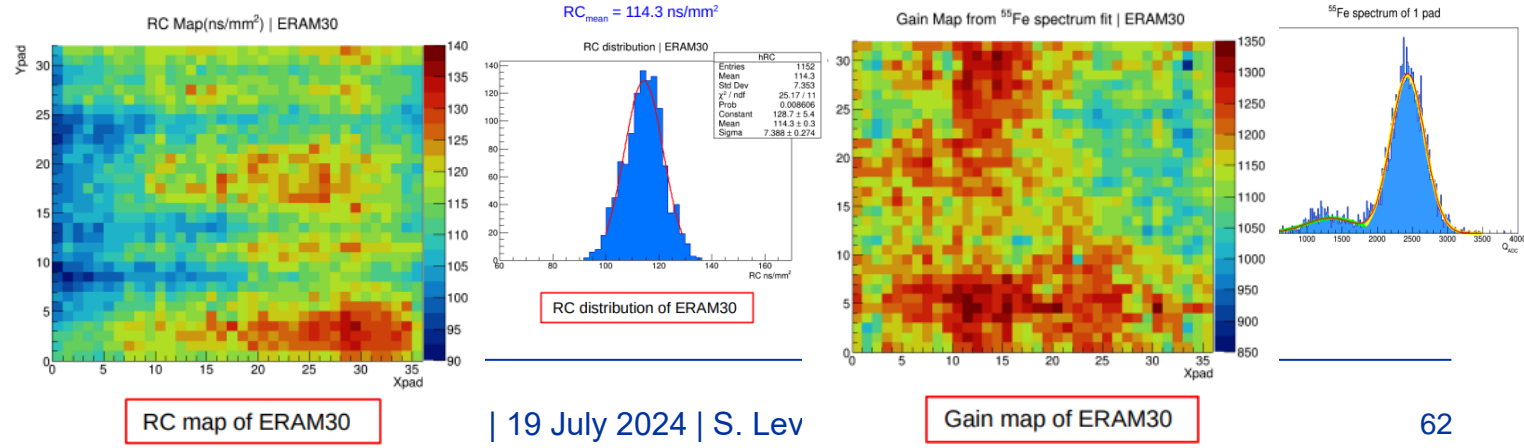
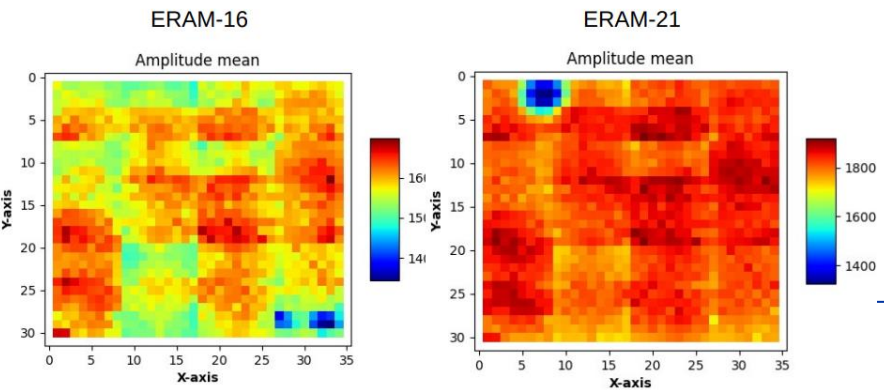
- 1) **Qualify, characterize and calibrate** all prototypes and series ERAMs
- 2) Support the development of **detailed ERAM response model**



A) Mesh Pulsing: before and after stiffener gluing
Aim: detector geom defects (eg pillar detach), stiffener gluing issues, electronic noise



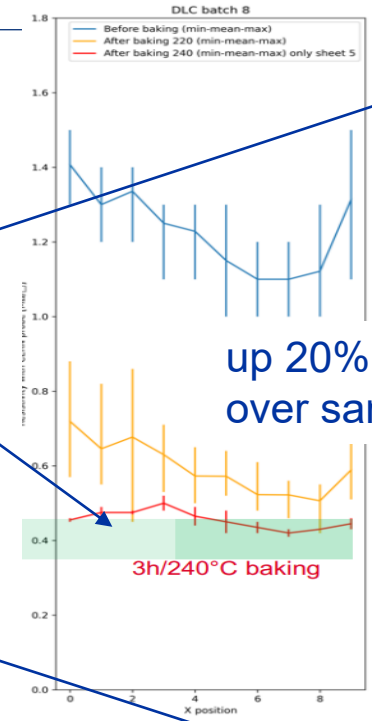
B) X-ray scan of finalized detectors with final electronic modules. Remote controlled station for scanning with mm step fine steps
Aim: QC and fine calibration in terms of gain, resolution and RC



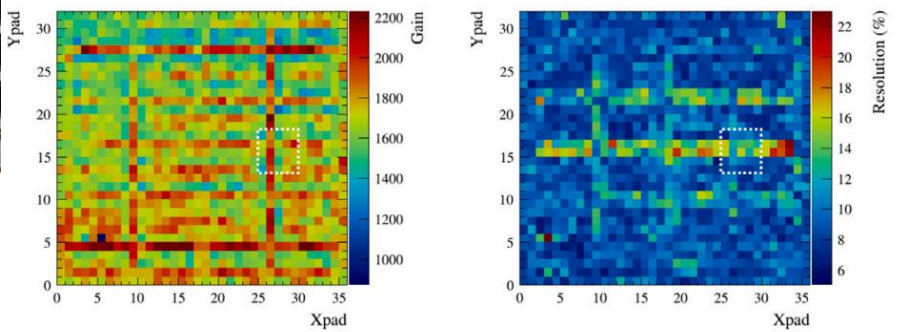
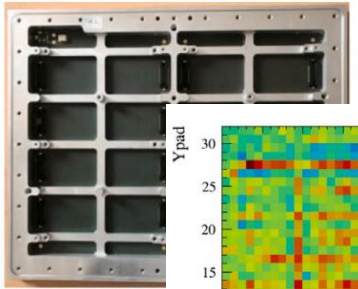
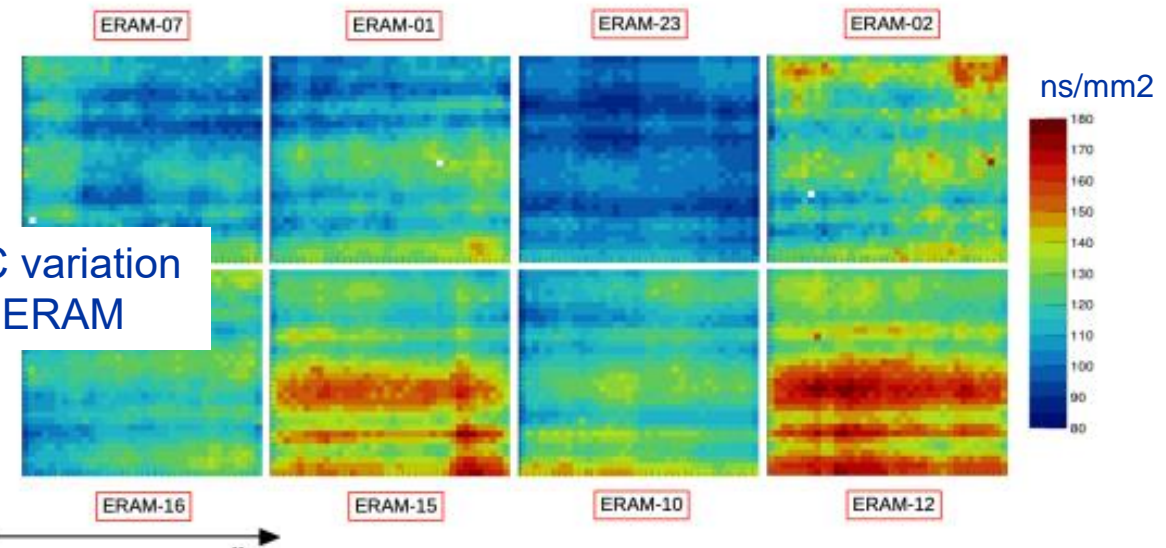
ERAM Series production experience: X-ray scan

Production steps: tough!
(needed long tuning)

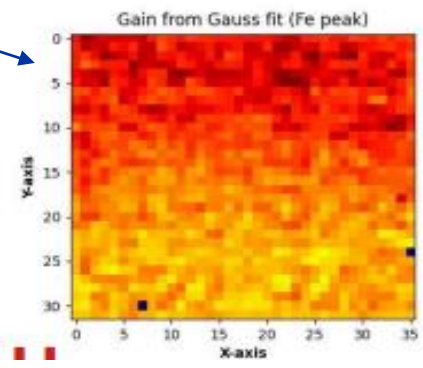
- 1) **Selecting DLC foil resistivity**
 - Large variations from DLC provider
 - Stable values only after annealing
- 2) **Gluing steps by Pressing**
 - DLC to PCB
 - Stiffener to DLC-PCB



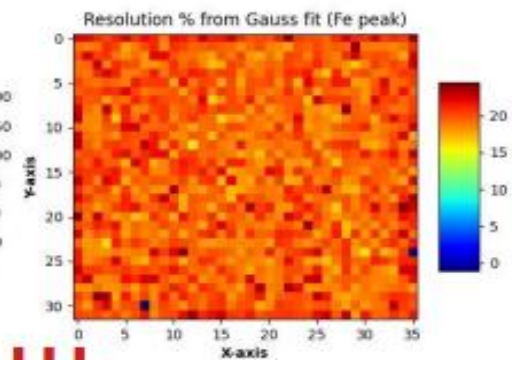
RC map of ERAMS on bottom HATPC EP1



ERAM with DLC-PCB gluing issue

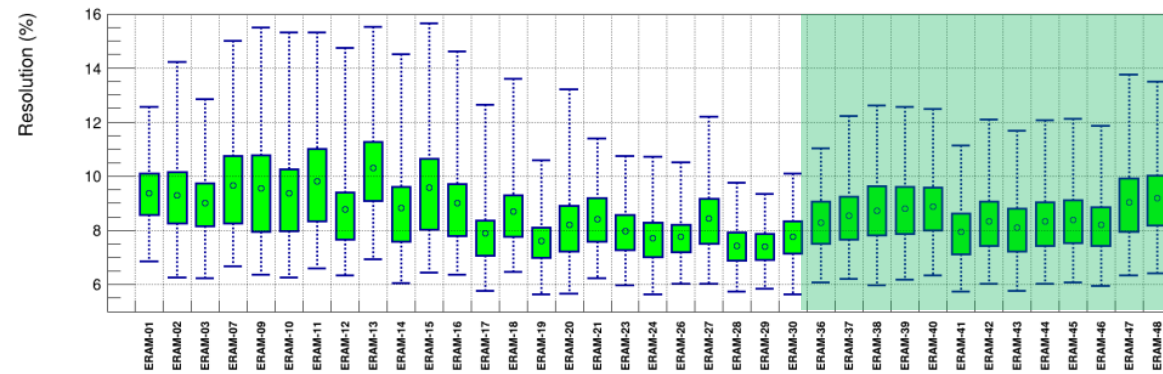
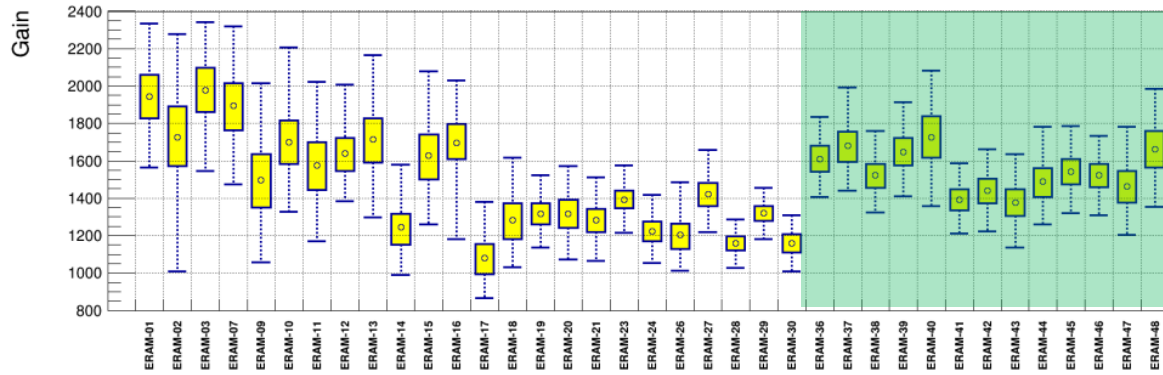


Gain map of ERAM OK

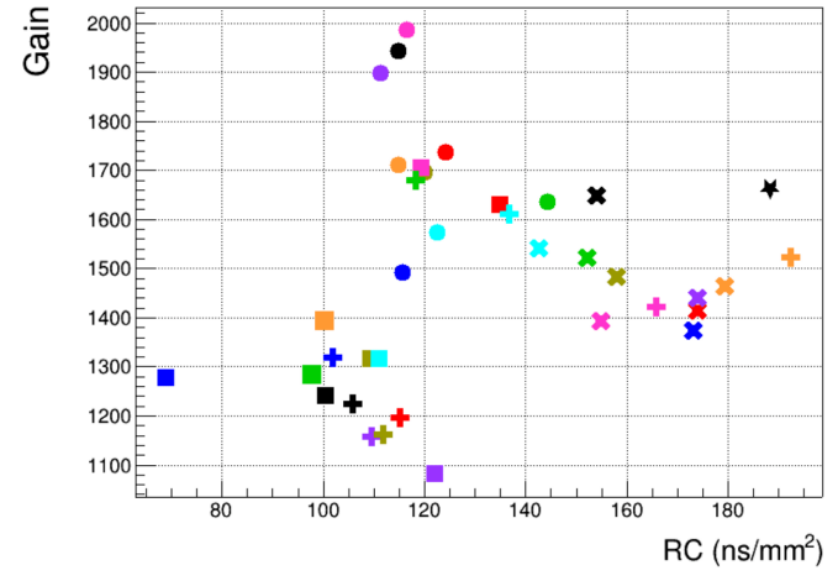


ERAM Series production experience

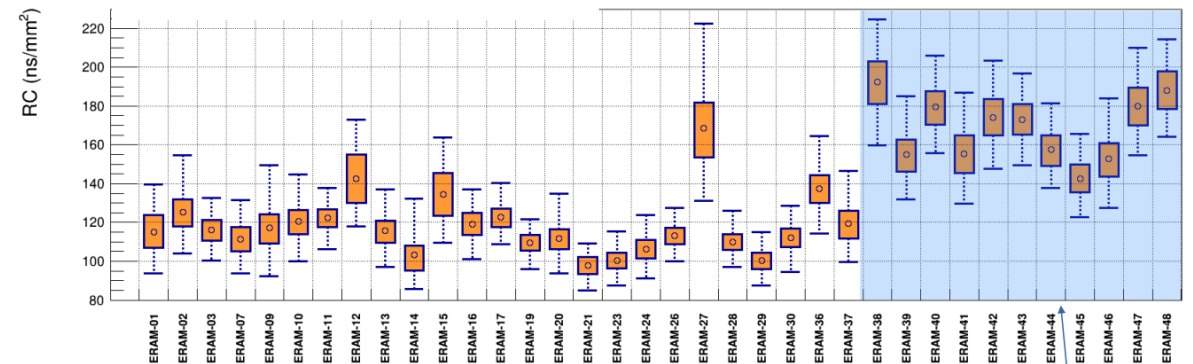
Gain distribution @350V



Energy resolution



RC distribution



- Lower and upper bounds of box: [Mean - 25%, Mean + 25%] of distribution (50% of values within box).
- Lower and upper bounds of bars: [Mean - 49%, Mean + 49%] of distribution (98% of values within bars).

DLC resistivity $\approx 500\text{k}\Omega/\square$
Glue thickness: 150 μm

ERAM Assembly and Operation experience

Low resistivity DLC O(500kΩ/□) [after annealing] features

- Optimal charge spread → uniform response across pad (combined with C ~ O(20pF/cm²))
- Fast Q removal and Effective Protection against sparks included at moderate rates ~ O(1kHz) tracks crossing pads
- Leakage currents at level of few nA in normal conditions (no beam)

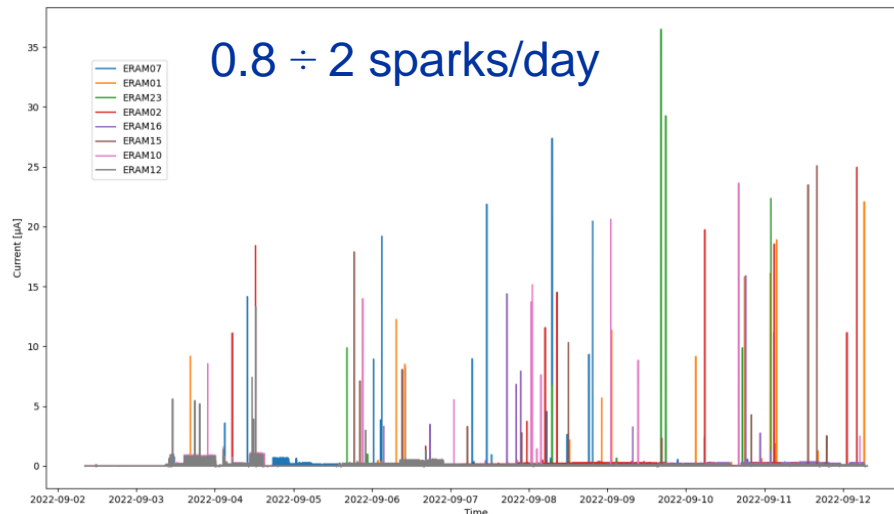
Challenging installation conditions

- high sensitivity to dust
- low H₂O level (100ppm) before HV on

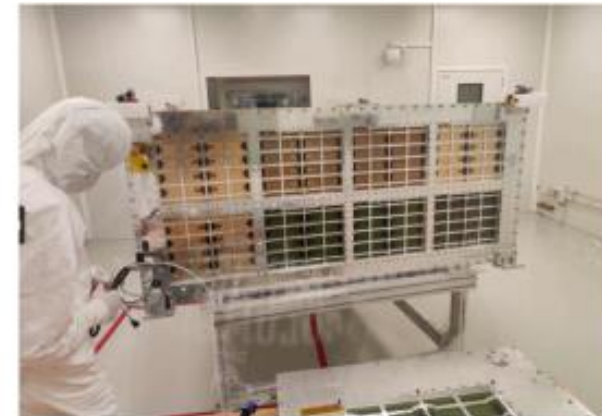
ERAM @ test beam 2022

ERAM stability

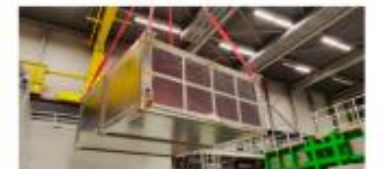
- We have operated 8 ERAM modules during ~ 7.7 days @ CERN 2022
 - Intense beam activity
 - One ERAM module was not working during cosmic test (solved by hammering on it)
- **We have observed no major issue**
- The spark rate is between 0.8 and 1.7 per day (higher than 2uA)



ERAM assembly (and storage) in Clean Room



Grey tent area in front of Clean Room large entrance for enhanced clean conditions



The ND280 experiment: High Angle TPC highlights

- Field Cage (FC)
 - Assembly and layout
 - Production
 - Characterization and Quality Assessment
 - Mechanical
 - Electrical

- Encapsulated Resistive Anode Micromegas (ERAMS)
 - Production of 50 sensors
 - Characterization
 - Detector response, signal and impact on reconstruction

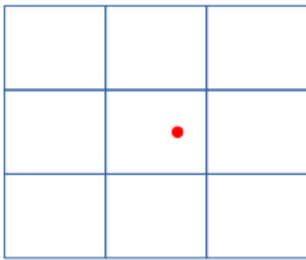


- Impact on HATPC performance

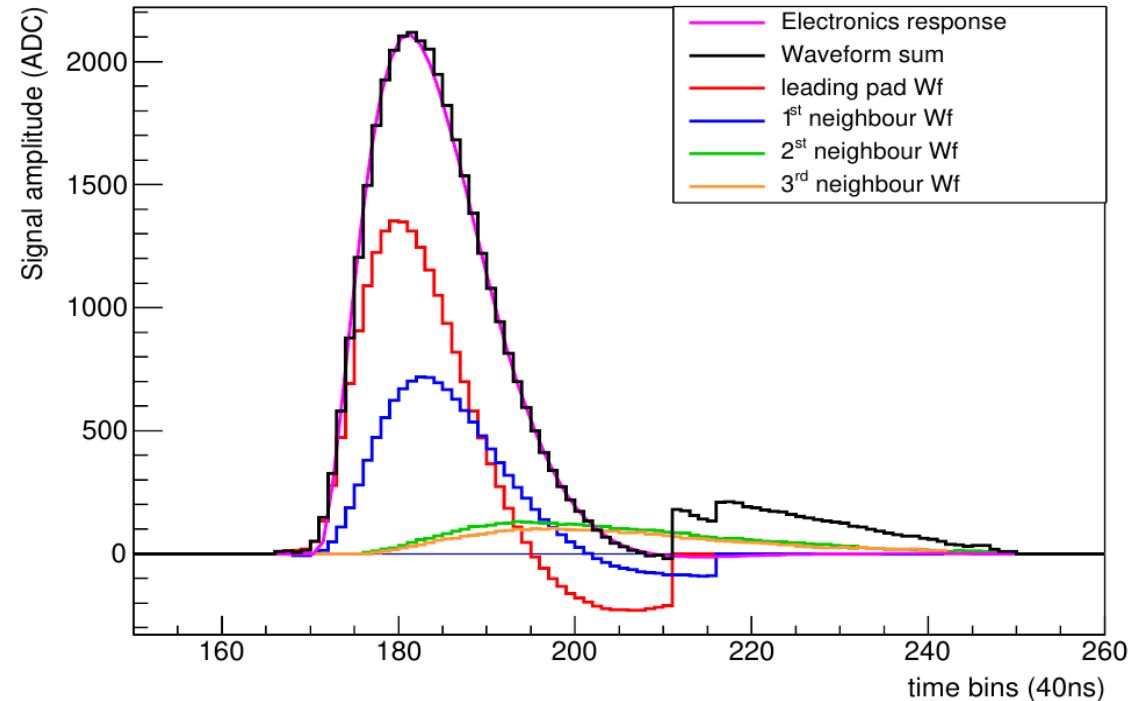
The ND280 experiment: High Angle TPC highlights

How does the signal look ? point deposition for example

Charge deposited punctually
on a pad (X ray)



ADC signal : max 4096 counts
Time window of 511 time bins
Time bin (typ.): 40 ns (25 MHz sampling)
Peaking time (typ.) : 412 ns



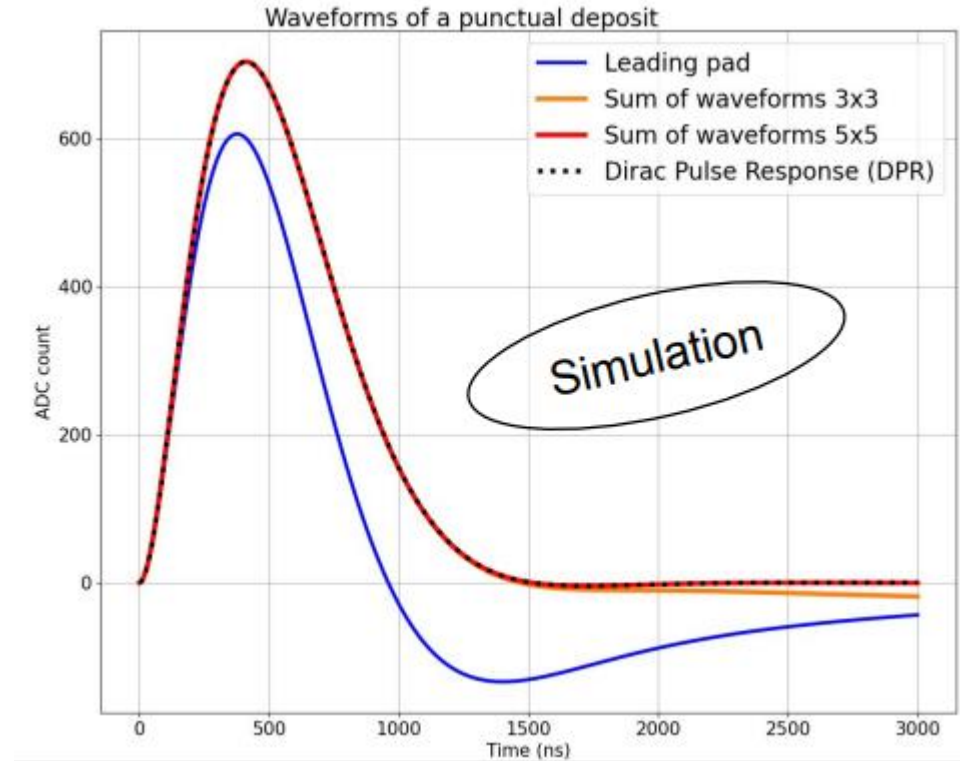
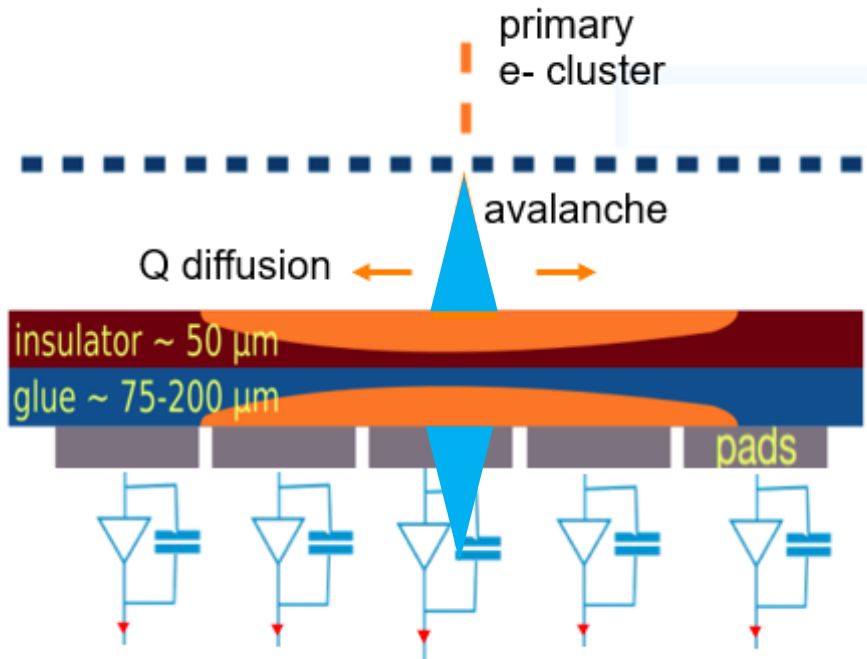
Leading pad: highest and earliest signal

⇒ current induced on pads from by avalanche, ie **ions** signal (as electrons' signal is too fast)

Adjacent pads: lower and later signals

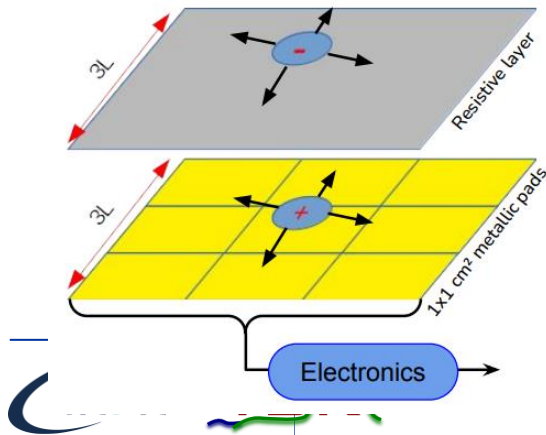
⇒ current induced by potential field adjustments after **electrons** are collected by on DLC
(current induction by “charge spread on resistive layer”)

Reconstruction of charge deposition 1/2

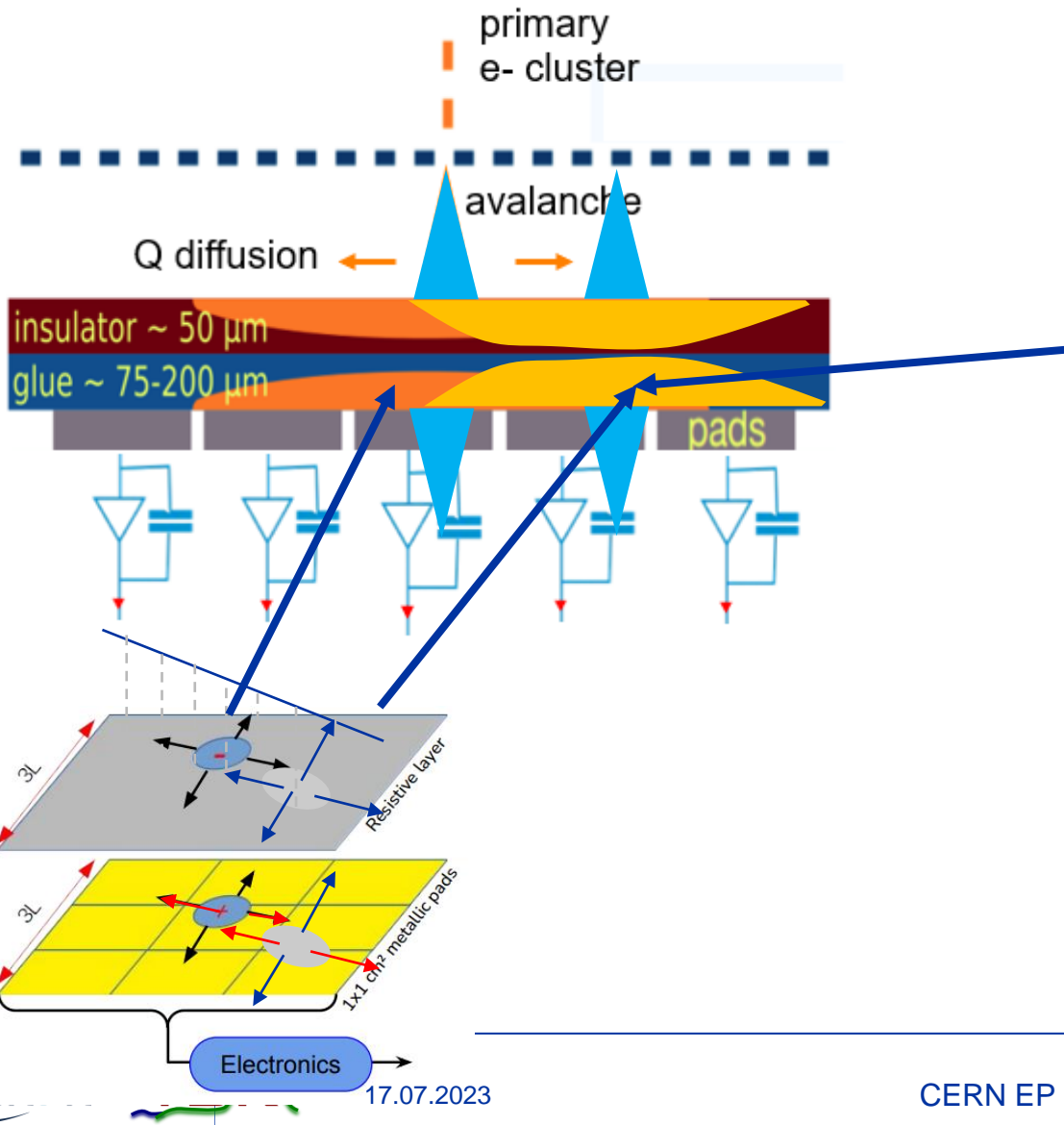


Recovering information about deposited Q is not trivial

Within our electronics shaping time scale
 in primary pads, the signal of ions is «diluted» by the signal of charge spreading
 => Need combining information of all pads (primary and secondary)



Reconstruction of charge deposition 2/2



Charge on DLC spreads along any direction including track direction
«**longitudinal correlation**» across primary pads within our electronics shaping time scale



requires a dedicated signal formation model

ERAM response – Signal formation model

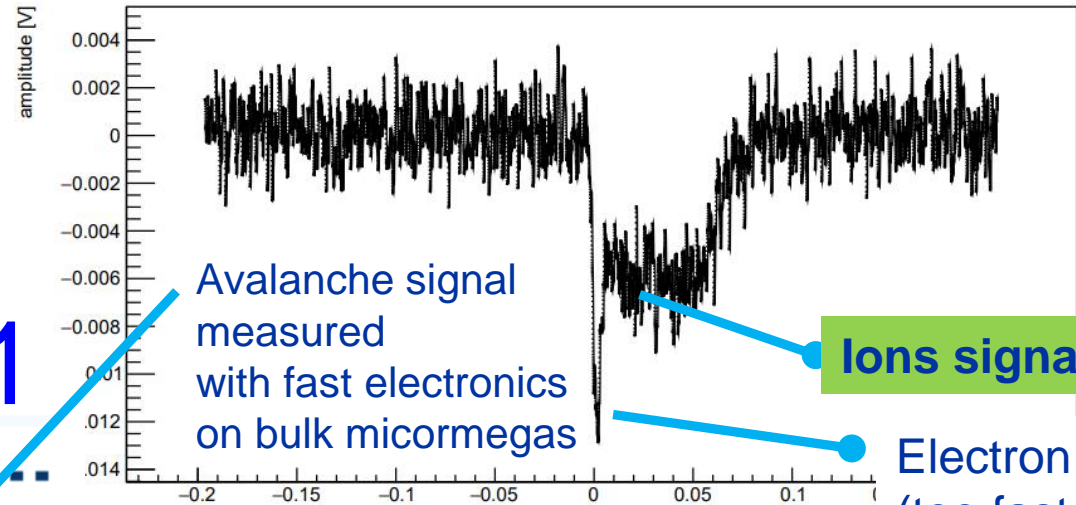
Vc = -350, Va = 460

Main ingredients

In the time scale of our shaping time O(100ns)
Charge spread is properly described by

Solutions of 2D diffusion eqn.

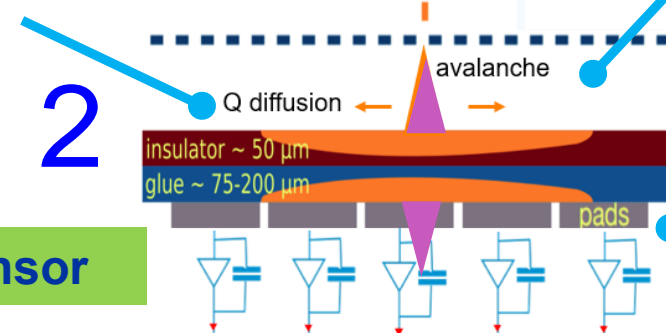
$$\Rightarrow \frac{\partial^2 \rho}{\partial^2 t} = \frac{1}{RC} \left(\frac{\partial^2 \rho}{\partial^2 x} + \frac{\partial^2 \rho}{\partial^2 y} \right) \text{ with } RC = \frac{C_s}{\sigma} \text{ in } s/m^2$$



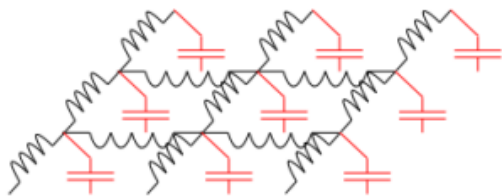
Avalanche signal measured with fast electronics on bulk micromegas

Ions signal (slow)

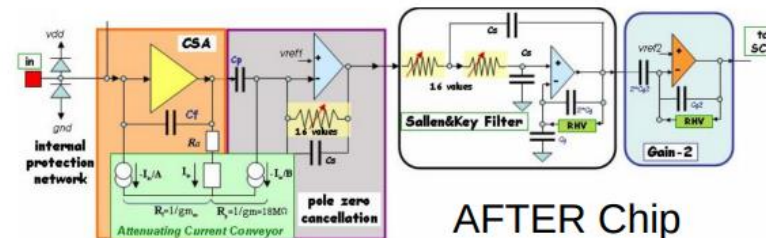
Electron signal (too fast for our shaping times)



Electrical model of the sensor



FEE Response Function



AFTER Chip

Note: of course **gas transport properties** (L, T diffusion) have to be accounted for

$$f(t; w_s, Q) = e^{-w_s t} + e^{-\frac{w_s t}{2Q}} \left[\sqrt{\frac{2Q-1}{2Q+1}} \sin\left(\frac{w_s t}{2} \sqrt{4 - \frac{1}{Q^2}}\right) - \cos\left(\frac{w_s t}{2} \sqrt{4 - \frac{1}{Q^2}}\right) \right]$$

ERAM detector response: reconstruction

Use of the model for Reconstructing the charge deposition

Due to square shape of ERAM pads, the classical method (**PRF+clustering**) works OK only for tracks with **horizontal or vertical direction** (wrt pads coordinates)

Better methods use solutions of 1D or 2D telegraph equation in order to

- 1) compute the pattern templates for charge diffusion on DLC
- 2) calculate the overall expected signal waveform per each pad
- 3) find the best matching with the recorded waveforms

Its computationally heavy → different approximations are used for different analysis some examples and illustration algorithms and TPC performances

- 1) X-rays analysis – ERAM characterization
- 2) Measurement of dE/dx – Particle Identification
- 3) Track reconstruction – momentum measurement

Reconstructing X-rays charge deposition

$Q_{pad}(t)$ = Solution of 2D Teq. for diffusion of initial Q deposited charge (point-like, delta-pulse initial conditions)

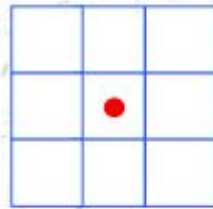
$$Q_{pad}(t) = \frac{Q_e}{4} \times \left[\operatorname{erf}\left(\frac{x_{high} - x_0}{\sqrt{2}\sigma(t)}\right) - \operatorname{erf}\left(\frac{x_{low} - x_0}{\sqrt{2}\sigma(t)}\right) \right] \times \left[\operatorname{erf}\left(\frac{y_{high} - y_0}{\sqrt{2}\sigma(t)}\right) - \operatorname{erf}\left(\frac{y_{low} - y_0}{\sqrt{2}\sigma(t)}\right) \right]$$

$$\sigma(t) = \sqrt{\frac{2t}{RC}}$$

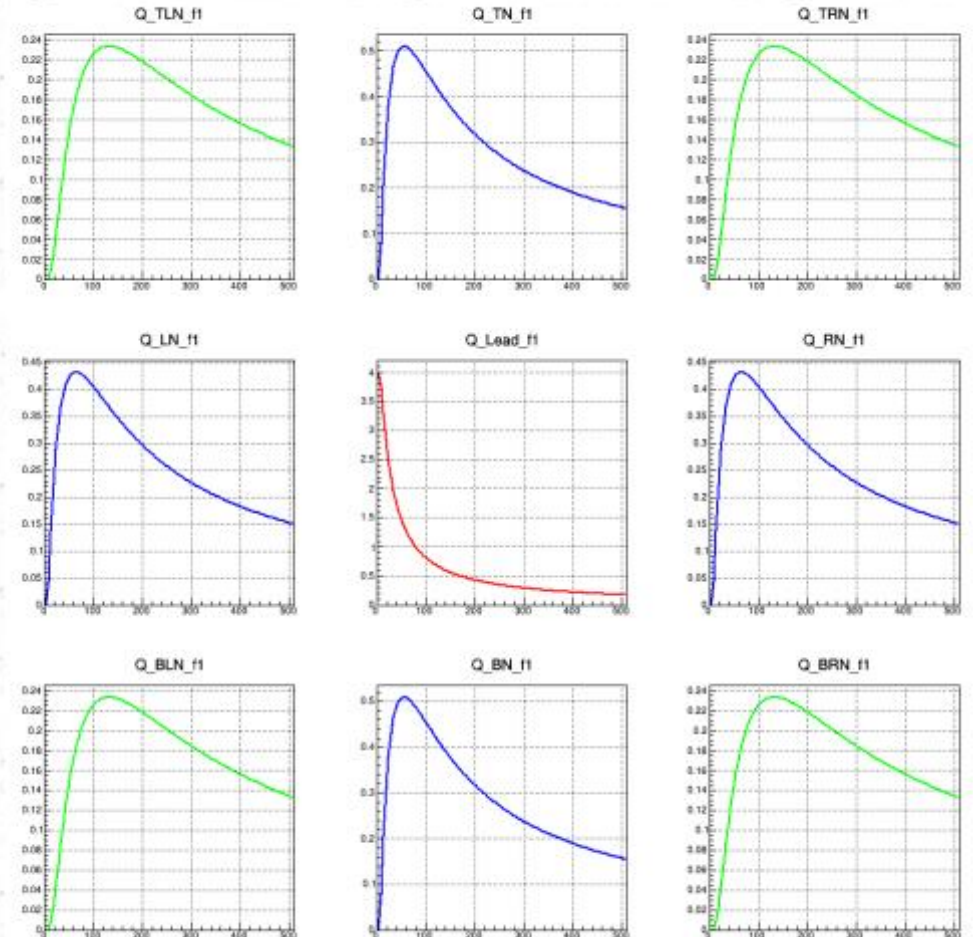
- Obtained from Telegrapher's equation for charge diffusion.
- Integrating charge density function over area of 1 readout pad.
- Parameterized by 5 variables:

- x_0 } Initial charge position
- y_0 }
- t_0 : Time of charge deposition in leading pad
- RC : Describes charge spreading
- Q_e : Total charge deposited in an event

x_H, x_L : Upper and lower bound of a pad in x-direction
 y_H, y_L : Upper and lower bound of a pad in y-direction



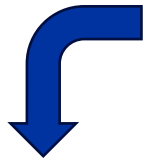
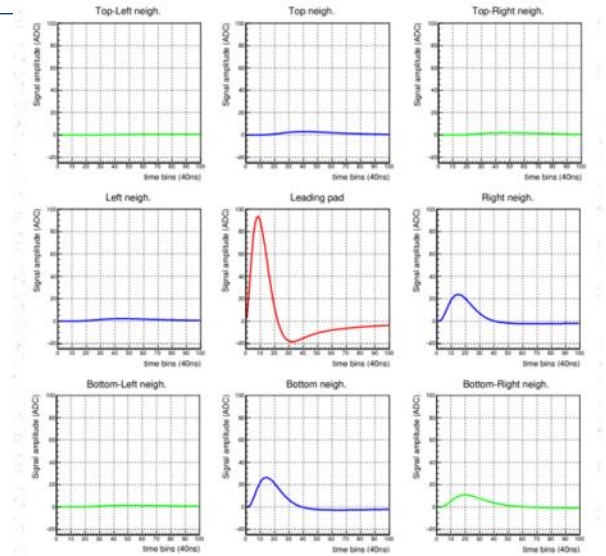
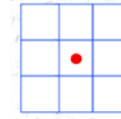
RC = 60 ns/mm²
 $Q_e = 4 e^-$



Reconstructing X-rays charge deposition

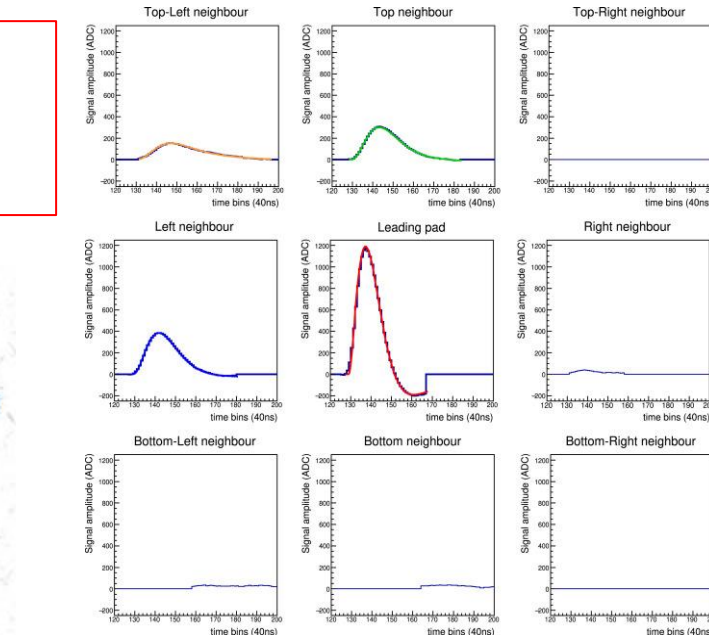
WF templates

Current induced on a pad $dQ_{\text{pad}}(t) / dt$
to be convoluted with
electronics transfer function $R(t)$
 $dQ/dt \otimes R(t) = Q(t) \otimes dR(t)/dt$
 $Q(t) \otimes dR(t)/dt$ is more practical



WF fit against templates

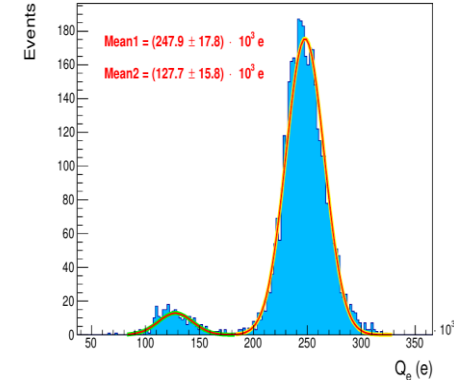
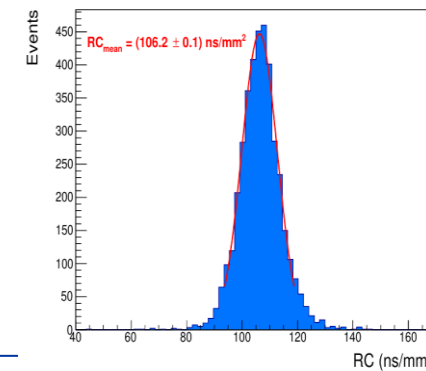
Simultaneous fit of waveforms of
Leading pad + Neighboring pads
to get the best 5 parameters



Results about Gain and RC

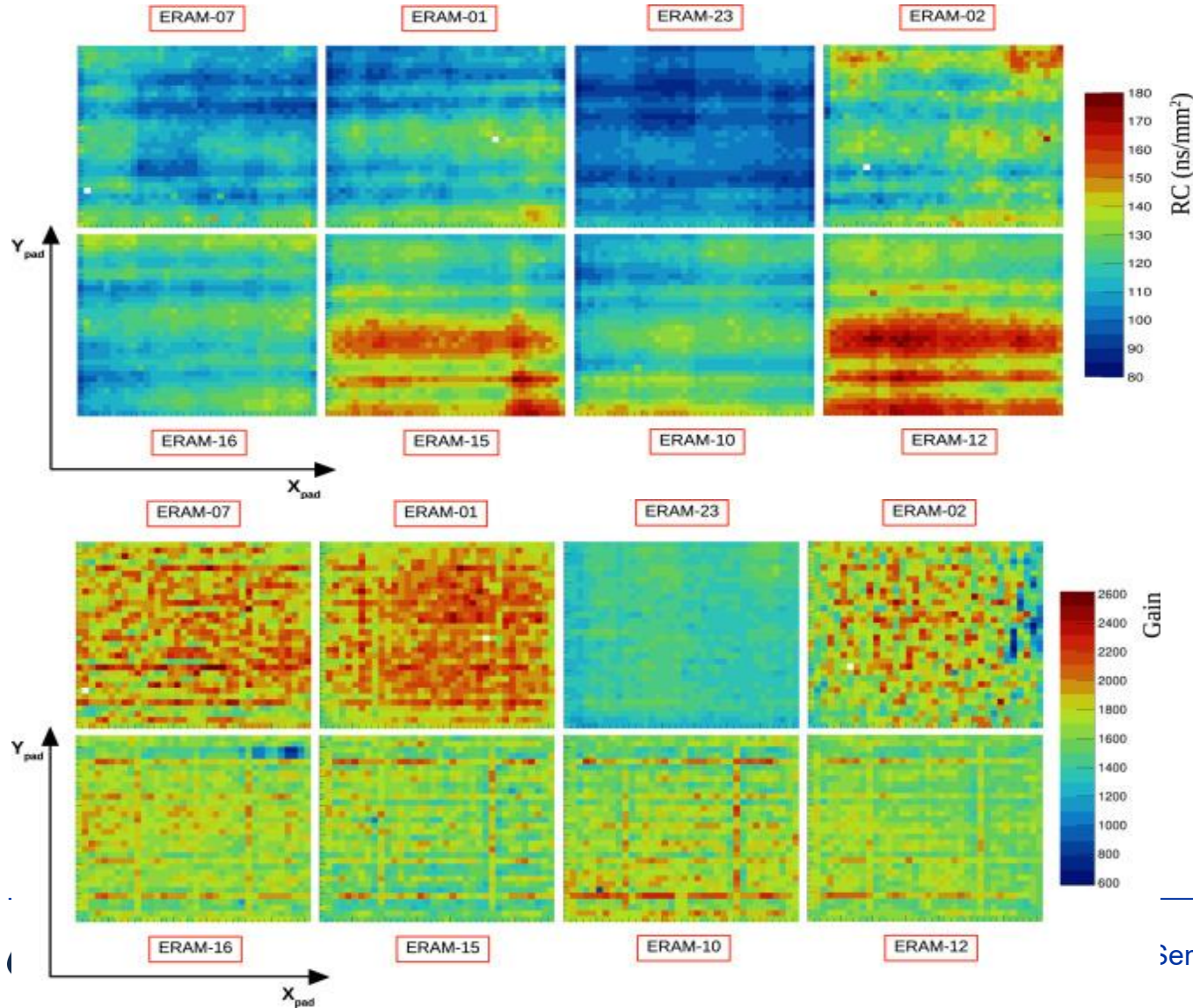
- x_0
- y_0
- t_0 : Time of charge deposition in leading pad
- RC : Describes charge spreading
- Q_e : Total charge deposited in an event

x_H, x_L : Upper and lower bound of a pad in x-direction
 y_H, y_L : Upper and lower bound of a pad in y-direction



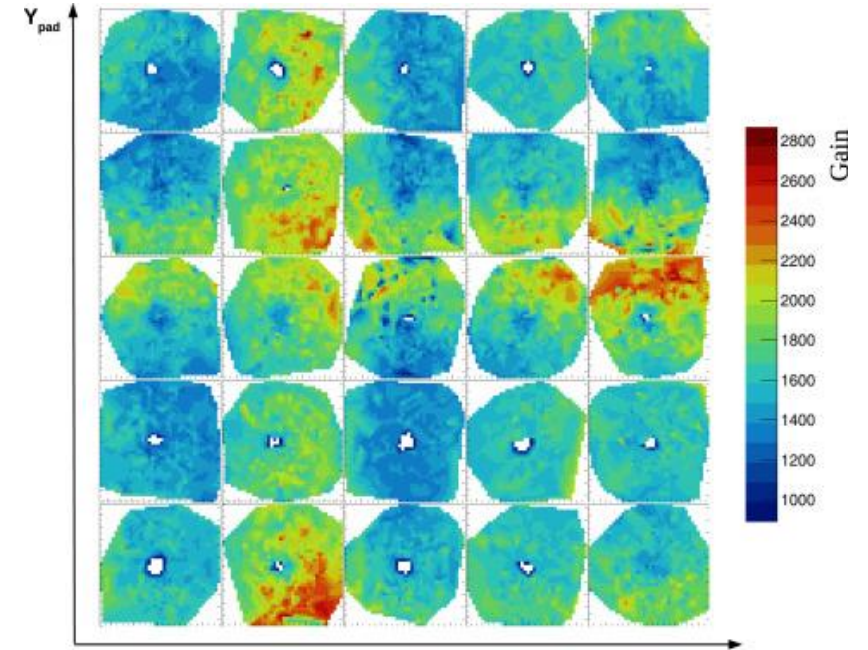
Extraction of RC and Gain maps from X-rays

Use of the method for the extraction of ERAM GAIN and RC



X-ray conversion position is also fitted
→ accurate maps of Gain and RC

Use for detailed studies of charge diffusion and ERAM response at fine PAD position level



Indications are that the **lower resistivity** the **better performances** (eg space resolution)

Reconstructing Q along tracks

For the reconstruction of the charge along the tracks two methods

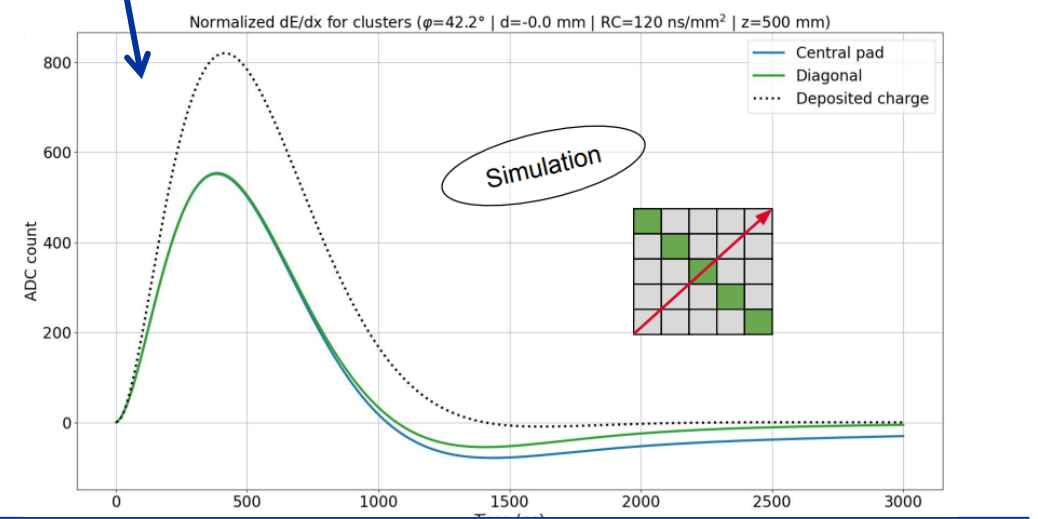
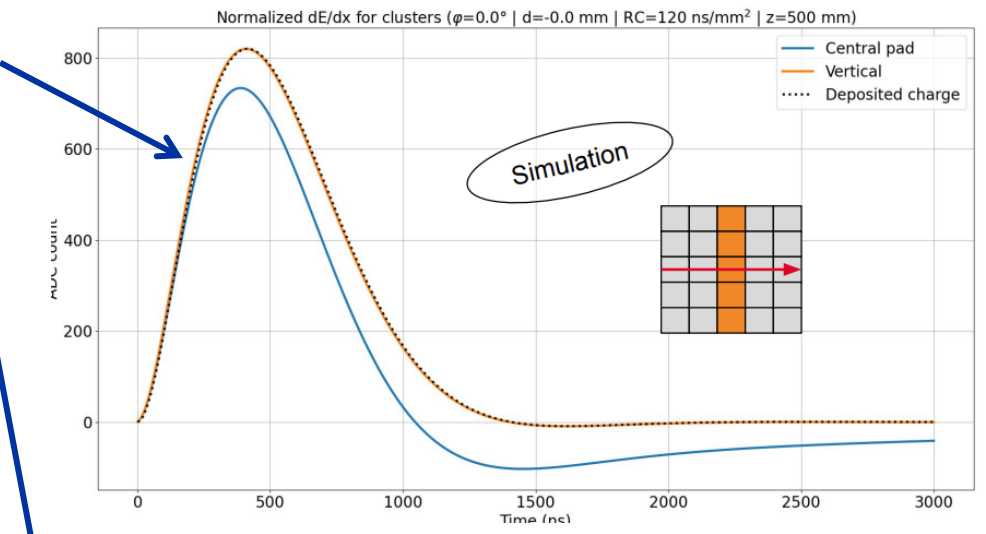
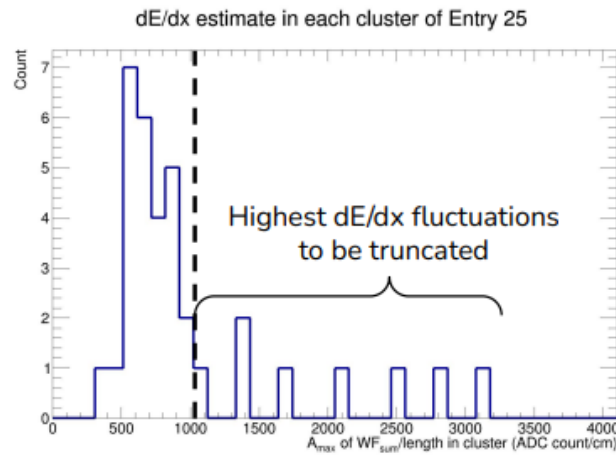
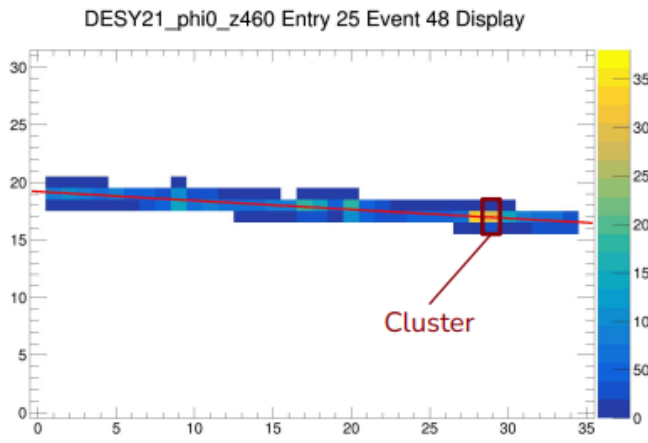
- **Waveform Sum (WS)**
- **Crossed Pad (XP)**

Compare the performance of the two methods for dE/dx extraction

Reconstructing Q along tracks: Waveform Sum

Simple method based on Sum of waveforms(t) (WS) over pads in a cluster

OK for almost H & V tracks
Q missing for included tracks



1. Clusterize the pads into slices and sum the waveforms in each slice to get dE

3. Truncate the clusters with the highest dE/dx (top 30%) to get rid of fluctuations

just like for vertical TPCs!

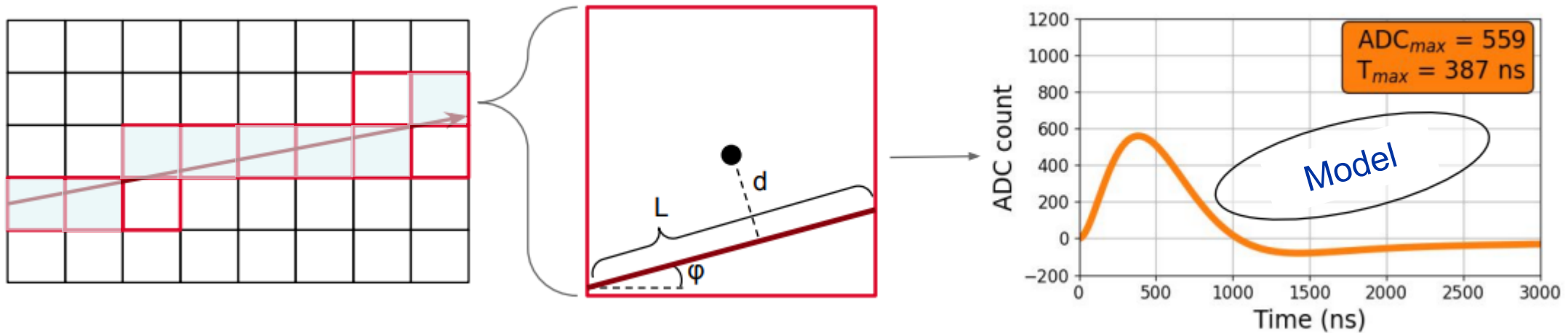
2. Get the track length in each cluster to get dx

4. Get the mean over remaining estimates dE/dx

Reconstructing Q along tracks: Crossed Pad (XP)

- 1) Reconstruct tracks and consider only pads crossed (XP) by the track (primary pads)
- 2) Reconstruct original (ion induced) charge (Q) for each XP (given the track parameters there) by $Q = A \times (Q/A)$ – where A is recorded amplitude on XP and rescaling ratio (Q/A) from Look Up tables (LUT)

LUTs build from model: original Q is distributed linearly over the segment for each XP so that solutions of 1D diffusion equations can be used



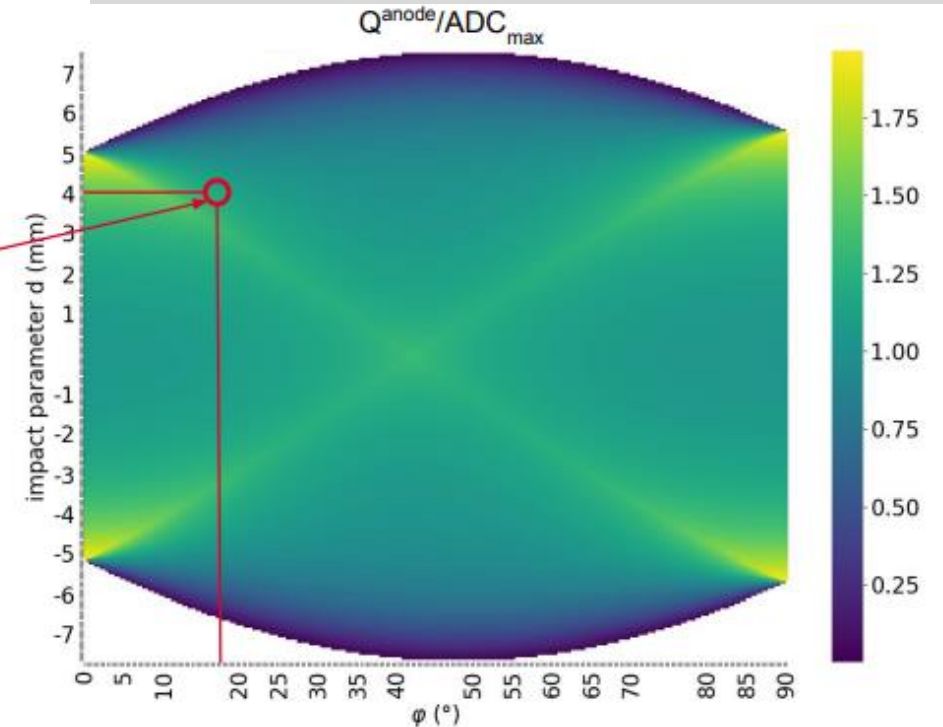
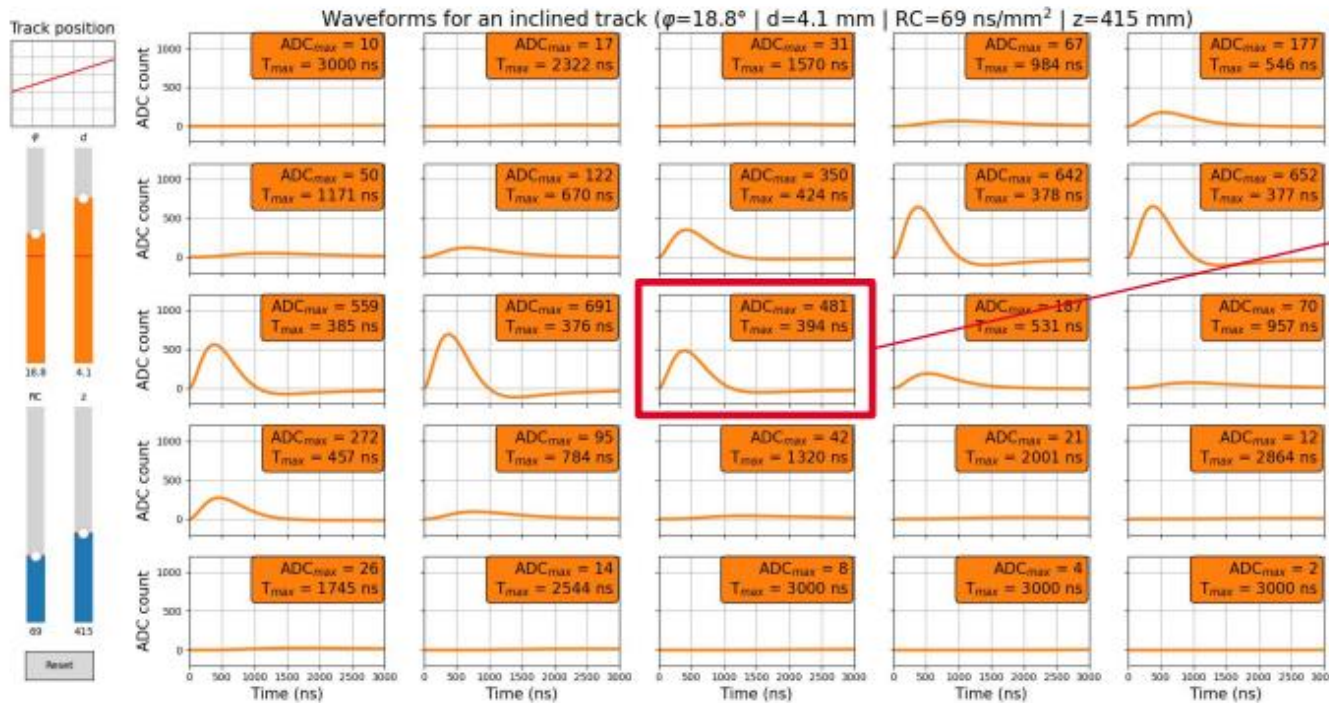
- 1) **No clustering** => potentially more accurate method **because reconstructing full induced charge on primary pads**
- 2) «dilution of ion signal» on a XP pad, due to charge spread over the pad is correctly taken into account
- 3) «longitudinal correlation» among adjacent XP pads, due to charge spread along track direction is accounted for
- 4) **Fast method** though based on model templates (long time is to generate LUTs ...)

Reconstructing Q along tracks: Crossed Pad (XP)

Building the rescaling ratio Q/A ratio 4D LUTs via model

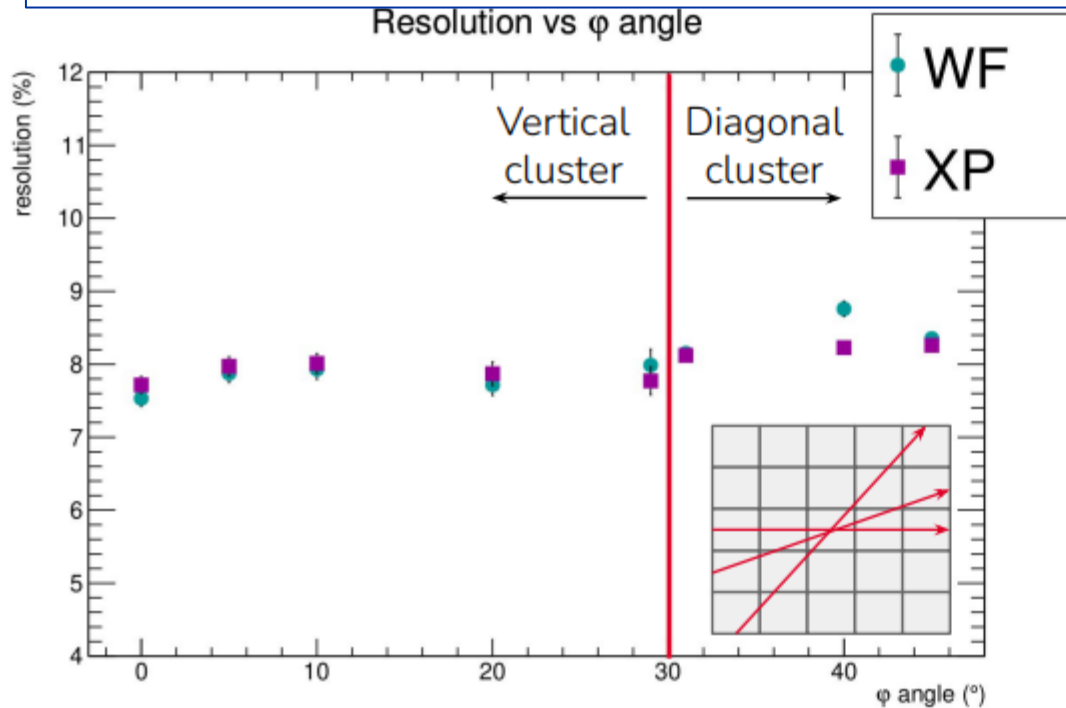
4D Look-Up Table (LUT):

- Angle φ : 200 steps $[0^\circ, 90^\circ]$
- Impact parameter: 200 steps $[-7.3, +7.3]$ mm
- Drift distance: 21 steps $[0, 1]$ m
- RC: 21 steps $[50, 150]$ ns/mm²

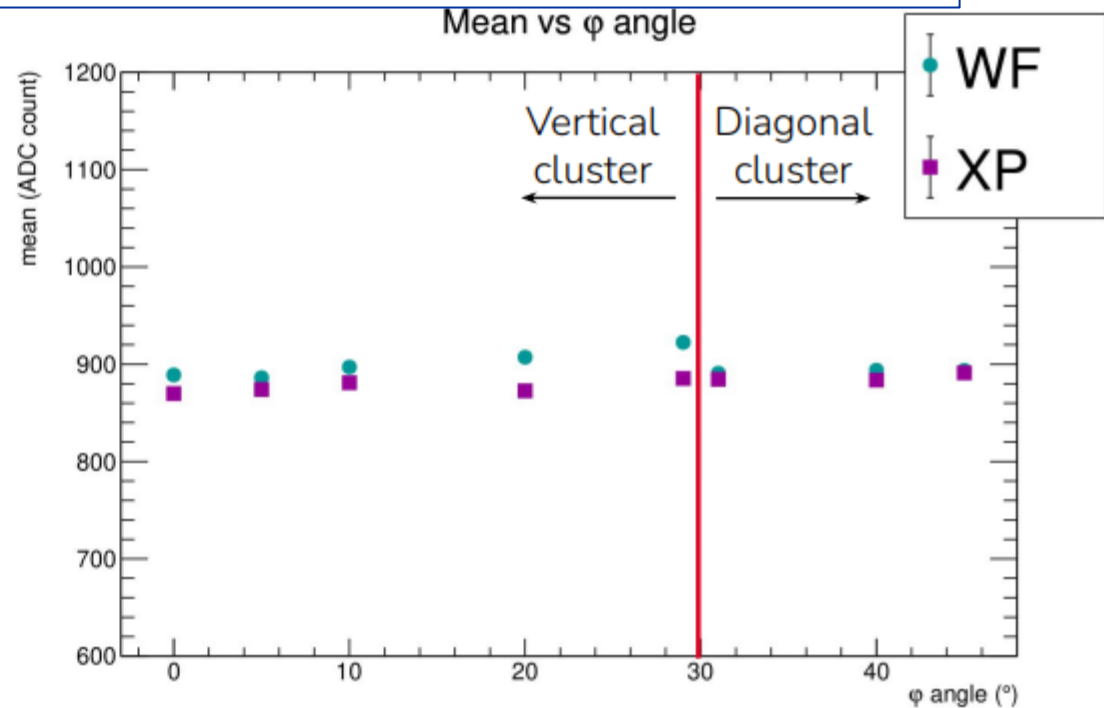


dE/dx preliminary results: (WS) and (XP) methods

dE/dx (4GeV electrons) – comparison of WF and XP methods on Test Beam data (DESY)



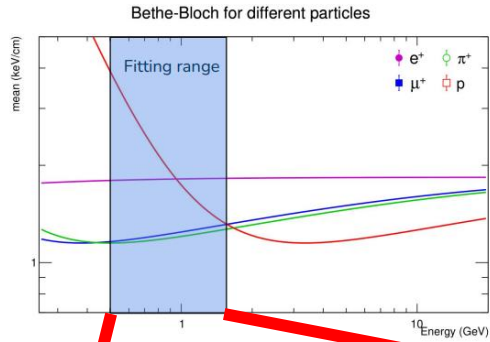
- Resolution $\sigma/\mu \sim 8\%$ and stable
- XP gives better results at diagonal angle



- Flat distribution of dE/dx across ϕ for XP
- Slight sink with WF_{sum} for diagonal clusters

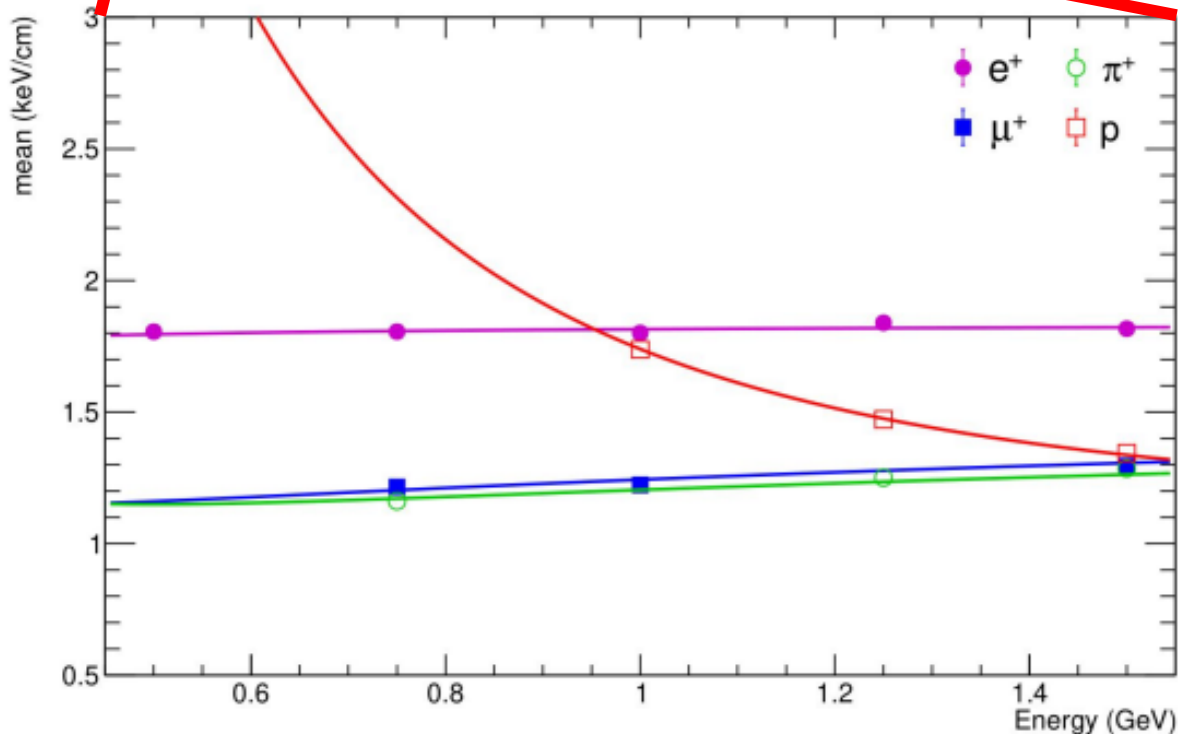
dE/dx preliminary results: (XP) method

dE/dx via XP method on Test Beam data (CERN PS T10)

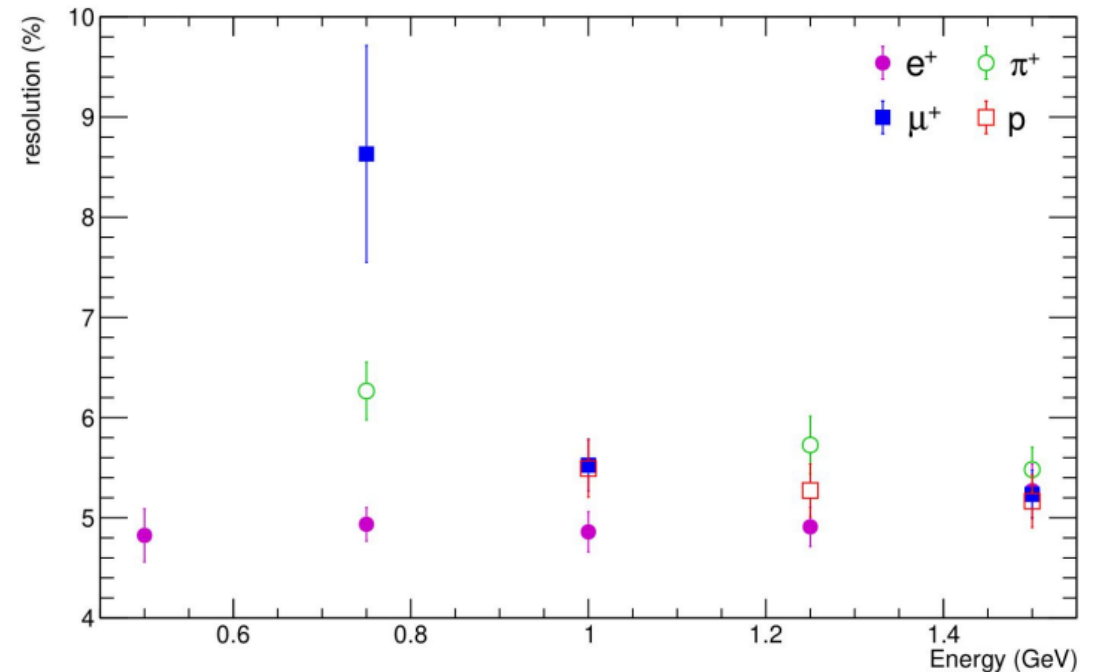


- Resolution < 6.5% (except low stat)
- e^+ stable < 5%

Mean vs energy with XP method



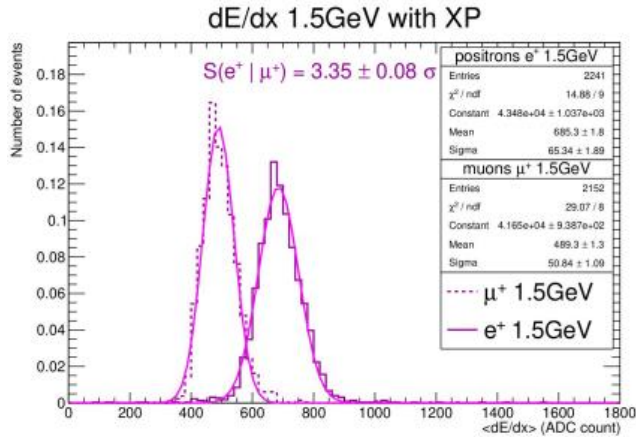
Resolution vs energy with XP method



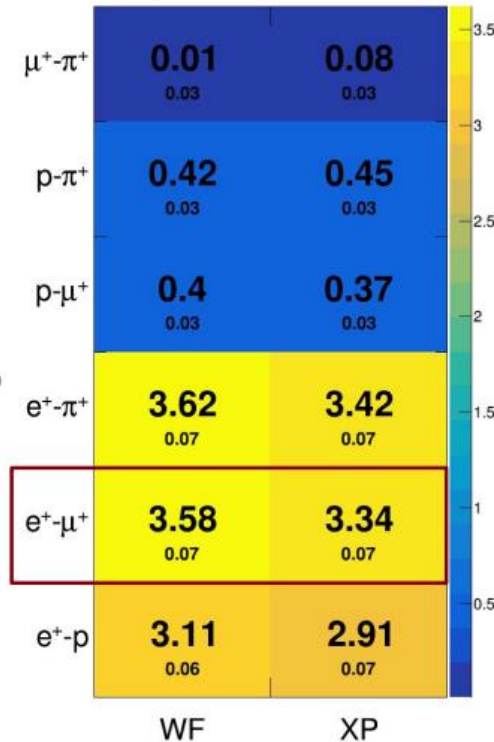
PID preliminary results (XP) vs (WS)

e/μ separation @ 1.5 GeV – Test Beam data (CERN PS T10)

Short tracks (~40cm)



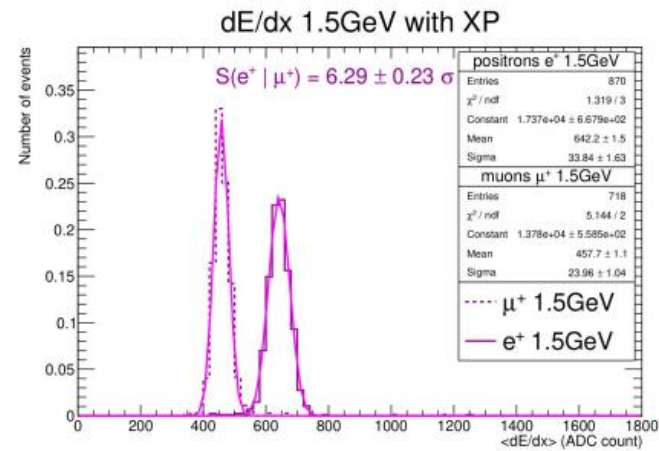
Separation power



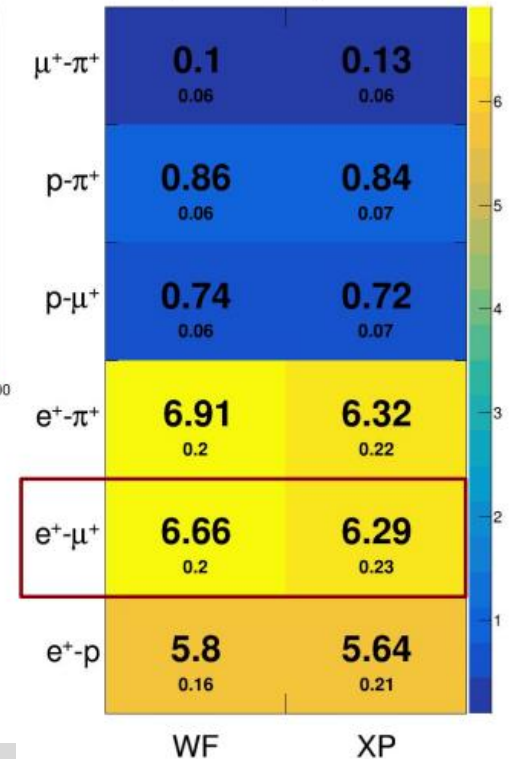
$$S(e^+, \mu^+) = \frac{|\mu_{e^+} - \mu_{\mu^+}|}{\sqrt{(\sigma_{e^+}^2 + \sigma_{\mu^+}^2)/2}}$$

■ μ^+ & e^+ split by more than 3σ

Long tracks (~160cm)



Separation power



$$S(e^+, \mu^+) = \frac{|\mu_{e^+} - \mu_{\mu^+}|}{\sqrt{(\sigma_{e^+}^2 + \sigma_{\mu^+}^2)/2}}$$

■ μ^+ & e^+ split by more than 6σ

Reconstructing tracks

For the reconstruction of the tracks

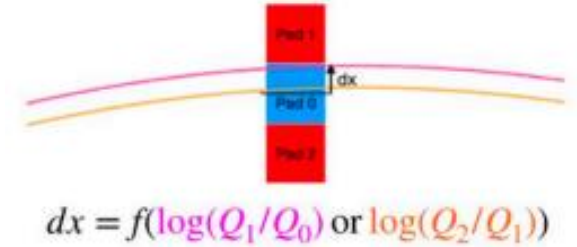
Log(Q) methods

Full Waveform fit Method

Reconstructing tracks: trajectory fitting

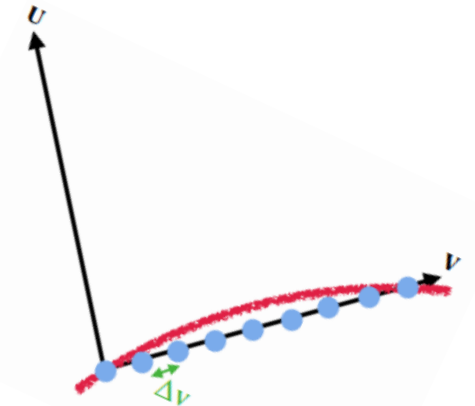
LogQ Method based on **clustering** & **Log[Q_{primary} /Q_{secondary}]**

- logQ method to reconstruct position in each cluster
- Helix fit performed on those reconstructed positions



Full Waveform fit Method – based on **model** & **no clustering**

- 1) Use all the pads associated to a track (Q_{max} values) to define a (v,u) local frame
- 2) Distribute “arbitrary” point charges along v axis separated by Δv (5mm)
the Q per each point is a free parameter
- 3) Diffusion model to predict the waveform generated by point charges in surrounding pads
- 4) Move all points along the u axis to minimize the chi-square difference **between measured waveforms and templates**

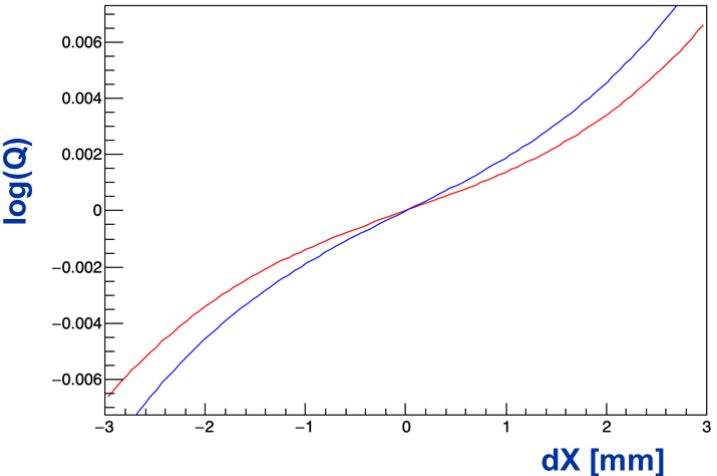
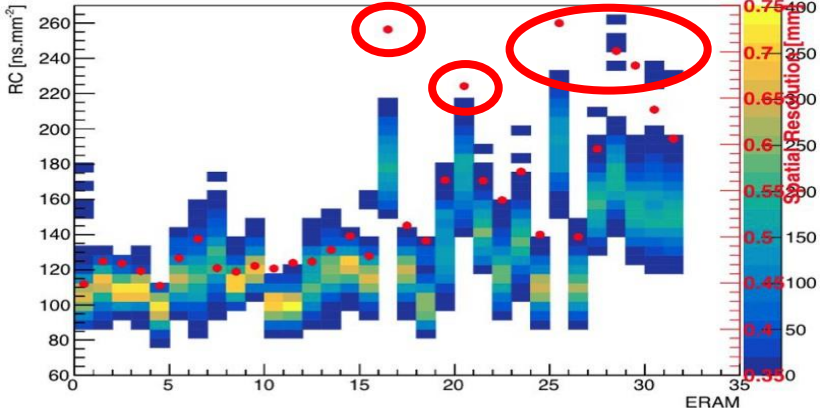
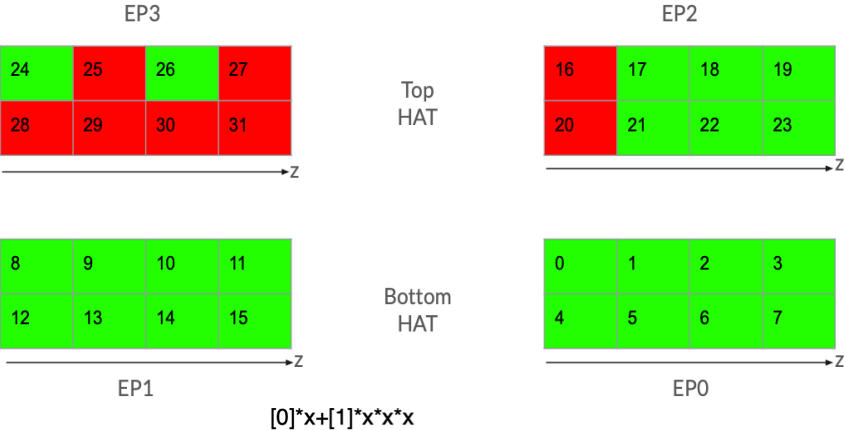


RungeKutta method to fit (u_0 , du/dv , q/p , t_0 , dv/dt)

$$\chi^2 = \sum_{i(pad)} \sum_{j(timebin)} \frac{(Q_{i,j}^{obs} - Q_{i,j}^{Dixit})^2}{\sigma_{i,j}^2}$$

Spatial resolution: HATPC Top and Bottom

Top HAT was equipped with ERAMs with larger RC variation w.r.t. Bottom



High RC → less charge spreading
 “flatter curve”
 Low RC → more charge spreading
 “steeper curve”

dX: distance from the center of the cluster and the real position

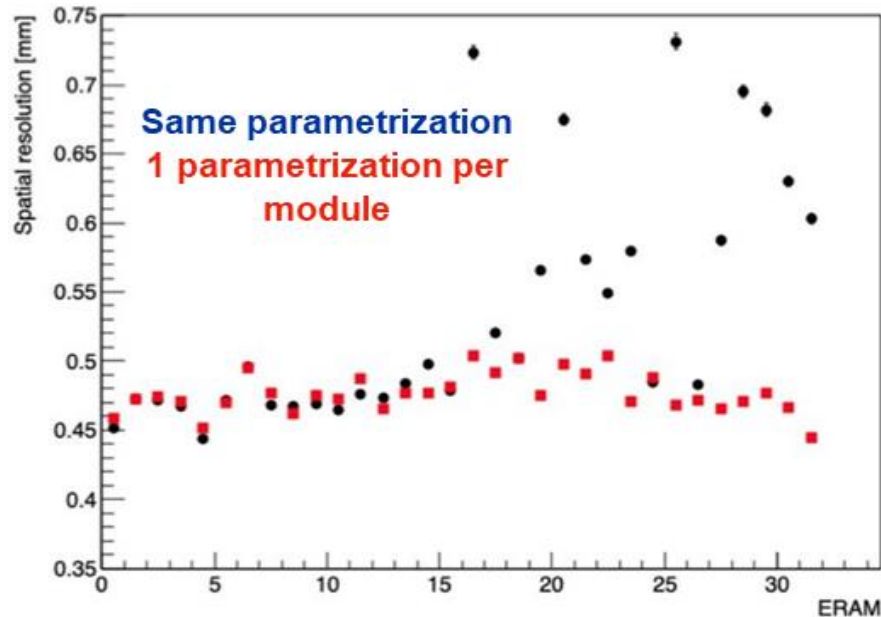
Non negligible RC variation among the same Endplate of the TPC



Instead of using one parametrization of the log(Q), ERAM dependent

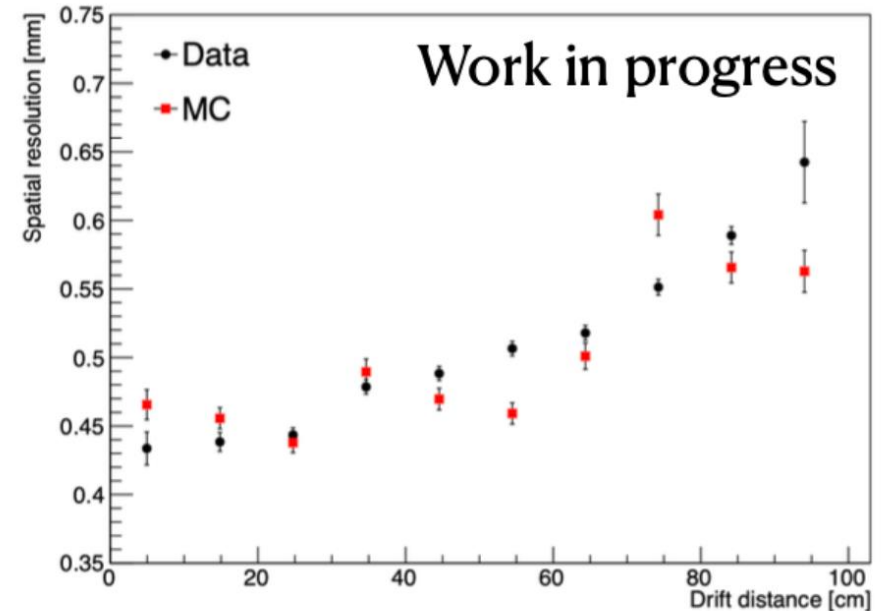
Spatial resolution after reparameterization

Work in progress, preliminary



With the new parametrization all modules have similar performances in terms of spatial resolution

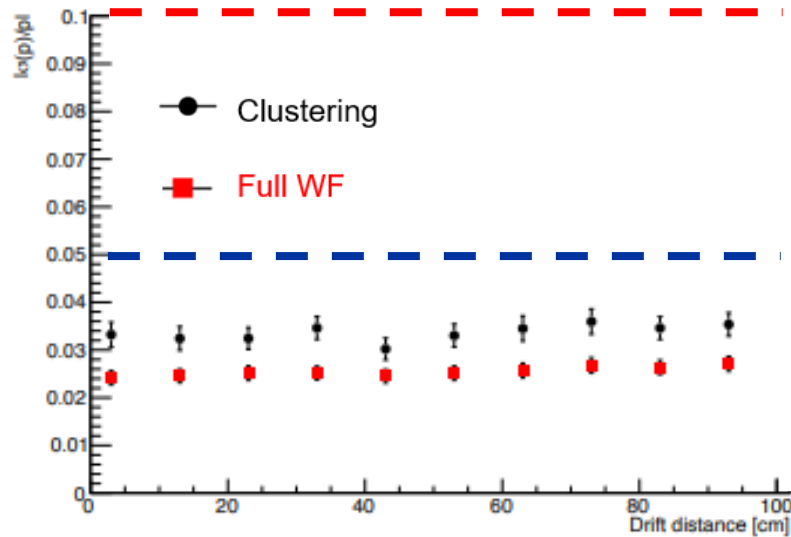
$$\sigma \approx 0.45 \text{ mm}$$



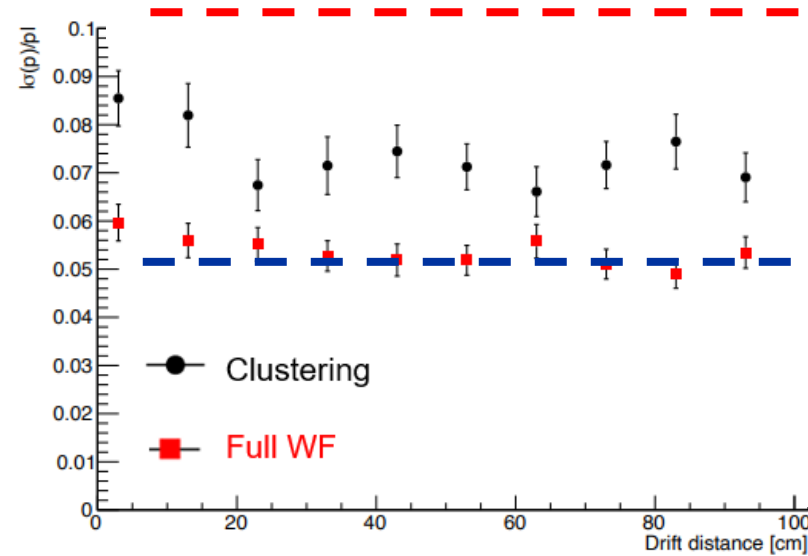
Reconstructing tracks: momentum resolution

σ_p/p momentum resolution as a function of track drift distance: simulated 700 MeV/c muons

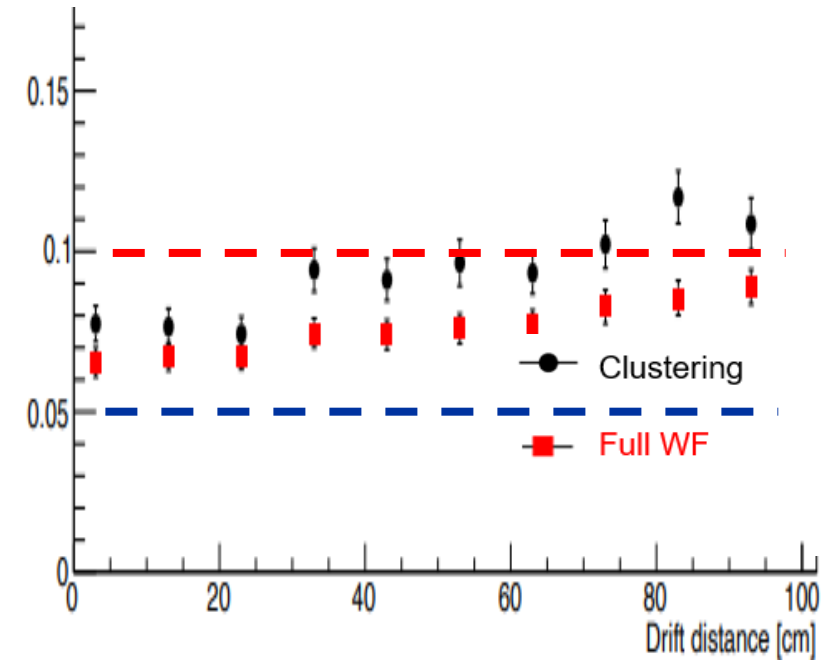
$\phi = 5.7^\circ$



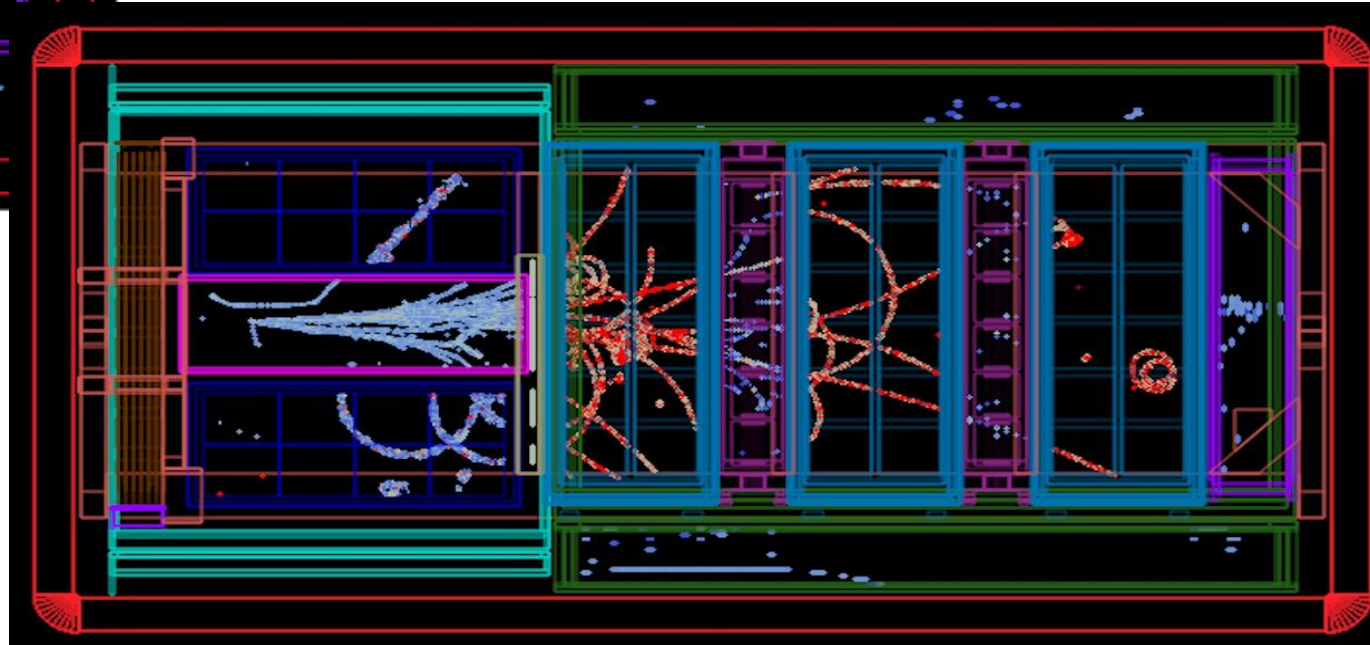
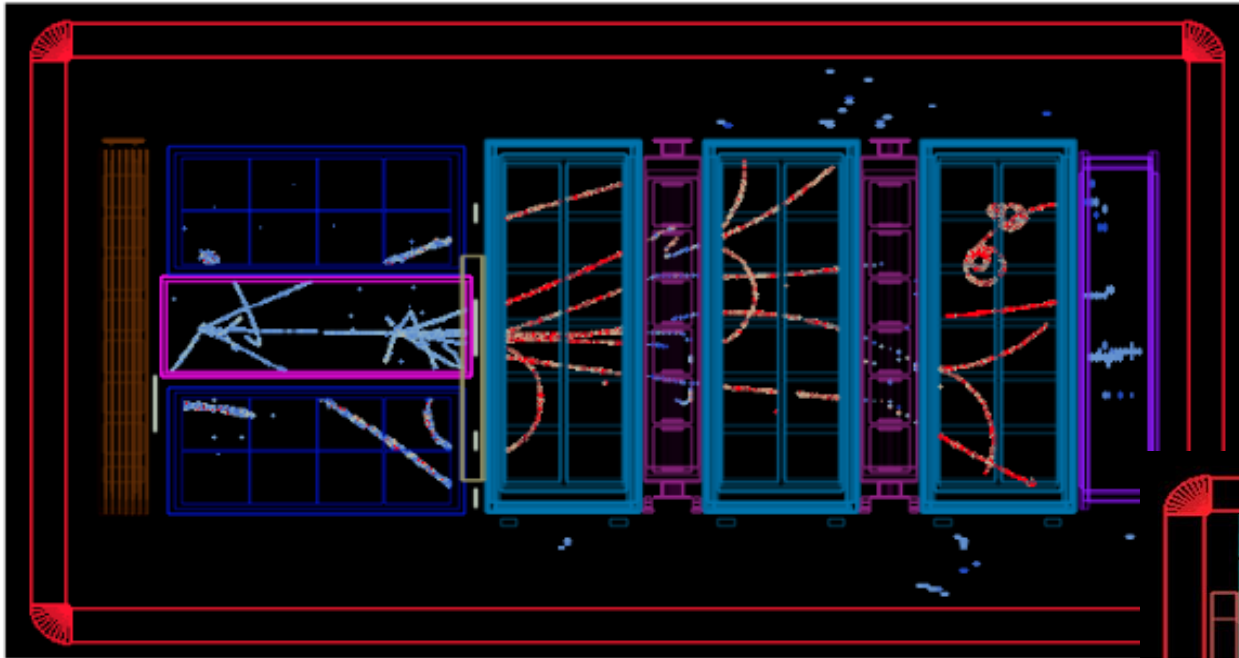
$\phi = 45^\circ$



$\phi = 84.3^\circ$



Event display, full ND280 detector!



Conclusions

Two new TPCs have been just installed in ND280 at JPARC

- Very stable operations in commissioning and technical runs
- First Neutrino Data taking just completed, restarting in October 2024

Field cages

- High ratio active/passive volume
- Highly effective insulation & E field uniformity
- Composite material technology exploited at the limit of the technology

Resistive MM with encapsulated anode

- Low resistivity & optimal charge spread & no sparks effects
- Series production allowed several detailed studies
- The ERAM technology is complex and delicate to produce as are all the resistive MPGDs. The expertise and excellent partnership with the CERN/PCB workshop enabled a high yield (~80%) of high-quality production
- New algorithms for square pads exploiting detailed response model under development

Conclusions

Two new TPCs have been just installed in ND280 at JPARC

- Very stable operations in commissioning and technical runs
- First Neutrino Data taking just completed, restarting in October 2024

Field cages

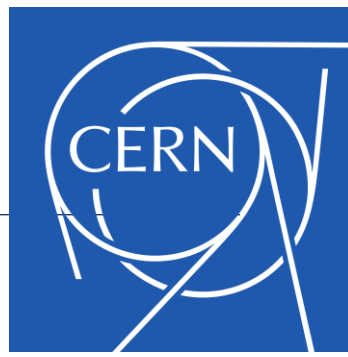
- High ratio active/passive volume
- Highly effective insulation & E field uniformity
- Composite material technology exploited at the limit of the technology

Resistive MM with encapsulated anode

- Low resistivity & optimal charge spread & no sparks effects
- Series production allowed several detailed studies
- The ERAM technology is complex and delicate to produce as are all the resistive MPGDs. The expertise and excellent partnership with the CERN/PCB workshop enabled a high yield (~80%) of high-quality production
- New algorithms for square pads exploiting detailed response model under development

Thanks!

Thanks to CERN



We would like to express our gratitude for the continuous and extremely valuable support from CERN

Burkard Schmidt, Roberto Guida, Frederic Merlet and colleagues → Gas system EP-DT/ED-DT-FS

Davide Tommasini, Roland Piccin, Sebastien Clement, Cedric Urscheler → Polymer lab/TE-MS

Rui de Olivera, Olivier Pizzirusso → EP-DT-EF

Eraldo Oliveri, Djunes Janssen → EP-DT-DD

Francesco Lanni, Lluís Secundino Miralles Verge Albert DE ROECK, Filippo Resnati → Neutrino Platform

Ahmed Cherif, Jean Philippe Rigaudt → Metrology/TE-MS-SMT

Antje BEHRENS, Jean Christophe Gayde → BE-GM-ESA

Mauro Taborelli, Colette Charvet, Marcel Himmerlich → TE-VSC-SCC

Paolo Chiggiato → TE-VSC

Patrick Muffat, Loredana ZENI Toberer, Laurence Planque, Stephanie Krattinger, Elsa Clerc → SCE-SSC-LS

Thanks to CERN



We would like to express our gratitude for the continuous and extremely valuable support from CERN

Burkard Schmidt, Roberto Guida, Frederic Merlet and colleagues → Gas system EP-DT/ED-DT-FS

Davide Tommasini, Roland Piccin, Sebastien Clement, Cedric Urscheler → Polymer lab/TE-MS

Rui de Olivera, Olivier Pizzirusso → EP-DT-EF

Eraldo Oliveri, Djunes Janssen → EP-DT-DD

Francesco Lanni, Lluís Secundino Miralles Verge Albert DE ROECK, Filippo Resnati → Neutrino Platform

Ahmed Cherif, Jean Philippe Rigaudt → Metrology/TE-MS-SMT

Antje BEHRENS, Jean Christophe Gayde → BE-GM-ESA

Mauro Taborelli, Colette Charvet, Marcel Himmerlich → TE-VSC-SCC

Paolo Chiggiato → TE-VSC

Patrick Muffat, Loredana ZENI Toberer, Laurence Planque, Stephanie Krattinger, Elsa Clerc → SCE-SSC-LS

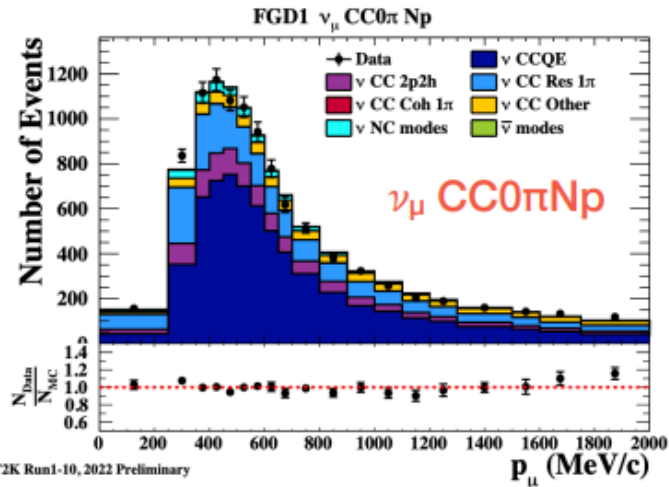
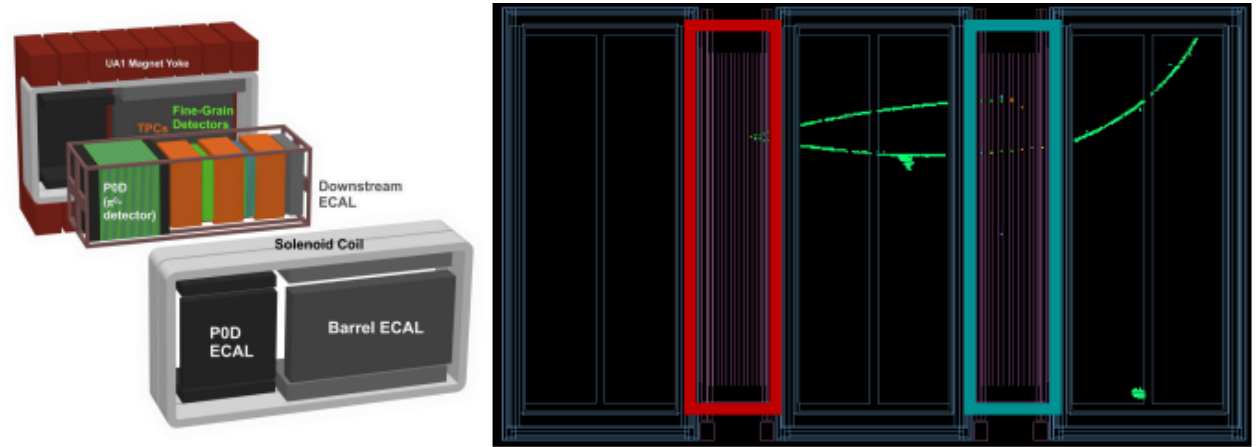
Thanks to INFN support at CERN and the CEA ANTENNA colleagues

Spare

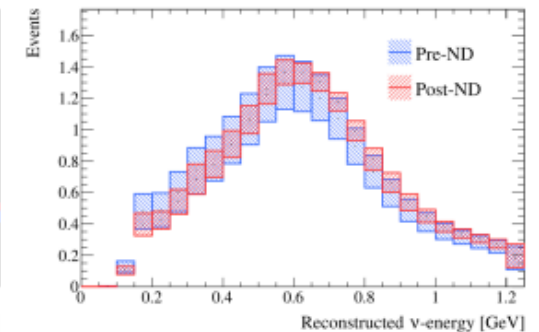
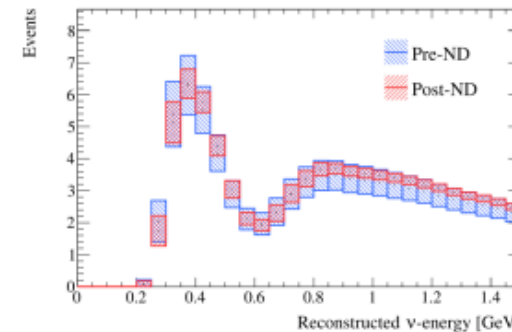
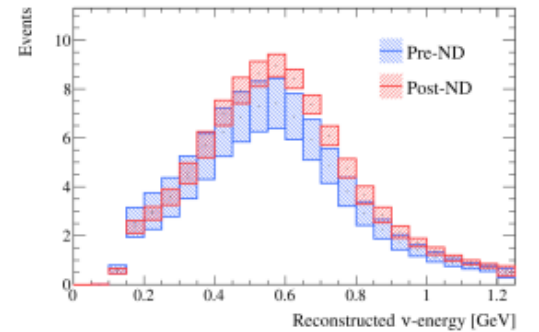
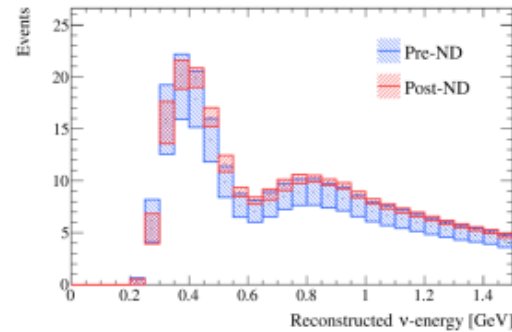
Just in Case

Near Detector impact on Oscillation Analysis

- ND280 magnetized detector
- Select interactions in FGD and measure muon kinematics in the TPCs
- Separate samples based on number of reconstructed pions (CC0 π , CC1 π , CCN π), protons, photons, etc
- Factor of ~ 3 reduction on the uncertainty on the event rates at the Far Detector



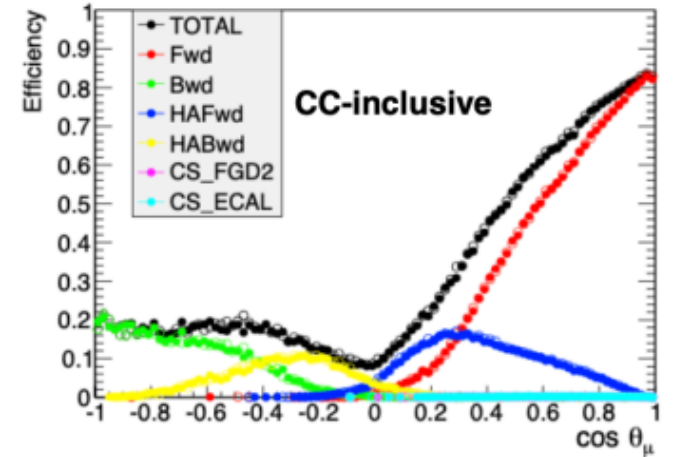
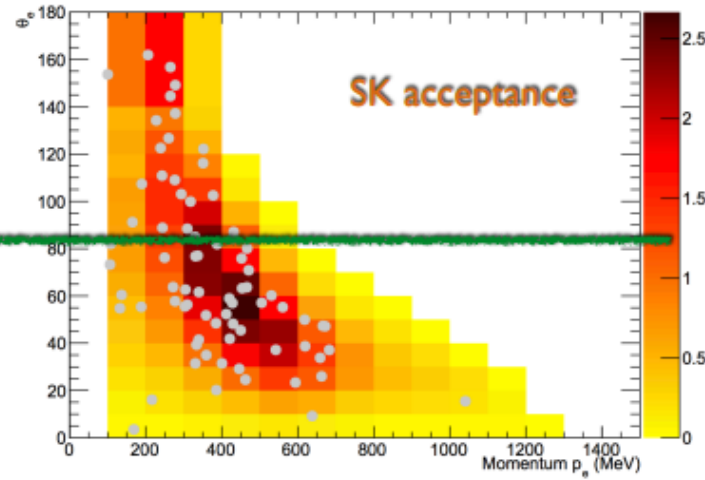
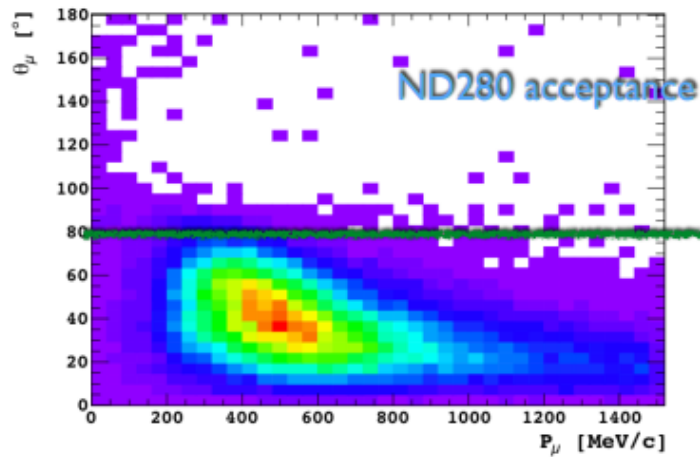
Sample	Pre-ND FIT error	Post-ND FIT error
FHC 1R μ	11.1%	3.0%
RHC 1R μ	11.3%	4.0%
FHC 1Re	13.0%	4.7 %
RHC 1Re	12.1%	5.9%
FHC 1Re 1d.e.	18.7%	14.3%



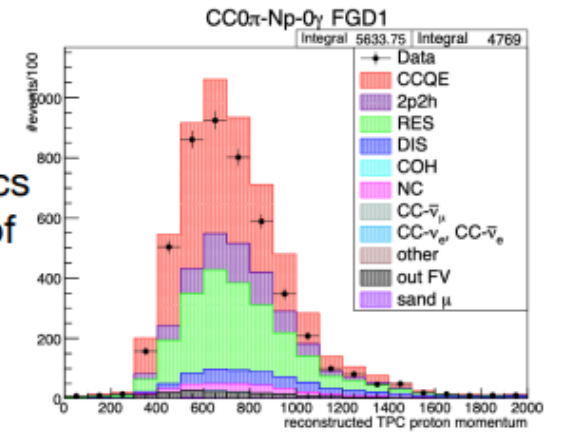
(d) $\bar{\nu}$ -mode 1R μ

(e) $\bar{\nu}$ -mode 1Re

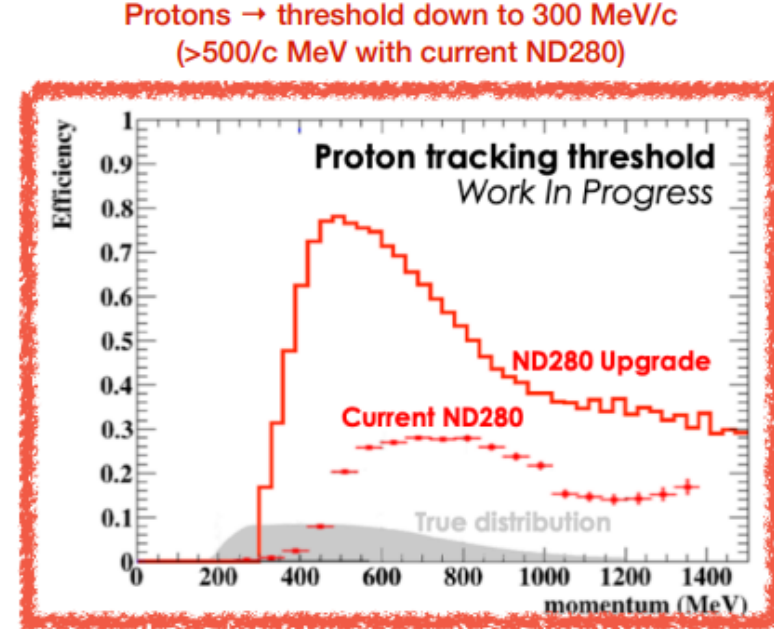
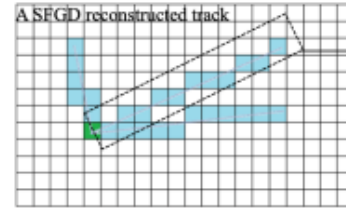
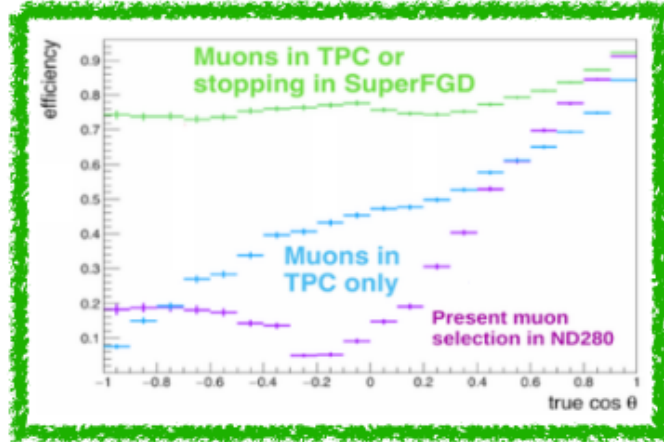
ND280 limitations



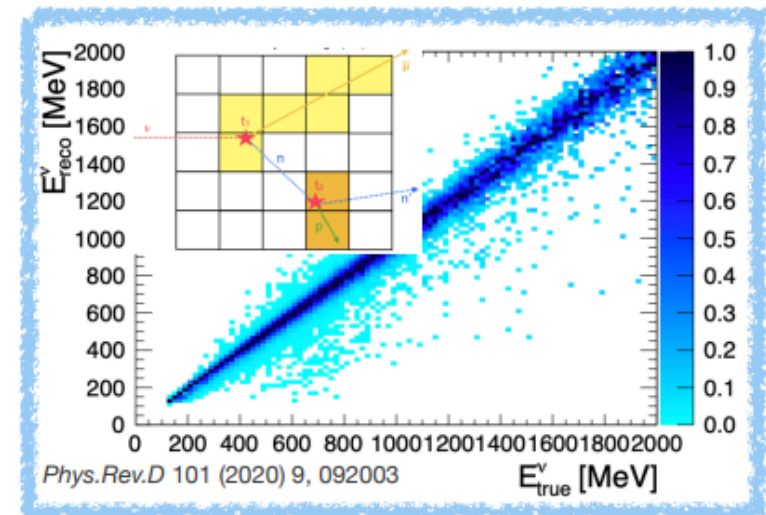
- Improve angular acceptance ν
- Better reconstruction and usage of the hadronic part of the interactions!
 - Currently samples are selected according to their topology (0π , 1π , $1p$, $N\pi$, ...) but the kinematics of the hadrons is not used in any way in the constraint on flux and x-sec systematics \rightarrow plenty of additional information to be exploited
 - This is due to both, a low efficiency from ND280 to reconstruct hadrons and the difficulties in modeling the x-sec systematics for the hadronic part
 - With the upgrade we plan to improve the efficiency to reconstruct hadronic part



ND280 Upgrade improvements



- High-Angle TPCs allow to reconstruct muons at any angle with respect to beam
- Super-FGD allow to fully reconstruct in 3D the tracks issued by ν interactions → lower threshold and excellent resolution to reconstruct protons at any angle
 - Improved PID performances thanks to the high granularity and light yield
- Neutrons will also be reconstructed by using time of flight between vertex of $\bar{\nu}$ interaction and the neutron re-interaction in the detector



Mantle resistance

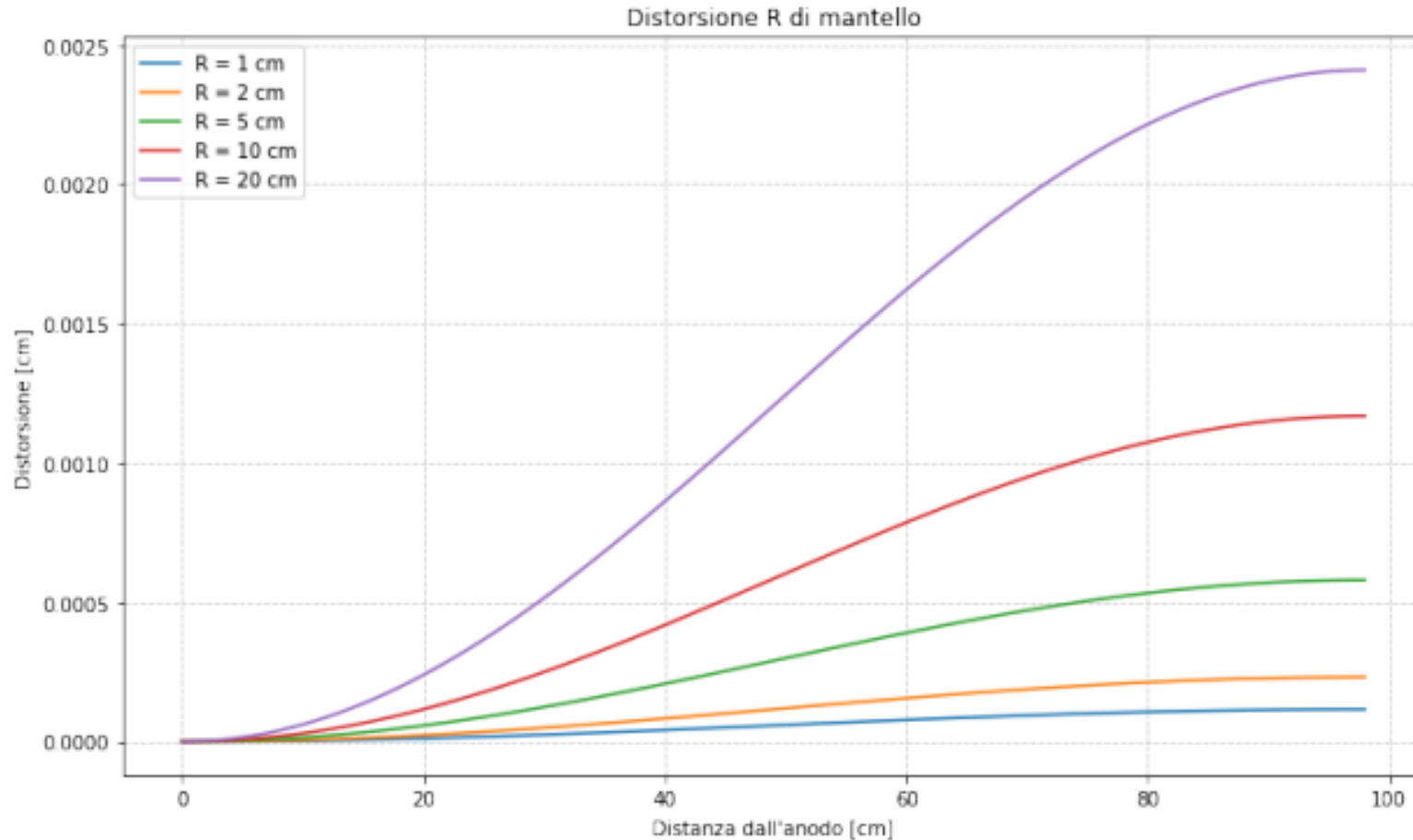


Figura 4.2: Spostamento lungo R del punto di arrivo di un elettrone causato da una resistenza R_{man} di un mantello isolante mille volte il valore della catena di resistori R. La distorsione é mostrata come funzione del punto di partenza z (Distanza dall'anodo).

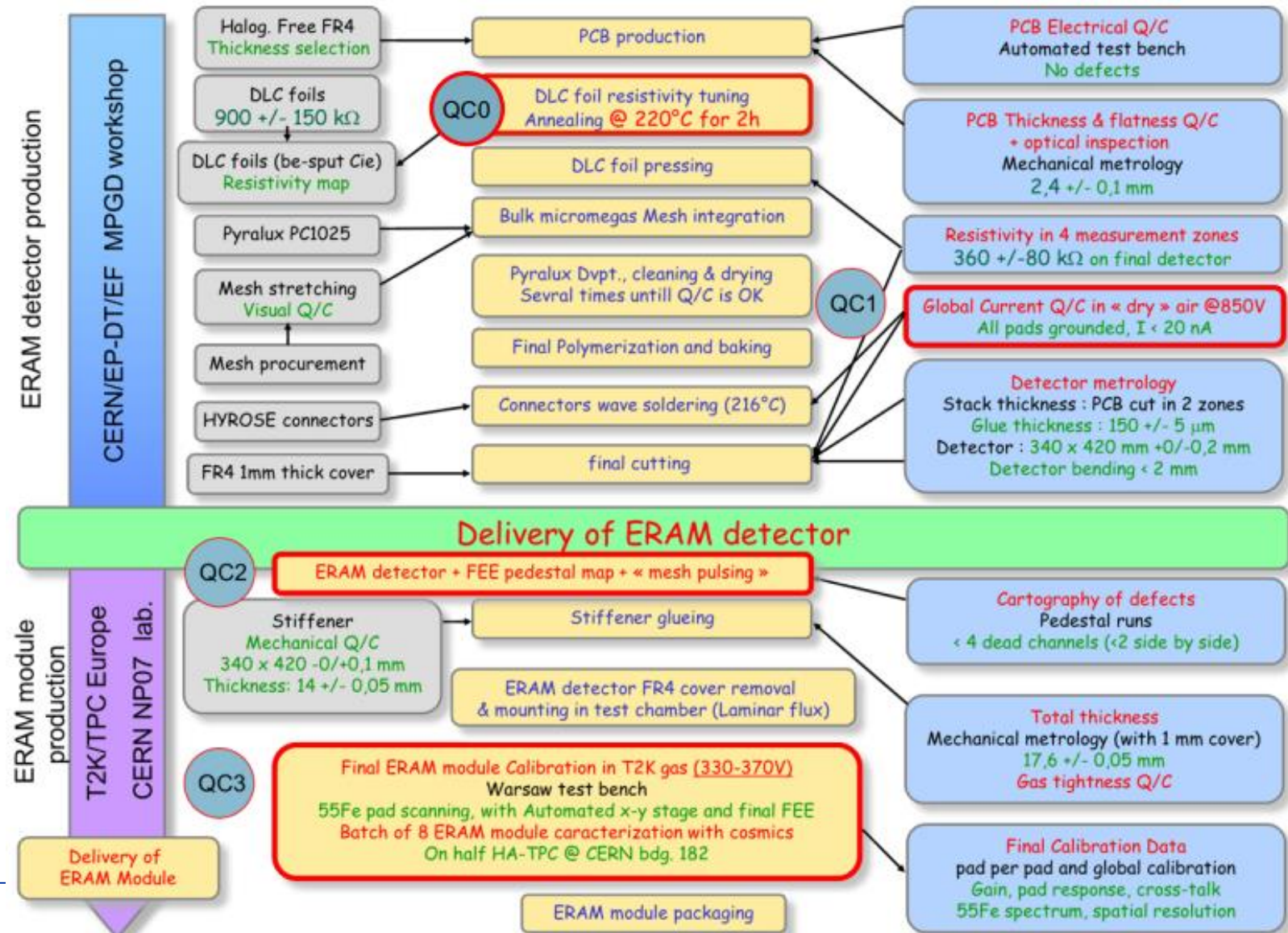
ERAM Production - about 50 detectors

Crucial steps in production (needed tuning)

- 1) **Selecting DLC foil resistivity**
 - Large variations from DLC provider
 - Value stable after annealing
- 2) **Gluing steps by Pressing**
 - DLC to PCB
 - Stiffener to DLC-PCB

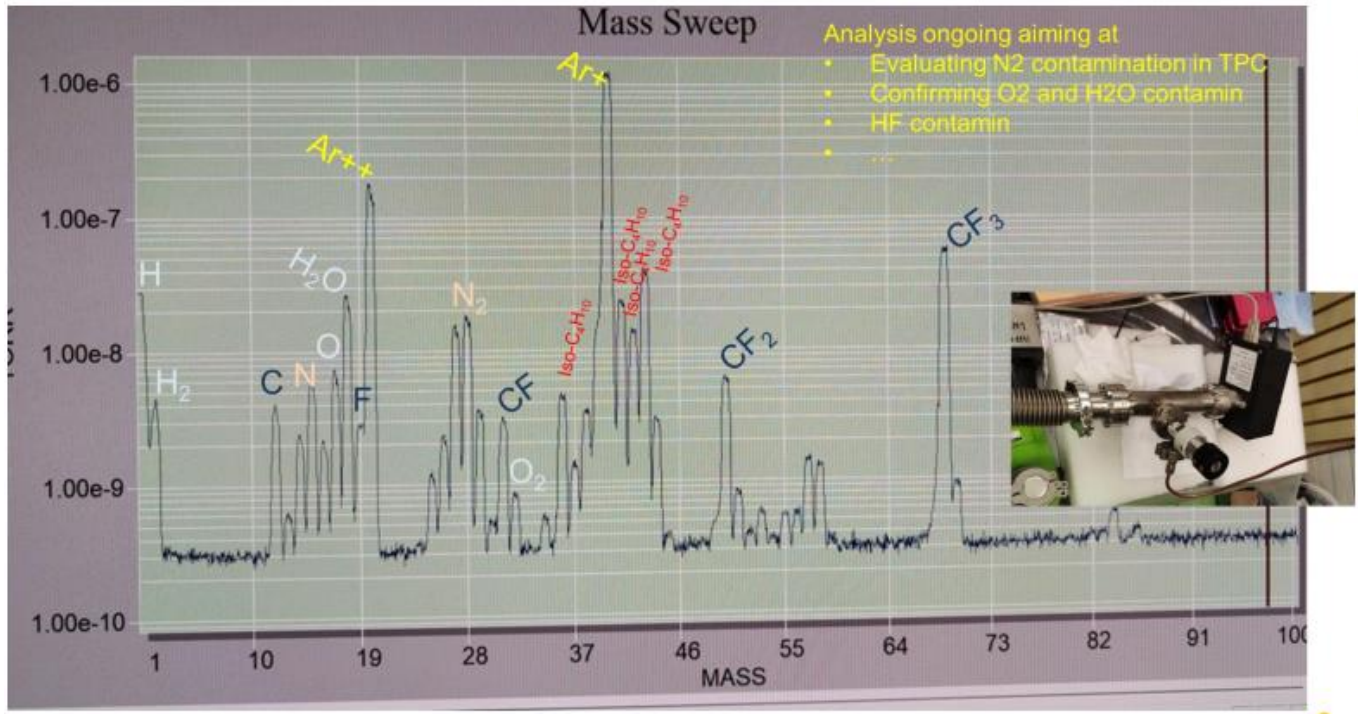
X-rays Test Bench at CERN was fundamental to

- 1) **Qualify, characterize and calibrate** all prototypes and series ERAMs
- 2) support the development of **detailed ERAM response model**



Field Cage assembling, characterization at CERN

Gas contamination from Field Cage – other contaminants



- Analysis ongoing aiming at
- Evaluating N₂ contamination in TPC
- Confirming O₂ and H₂O contaminin
- HF contaminin
- ...

Analysis of gas composition during cosmetics test in May

- More accurate estimates ongoing
- N₂ analysis ←
 - HCl acid
 - Evolution in time of components

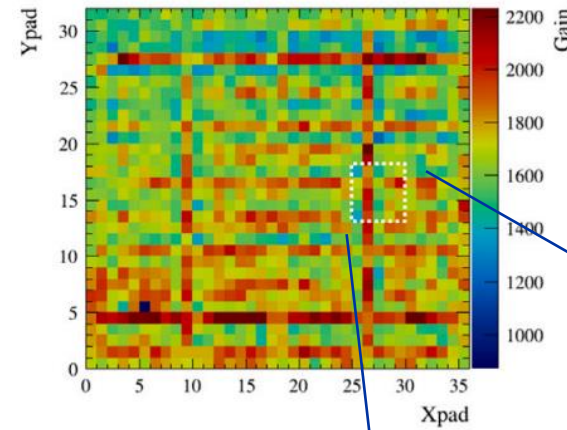
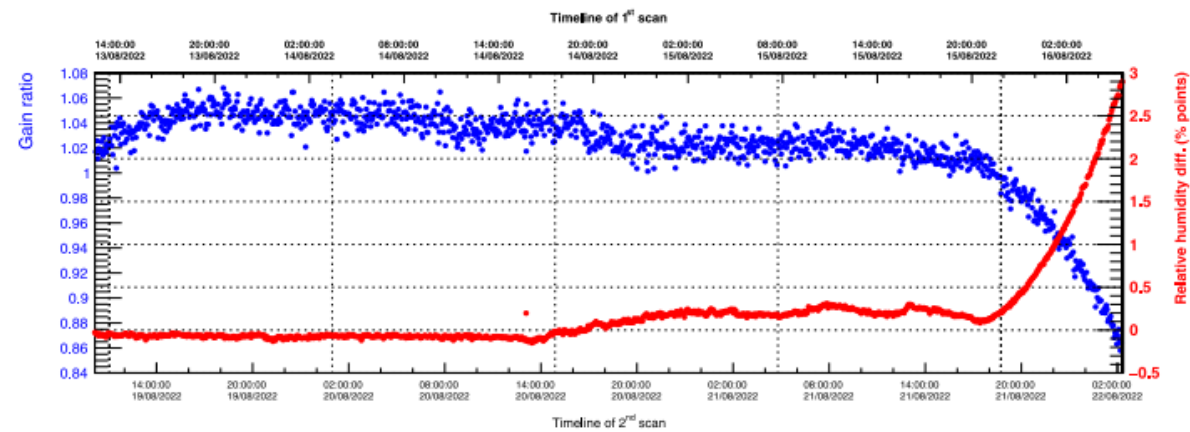
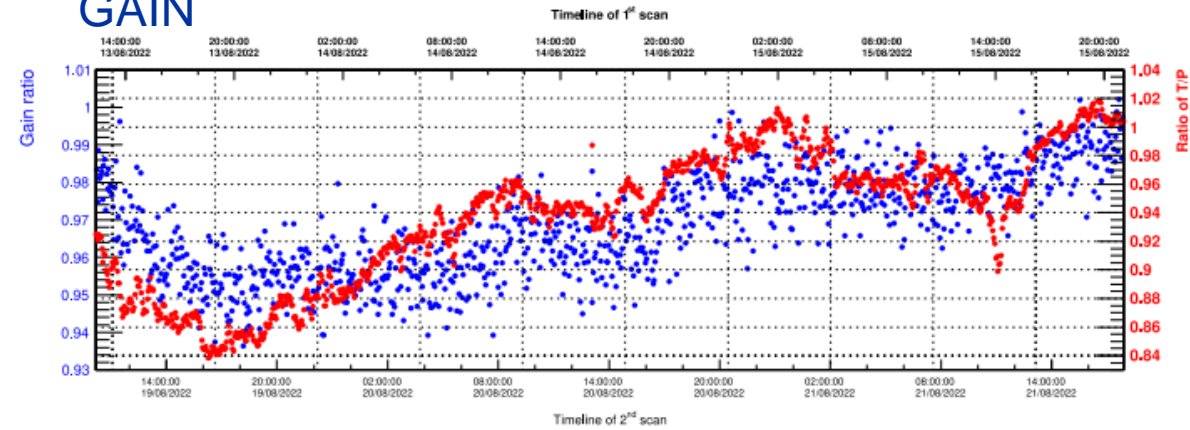
Main components → multi-peaks consistent with ratios found in literature

- H₂O (+ HO) contamination ~2% → consistent with other sensors (Vaisala)
- O₂ peak below sensitivity → consistent with ppm level → need further checks
- No HF acid apparently (below Ar++)



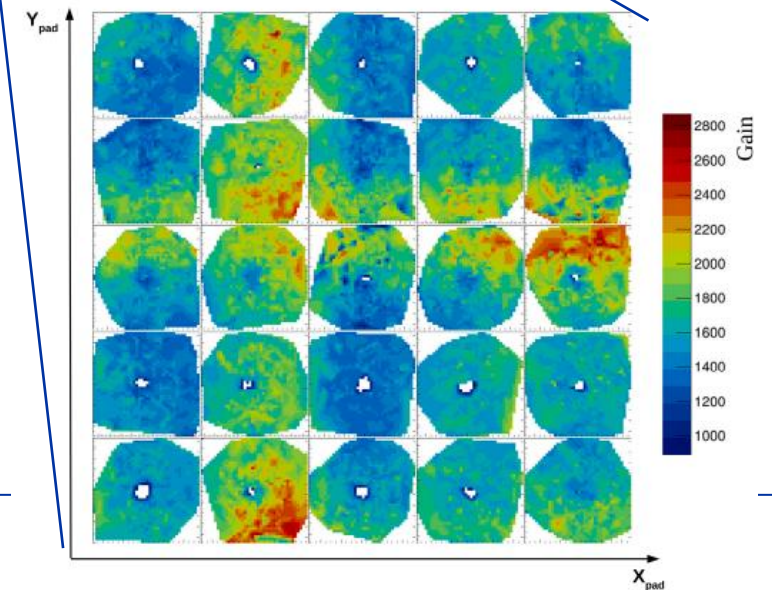
ERAM Series Production experience

Effect of gas density on (gas) GAIN



Fine grain scan

GAIN as a function of Pad position

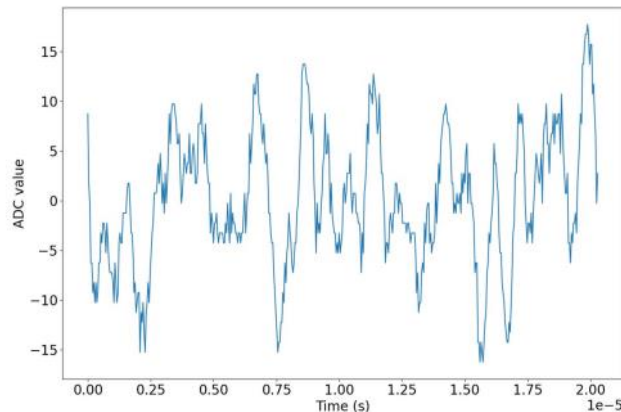


ERAM detector response – Simulation

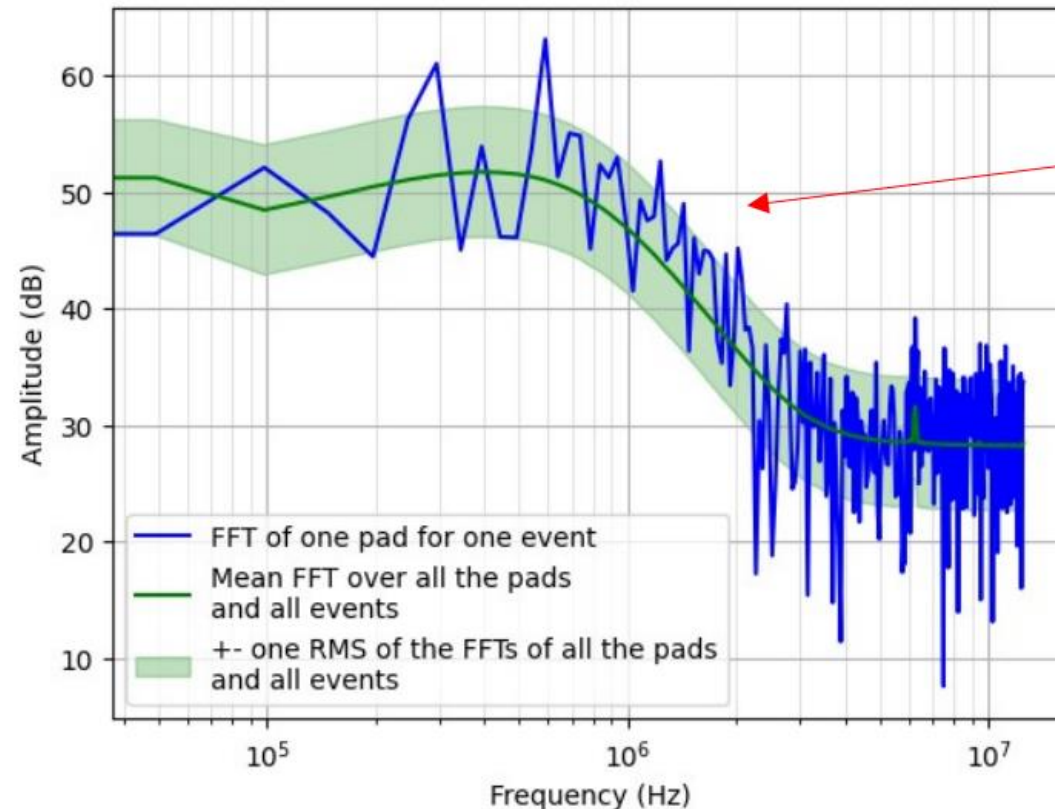
Use of the model for Simulation of charge deposition in events
 Where additional ingredient is **noise detailed modeled**

$T_p = 412 \text{ ns}$
 $F_s = 25 \text{ MHz}$

Record of the baseline (no trigger) by D. Calvet



One record
 $T_p = 412 \text{ ns}$
 $F_s = 25 \text{ MHz}$



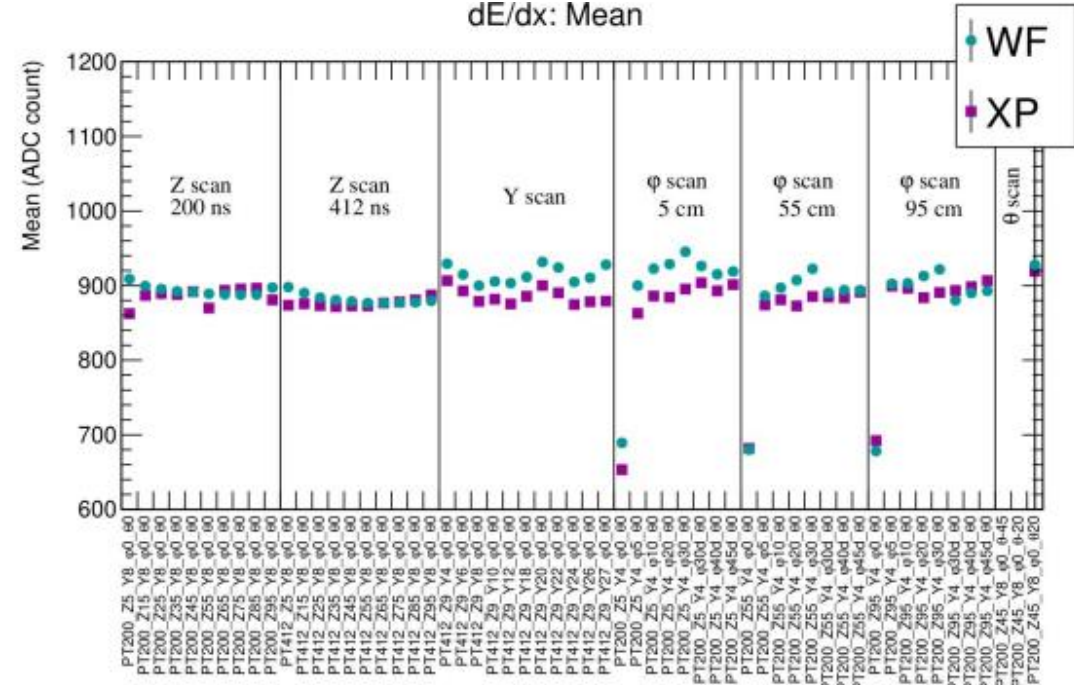
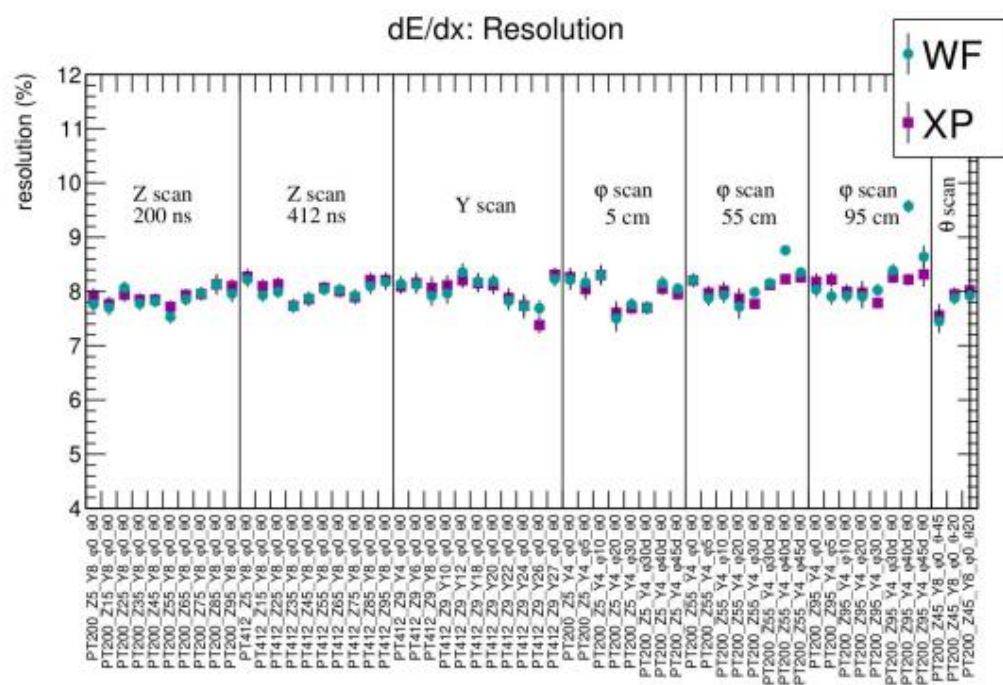
Dominated by frequencies lower than 1 MHz

The spectrum can be fitted quite decently with a "simple" analytical function

$$\sqrt{\left[\frac{A_0}{f^2}\right]^2 + [A_1 \sqrt{f} H_{after}(f)]^2 + A_2^2}$$

Reconstructing tracks dE/dx

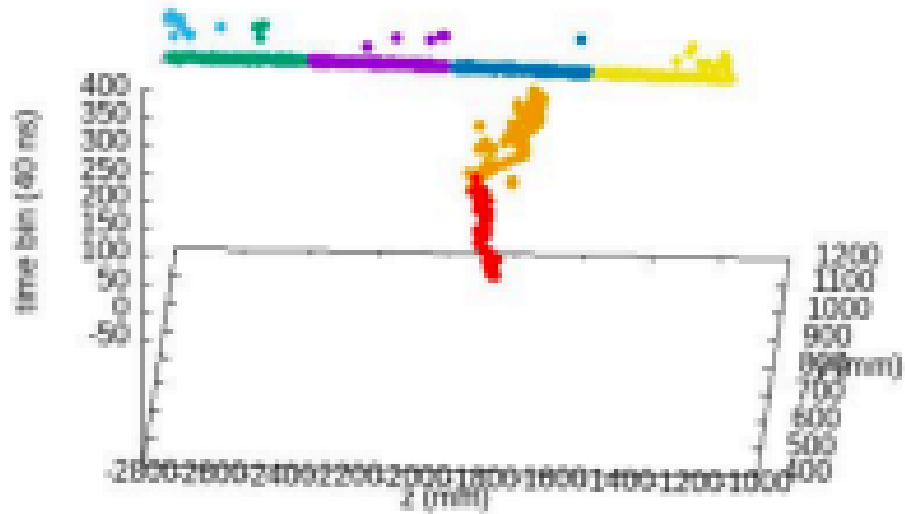
dE/dx – comparison of SWF and XP methods on Test Beam data (4GeV electrons, DESY)



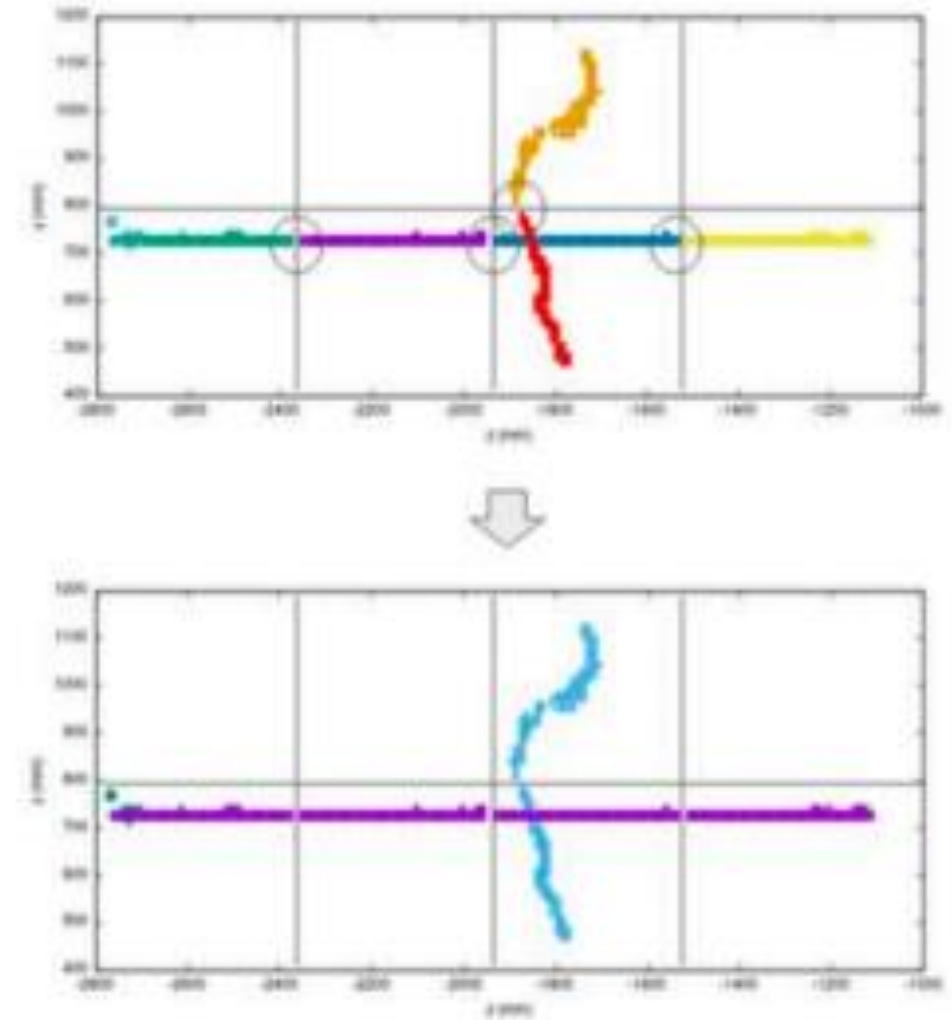
- Very good agreement overall
- Better resolution with XP with diagonal tracks

- Disagreement at small drift distance: reflects the track fitting quality
- Disagreement for Y scan: taken at small drift distance
- Disagreement for diagonal tracks: using only on correction function for WF_{sum} is not suitable

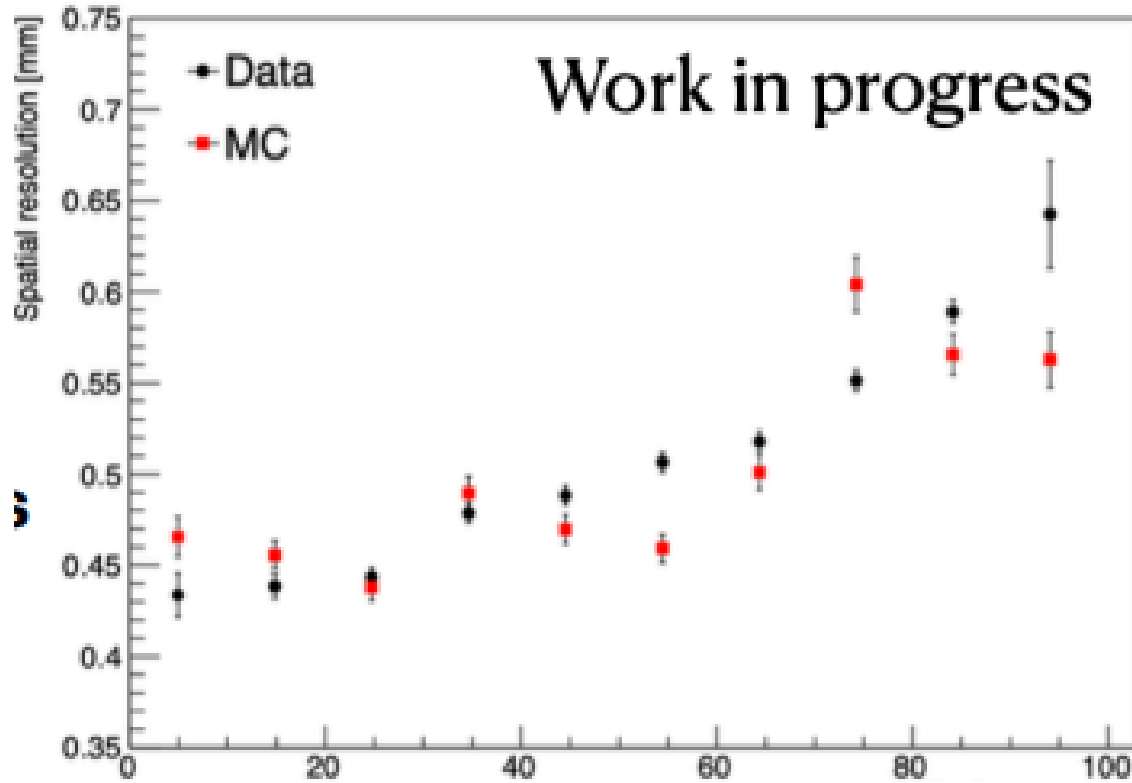
Reconstructing tracks – pattern recognition



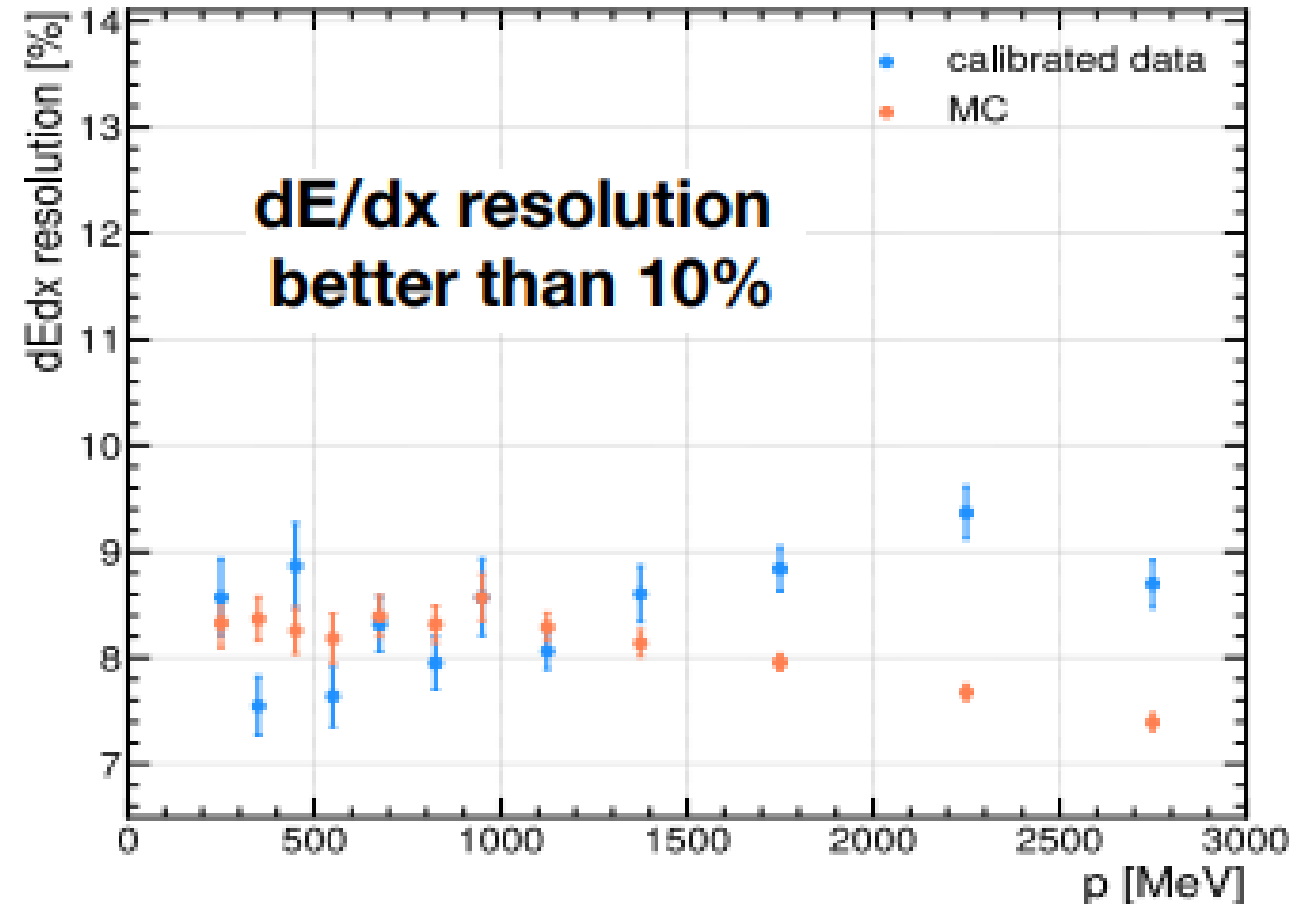
- Time and charge definition for each hit
- Waveform multipeak search in order to differentiate vertices and crossing trajectories
- Merging between different ERAMs and End Plates



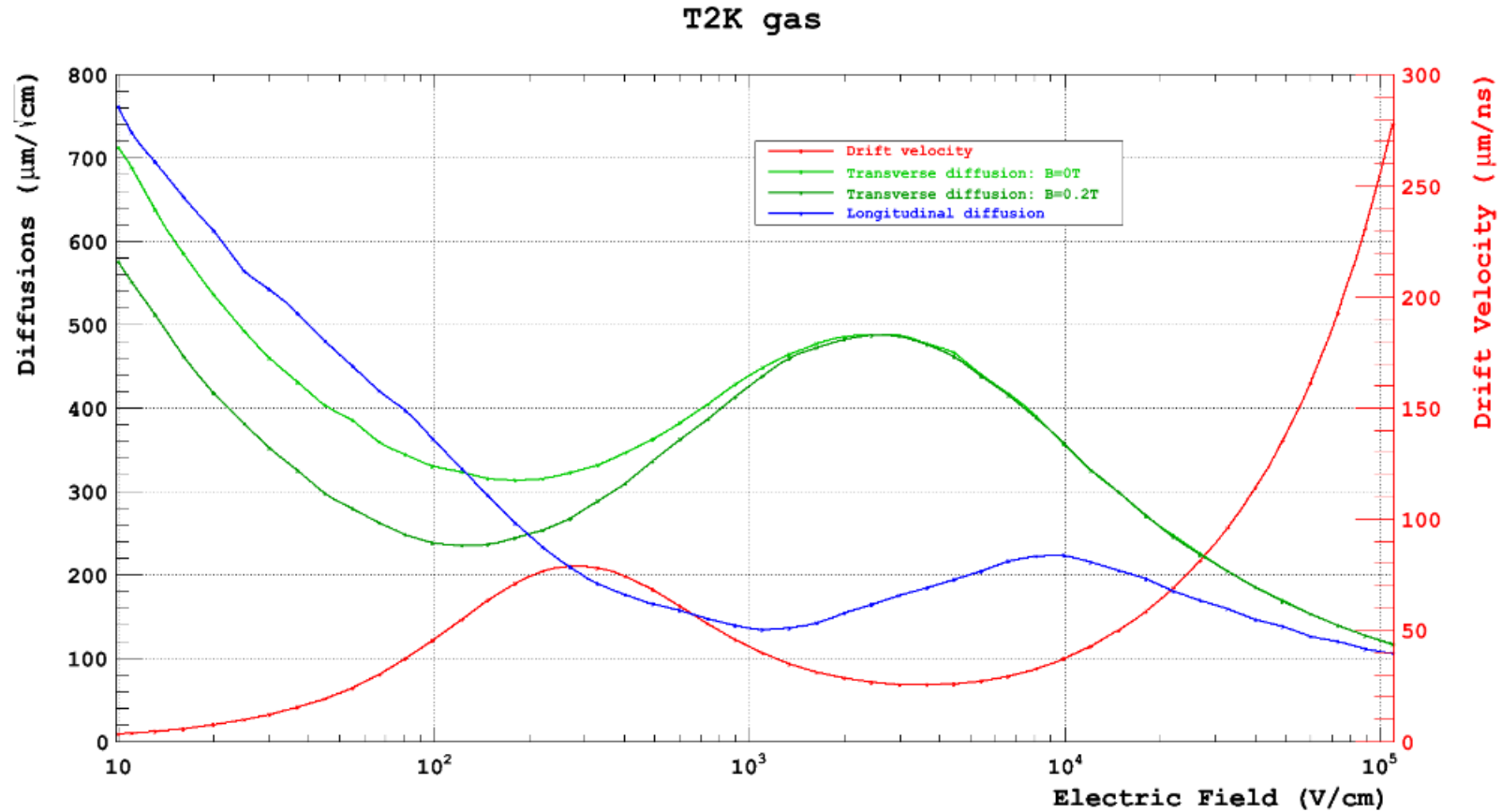
Reconstructing tracks – trajectory fitting



**Spatial resolution
~500 μm with muons**

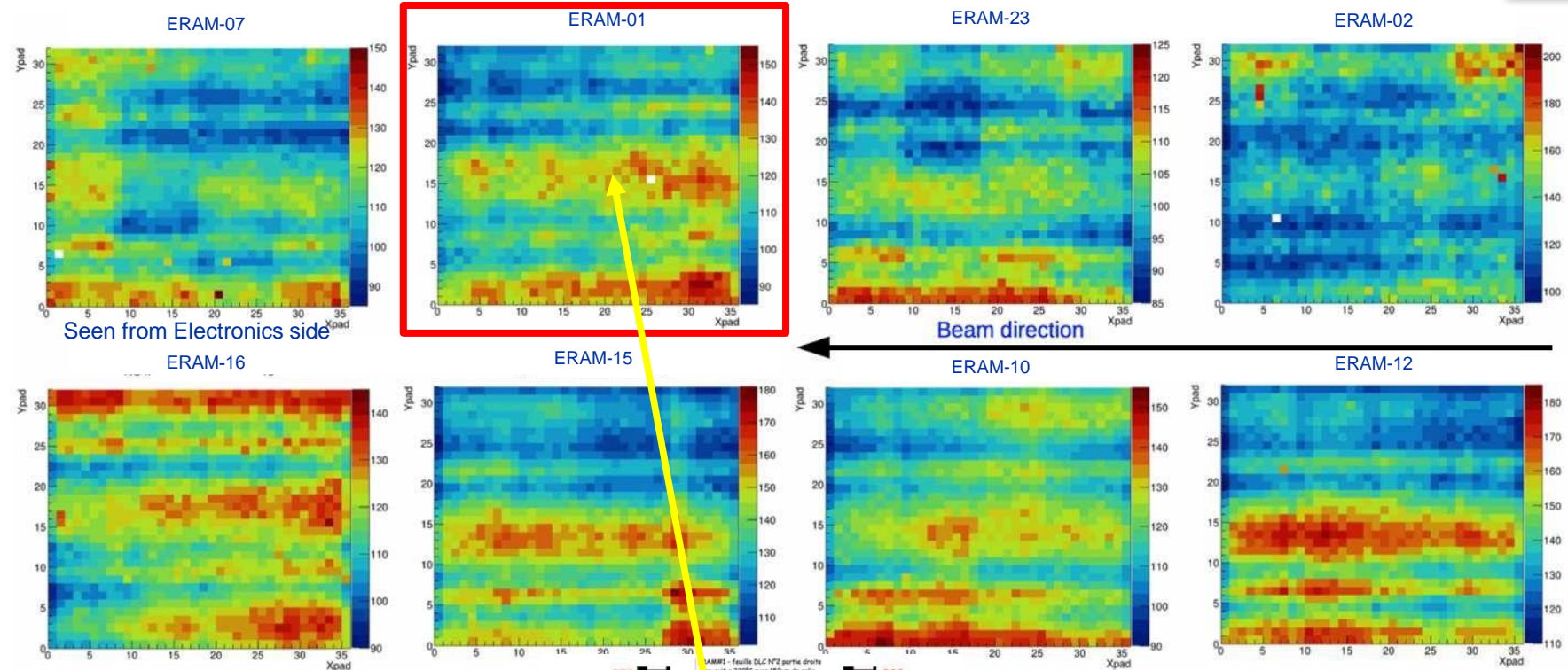


T2K gas properties

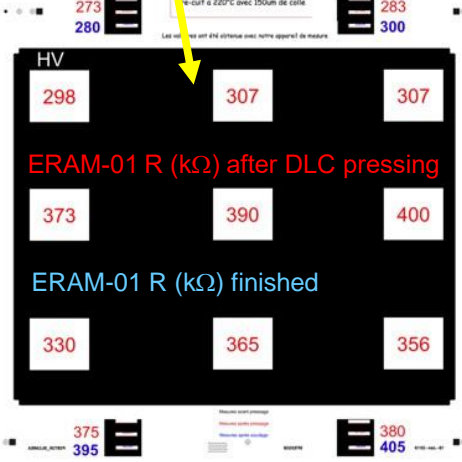




Ref: S. Joshi (Irfu/PhD)



RC is derived from the fit of the pad signal waveforms datas (leading and neighbours) with the complete modelization of the detector response



ERAM	RC _{mean} (ns/mm ²)	Gain _{mean}	
01	116.9	1944	
02	128.6	1736	
03	116.4	1987	
07	111.8	1898	
10	120.9	1697	
12	145.4	1635	
15	135.1	1629	
16	120.4	1705	
18	68.98	1277	~1/2 RC as expected
23	101.6	1393	
29	102	1318	~ RC as expected
30	114.3	1161	

RC is quite well correlated to the measured DLC resistivity

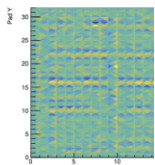


Figure 31: A map of gain non-uniformity shift of the mean amplitude reconstruct pad under study with respect to the me

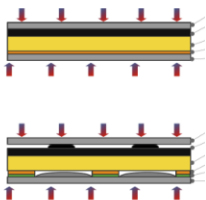
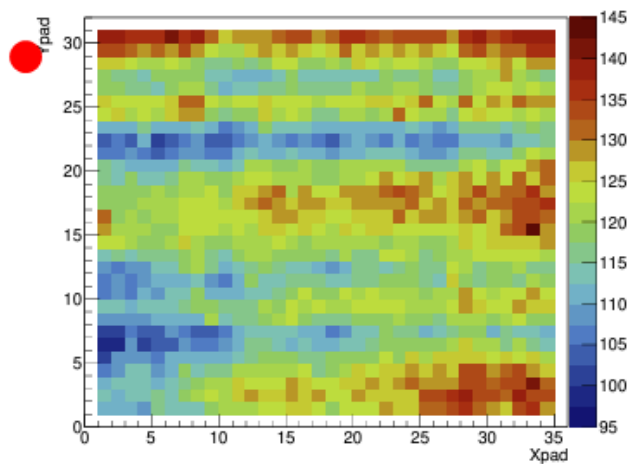
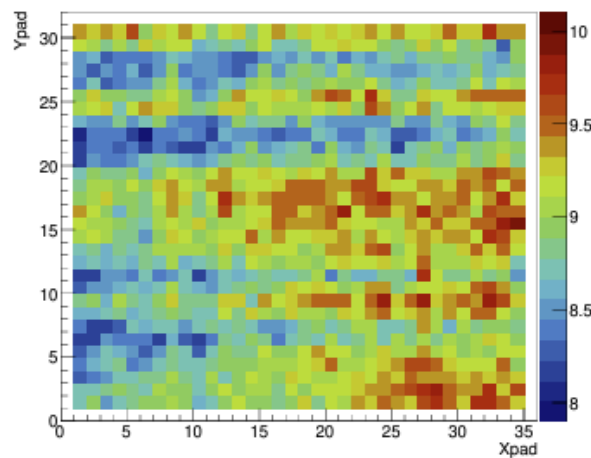


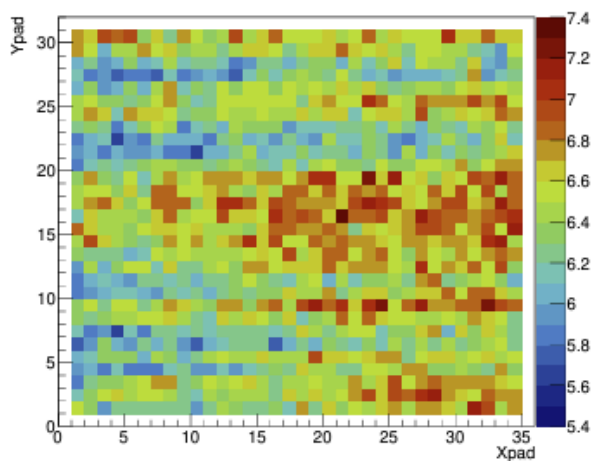
Figure 32: Schematic view of the DLC resulting in the non-uniformities observed. The arrows represent the mechanical stress when the soldermask is removed and re



(a)



(b)



(c)

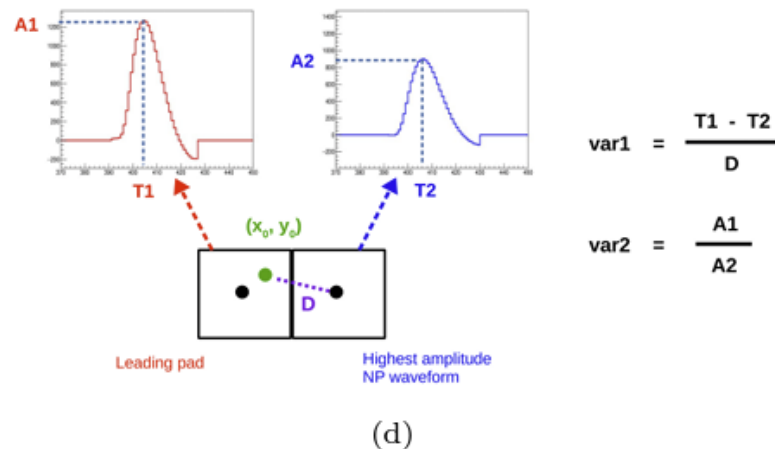
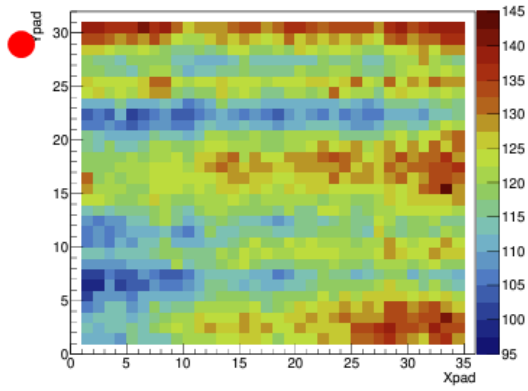
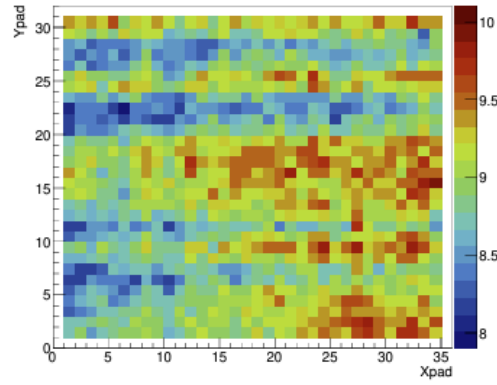


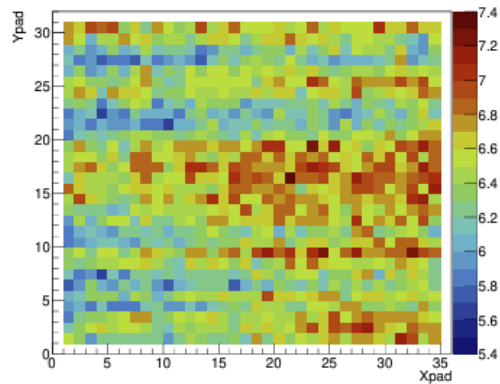
Figure 23: Comparing the features of an RC map (a) with the maps of two different basic-level variables (b) and (c) for ERAM-16. Variables var1 and var2 described in plot (d) are used to construct the maps (b) and (c) respectively.



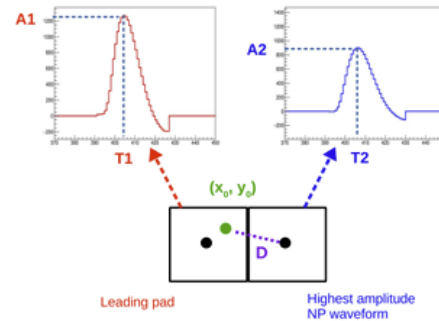
(a)



(b)



(c)



(d)

$$\text{var1} = \frac{T1 - T2}{D}$$

$$\text{var2} = \frac{A1}{A2}$$

x_0, y_0 extracted by baricentrum
Fit independent

Figure 23: Comparing the features of an *RC* map (a) with the maps of two different basic-level variables (b) and (c) for ERAM-16. Variables var1 and var2 described in plot (d) are used to construct the maps (b) and (c) respectively.

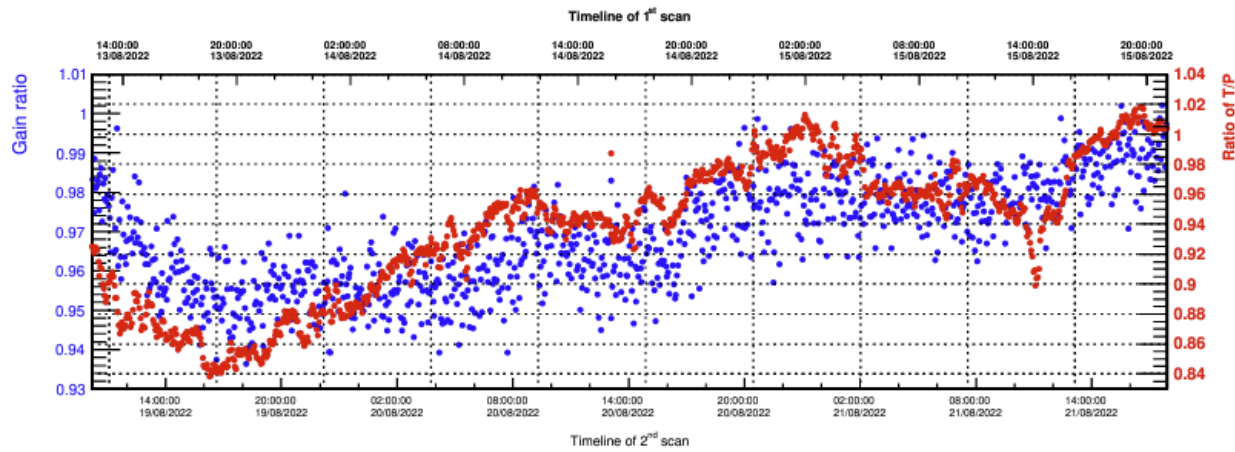


Figure 35: Effect of T/P on gain of an ERAM. The top and bottom x -axes represent the timelines of the two full detector scans.

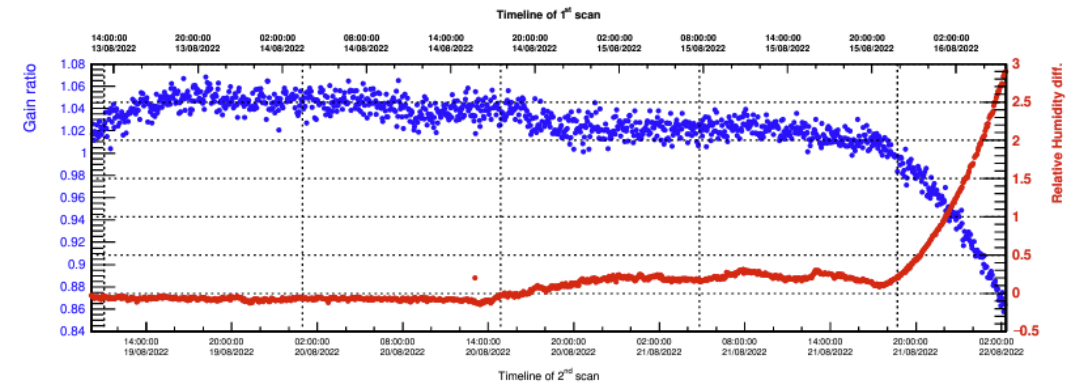


Figure 36: Effect of relative humidity on gain of an ERAM. The top and bottom x -axes represent the timelines of the two full detector scans.

Table 7. Typical Electrical Properties of Kapton® Type HN and HPP-ST Films

Property Film Gauge	Typical Value		Test Condition	Test Method
Dielectric Strength	V/μm (kV/mm)	(V/mil)		
25 μm (1 mil)	303	(7700)	60 Hz 1/4 in electrodes 500 V/sec rise	ASTM D-149
50 μm (2 mil)	240	(6100)		
75 μm (3 mil)	201	(5,100)		
125 μm (5 mil)	154	(3900)		
Dielectric Constant				
25 μm (1 mil)		3.4	1 kHz	ASTM D-150
50 μm (2 mil)		3.4		
75 μm (3 mil)		3.5		
125 μm (5 mil)		3.5		
Dissipation Factor				
25 μm (1 mil)		0.0018	1 kHz	ASTM D-150
50 μm (2 mil)		0.0020		
75 μm (3 mil)		0.0020		
125 μm (5 mil)		0.0026		
Volume Resistivity		$\Omega\cdot\text{cm}$		
25 μm (1 mil)		1.5×10^{17}		ASTM D-257
50 μm (2 mil)		1.5×10^{17}		
75 μm (3 mil)		1.4×10^{17}		
125 μm (5 mil)		1.0×10^{17}		

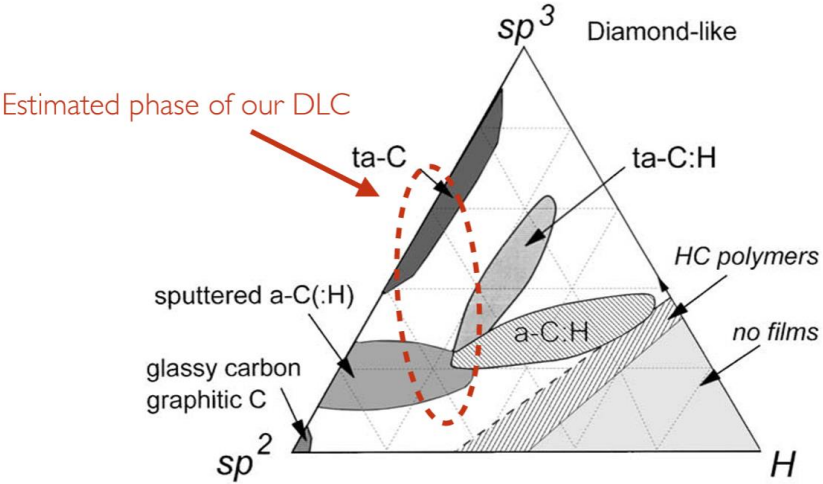
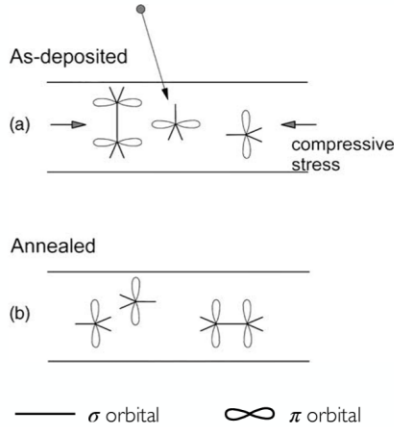
Although a-C:H and ta-C belong to the same material family, they are not produced by the same coating process. a-C:H is achieved by **PECVD** (Plasma Enhanced Chemical Vapor deposition) in a gaseous environment. Whereas ta-C is produced by PVD-arc (Physical Vapor deposition arc) from a solid carbon target. PVD-arc technology enables the production of a ta-C coating with a higher percentage of sp³ hybridization without hydrogen and providing a higher hardness.

• Thermal annealing of ta-C is well known

- a-C:H as well. But,
- “Thermal annealing of a-C:H also reduces the stress, as in ta-C. However, as the bonding in a-C:H is less stable during annealing, annealing is less useful in this case.”

• Mechanism described

- Thermal annealing converts a small fraction of sp³ (2%) to sp²
 - Distance between atoms is different between sp² and sp³
 - New sp² structure has aligned electron orbitals
- The conversion causes **exponential decrease** in resistivity
- Compressive stress relieved by new sp² structure with electron orbitals aligned



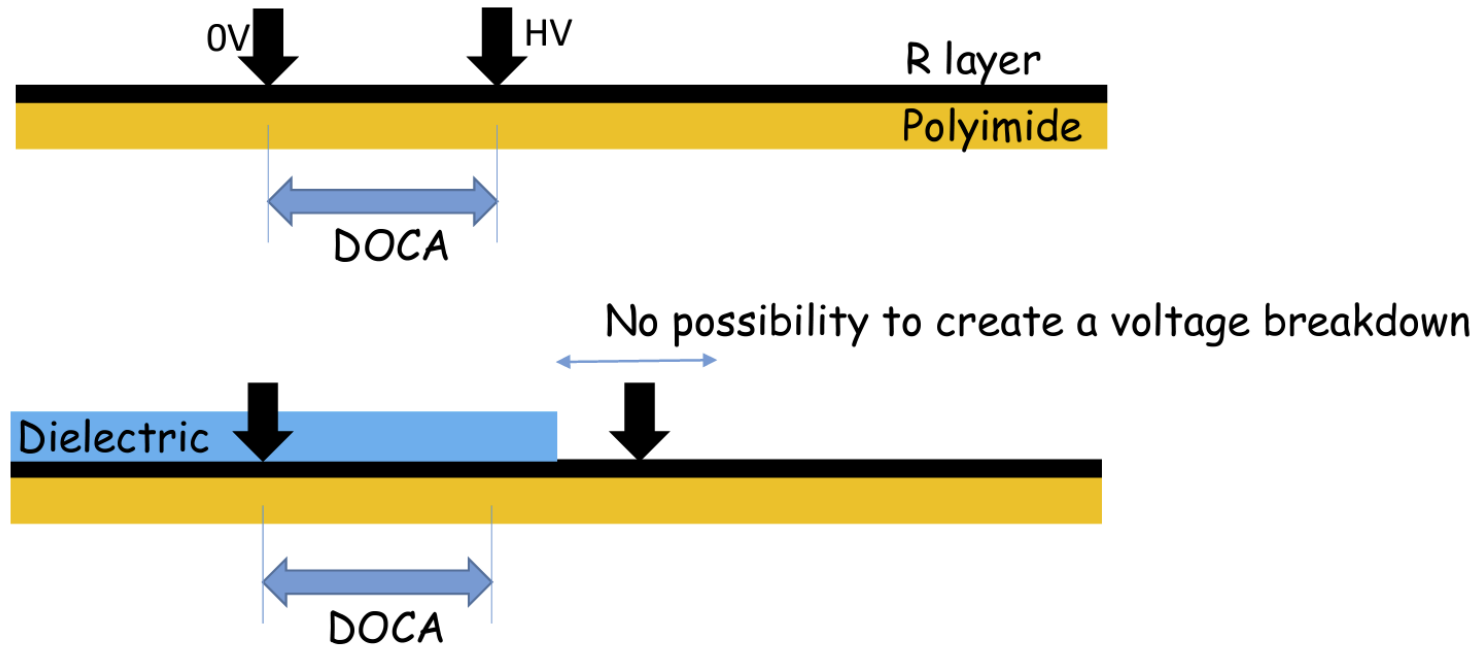
Kensuke Yamamoto^A

S. Ban^A, W. Li^A, A. Ochi^B, W. Ootani^A, A. Oya^A, H. Suzuki^B, M. Takahashi^B
 (^AThe University of Tokyo, ^BKobe University)

DOCA

(Distance Of Closest Approach)

Breakdown of the resistive layer ←   No effect on the resistive layer



A breakdown of the resistive layer means creating a low Ohmic channel in the layer

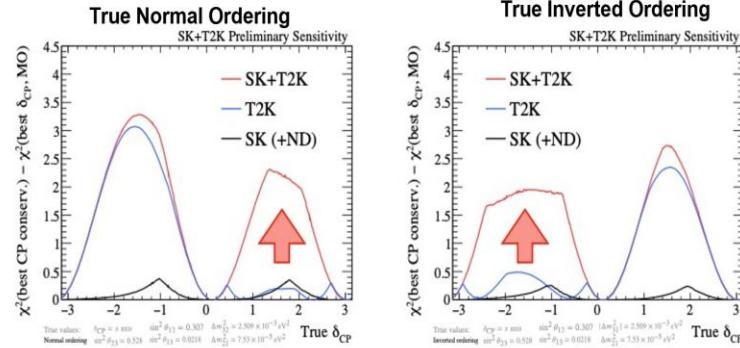
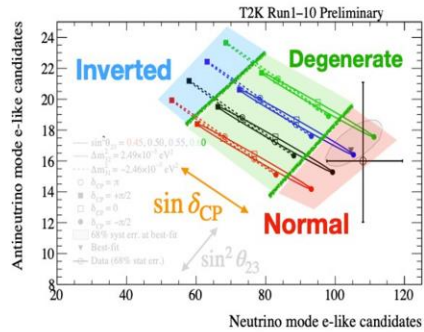
T2K+SK joint analysis

- T2K has good sensitivity to δ_{CP} but mild sensitivity to mass ordering
- SK has good constraint on mass ordering but not on δ_{CP}
- Adding SK atmospheric sample allows to break the degeneracies between the CP violation parameter δ_{CP} and the mass ordering \rightarrow boost sensitivity to CP

Both experiments individually prefer normal ordering and $\delta_{CP} \sim \pi/2$, T2K prefers upper octant, SK prefer lower octant

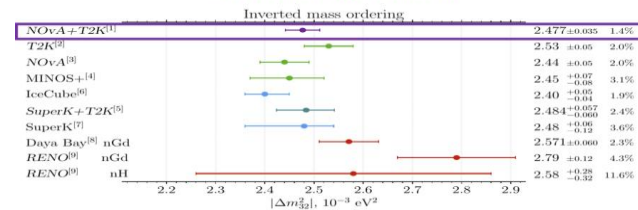
We performed Bayesian and Frequentist analyses \rightarrow frequentist analyses shown today

The CP-conserving value of the Jarlskog invariant is excluded with a significance between 1.9 and 2 σ



NOvA-T2K joint fit: takeaways

Advancing the precision frontier on $|\Delta m_{32}^2|$
 $< 2\%$ measurement!

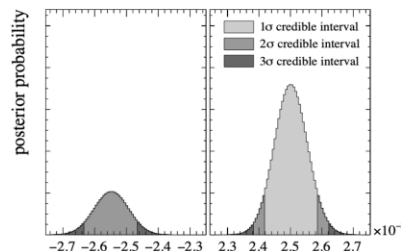
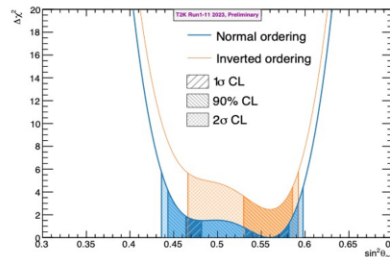


Mild preference for Inverted Ordering but influenced by θ_{13} constraint

NOvA+T2K only	NOvA+T2K + 1D θ_{13}	NOvA+T2K + 2D ($\theta_{13}, \Delta m_{32}^2$)
IO (71%)	IO (57%)	NO (59%)

Mass ordering and θ_{23} octant

- Slight preference for normal ordering and upper octant but none of them is significant
- Bayes factor NO/IO = 3.3
- Bayes factor $(\theta_{23} > 0.5) / (\theta_{23} < 0.5) = 2.6$

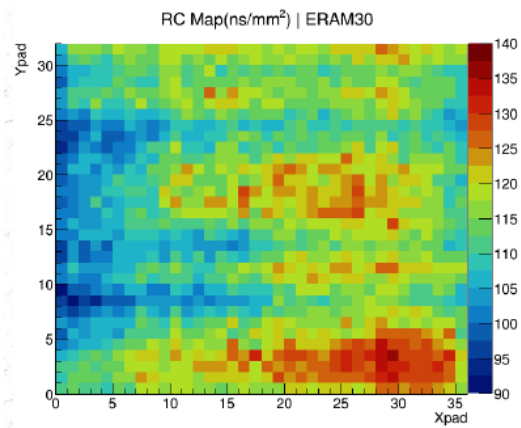
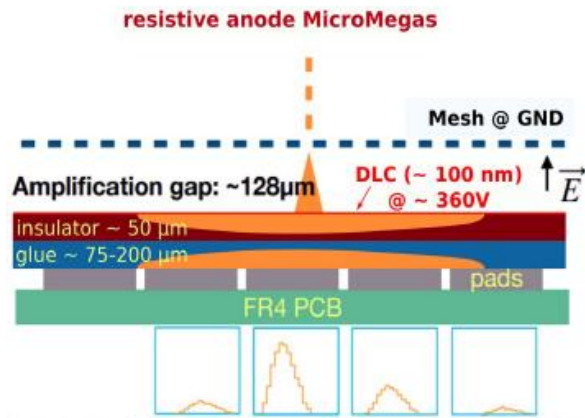


	$\sin^2 \theta_{23} < 0.5$	$\sin^2 \theta_{23} > 0.5$	Sum
NH ($\Delta m_{32}^2 > 0$)	0.23	0.54	0.77
IH ($\Delta m_{32}^2 < 0$)	0.05	0.18	0.23
Sum	0.28	0.72	1.00

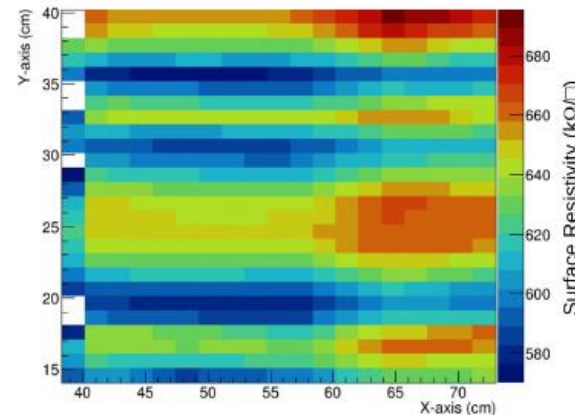
NOvA & T2K's first joint results:

- Yield **strong constraint on Δm_{32}^2**
- Weakly prefer IO or NO depending on which reactor constraint is applied
- **Strongly favor CP violation in Inverted Ordering**

Collaborations in active discussion about joint fit next steps



And this matches the resistivity direct measurement (C is very well constrained by the thickness of insulator)



R inhomogenities in the sputtering are clearly visible in the direction perpendicular to the drum rotation axis.